THE PETROGRAPHY, MINERALOGY AND
GEOCHEMISTRY OF THE GREAT
WHIN SILL, MIDDLETON-IN-TEESDALE,
N.E. ENGLAND.

DARREN NEIL CLARK

1992

B.Sc. (Honours) COMBINED SCIENCE

ANGLIA POLYTECHNIC

DARREN NEIL CLARK.
30 THE ORCHARD,
SEDGEFIELD.
STOCKTON-ON-TEES,
Co. CLEVELAND.
TS21 3AF.

CONTENTS

LIST OF FIGURES

LIST OF TABLES

LIST OF PLATES

LIST OF SYMBOLS AND ABBREVIATIONS

<u>Crystallographic properties of minerals</u>

a, b, c	Crystallographic axes
(111)	A single plane or face
{111}	A form; all planes with same geometric relationship to axes
β	Angle between *a* and *c* in the monoclinic system
α, β, γ	Angles between *b* and *c*, *a* and *c*, and *a* and *b* in the triclinic system

<u>Microscopy</u>

P.P.L.	Plane polarized light
X.P.L.	Cross polarized light

<u>Optical properties</u>

nα	Minor refractive index
nβ	Intermediate refractive index
nγ	Major refractive index
2V	Optic axial angle
2Vα	Optic axial angle bisected by α
2Vγ	Optic axial angle bisected by γ
OAP	Optic axial plane

<u>General</u>

mm	Millimeter
cm	Centimeter
m	Metre
km	Kilometer
SE	South-east
NW	North-west
N	North
$\Uparrow$	Up
$\Downarrow$	Down
+VE	Positive
°C	Degrees Centigrade
mg	Milligram
ml	Milliliter
AA	Atomic Absorption
ppm	Parts Per Million
c.	Approximately

1.0   <u>ABSTRACT</u>

The petrography, mineralogy and geochemistry of the Whin Sill and its contact rocks in the Middleton-in-Teesdale area are described using microscopic and analytical techniques. The sill consists of plagioclase feldspar (An_{88} to An_{25}); augite, pigeonite and subcalcic augite; orthopyroxene; magnetite – ulvöspinel solid solution with ilmenite lamellae; and micropegmatic intergrowths of quartz and alkali feldspar. Minor quantities of quartz, calcite, biotite, apatite and sulphides are also present. Grain size measurements confirm an increase in grain size away from the contacts and the presence of microphenocrysts indicate crystallization in the magma before intrusion. Major element analysis of the chilled margins, sill interior and pegmatite indicate that the sill complex magma shows significant variations. There is an increase in SiO_2 and a decrease in Na_2O and K_2O towards the contacts indicating possible magmatic differentiation or contamination. The chemistry of the sill has characteristics intermediate between tholeiitic and alkaline dolerites, and the initial magma itself may be a differentiate. Crystal settling is absent though large droplets of sulphides have been identified at the base of the sill. The contact rocks of the Whin Sill consists of partially metamorphosed limestones, sandstones and silt/mudstones. The metamorphosed rocks, even form rafts within the sill, frequently retain identifiable fossils and show occasional spotting and hardening.

2.0 INTRODUCTION

The Whin Sill is one of the best known geological features of the north of England. Because of its resistance to weathering relative to the Carboniferous sediments into which it has intruded, it inevitably forms an impressive topographic feature. This feature of the sill is magnificently exposed along the north facing scarp of the Roman Wall, to the west of the North Tyne, and is excellently exposed in the magnificent natural sections at High Force (Clough, 1876), Low Force ($_{NY}$ 904 280) (Plate 2.0), Cronkley Fell and along the River Tees.

Plate 2.0: Low Force water falls.
(Wynch Bridge looking North West)

It is frequently cited as one of the best examples of an extensive dolerite sheet whose main outcrop runs along the western edge of the northern Pennines, then turns north-east along the Roman Wall, across Northumberland and up to the Farne Islands. The outcrop of the Whin Sill and its related dykes can be seen in Figure 2.0, (Robson, 1980), along with other related dykes and also the locations of deep boreholes which have encountered the sill.
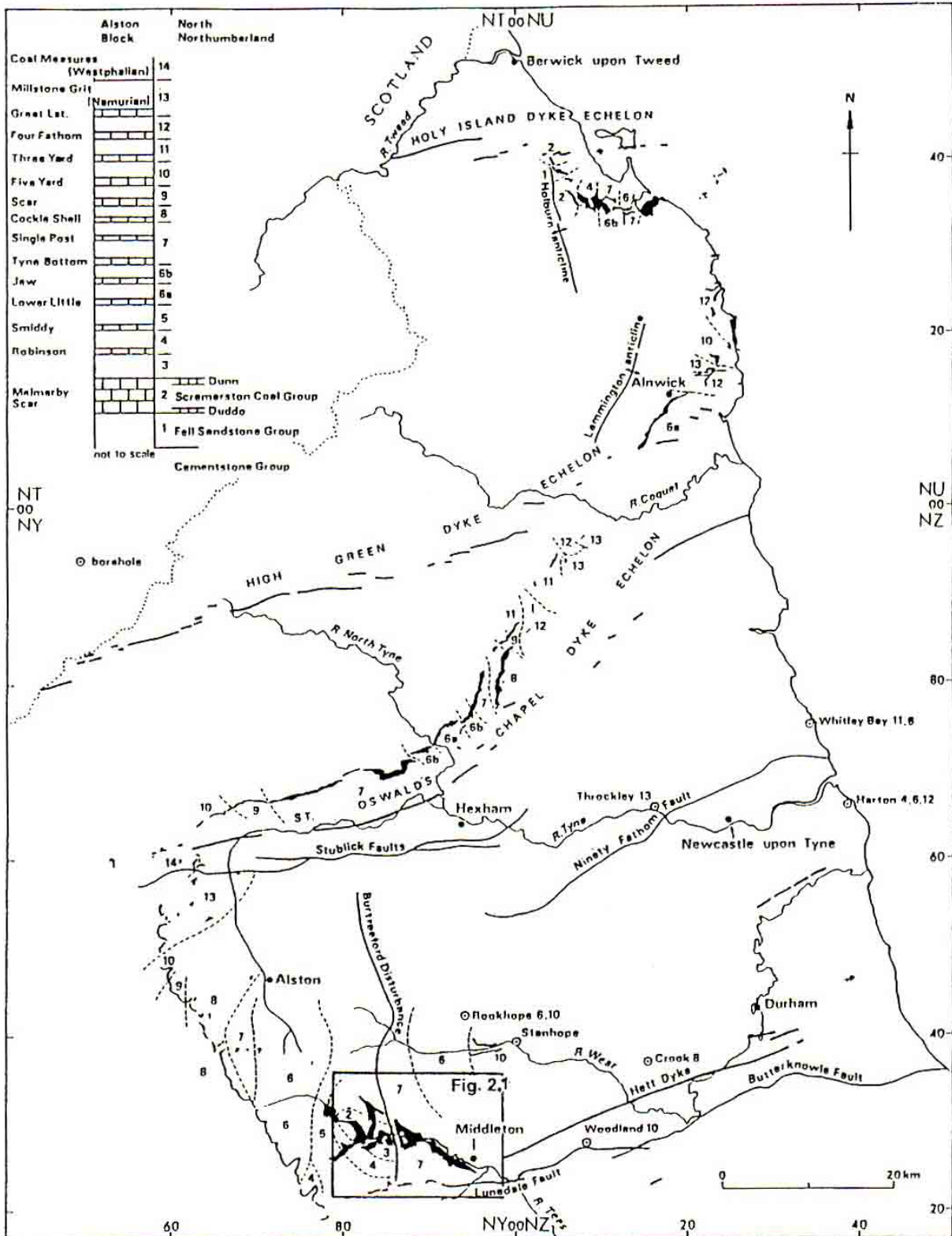
Figure 2.0: Map showing the outcrop of the Whin Sill, associated dykes and the location of deep boreholes in north-east England (Robson, 1980).

The Whin Sill forms a line of extensively quarried crags between Middleton-in-Teesdale and Cronkley Fell on the southern upthrown side of the Teesdale Fault. Figure 2.1 shows the outcrop of the Whin Sill in the Teesdale area (Based on Johnson and Dunham, 1973). The sill is limited to the east by the Butterknowle – Lunedale fault system. To the west the Sill passes from the horizon of the Tynebottom limestone at High Force ($_{NY}$ 880 284), cutting through the monoclinal structure associated with the Burtreeford Disturbance into the much lower Melmerby Scar limestone. It also reaches its maximum thickness of *c.* 73 m (240 ft) in this vicinity, (Dunham, 1948), recorded in a borehole near Dirt Pit Farm ($_{NY}$ 891 291).

The total Whin Sill complex is broadly concordant with the eastward dipping geological structure of the region, and underlies *c.* 4000 – 5000 km^2 in area, and has a volume estimated at being *c.* 215 km^3, (Francis, 1982), but as the sill dips below the North Sea to the east it thickens, so these values represent only a small percentage of the total volume of the Whin Sill. The sill occurs at its lowest stratigraphic level in upper Teesdale, where it is found in the Melmerby Scar limestone and as can be seen in Figure 1, the Whin Sill rises in stratigraphic level as you move northwards away from Teesdale. On the bases if this, Dunham and Kaye (1965) suggest that the original form may be regarded as a shallow, stepped saucer, thinning towards its edges. Figure 2.2 is a sketch-map of the Cronkley Fell area with a line of section showing the horizon changes made by the Whin Sill, from the Melmerby Scar limestone at the base to the Lower Little limestone of the roof.
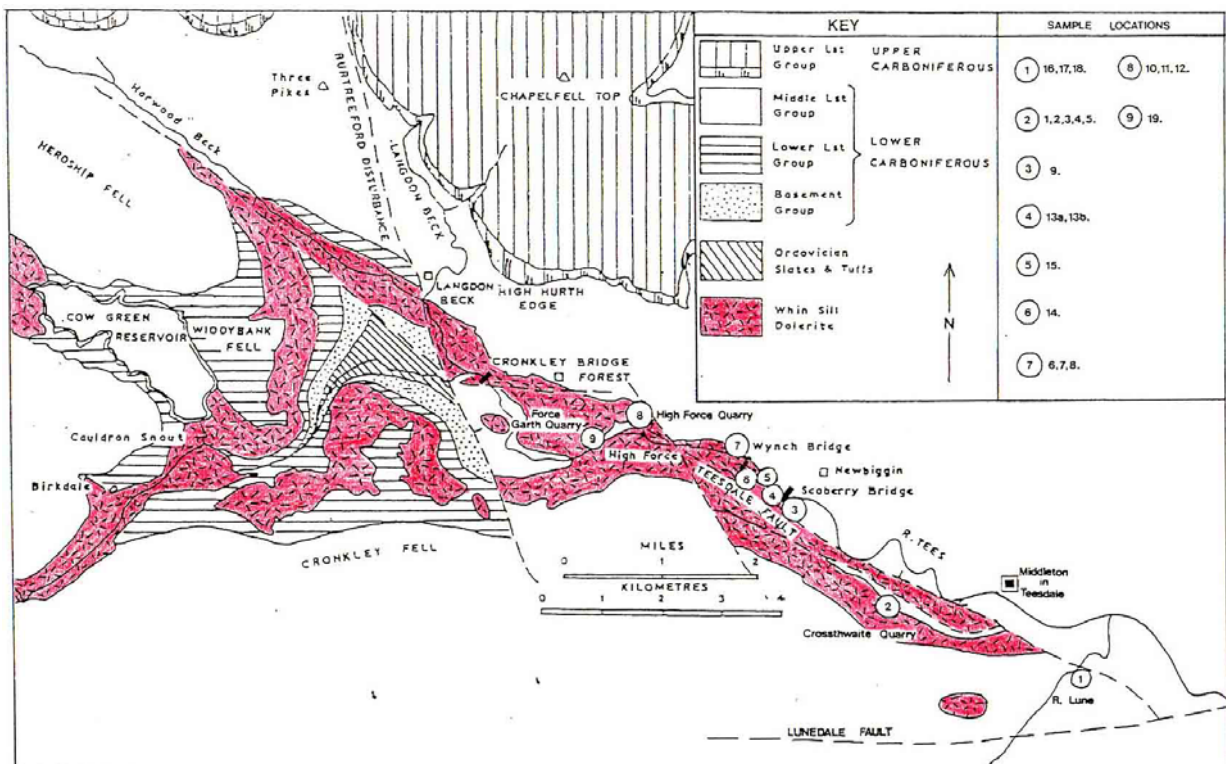
Figure 2.1: Geological sketch-map of Middleton-in-Teesdale,
based on Johnson and Dunham, 1973.

2.1 Age of the Whin Sill

The Whin Sill and associated dykes intruded Upper Carboniferous (Westphalian) rocks, but do not penetrate into the Permian strata. Pebbles of Whin Sill dolerite are known from Permian continental breccias, known as brockram, on the west of the Pennines. The age of emplacement of the sill is therefore found between the Upper Carboniferous and the Lower Permian, this is confirmed by Fitch and Miller (1987) where K-Ar dating suggests an age of 295±6 Ma.

2.2 Emplacement of the Whin Sill

Studies of the Whin Sill have produced many ideas as to the source and emplacement of the Whin magma. The magma which produced the Whin Sill complex was presumably generated in the mantle from many batches of mantle derived tholeiitic magma, and it has been recognised by Fitch and Miller (1967) that the magma moved towards the surface through tensional dyke channels in the crust as far as magmatic and hydrostatic pressures would allow (<1 km depth) and then flowed down-dip to stratigraphic levels controlled by magma density (Francis, 1982). Two noteworthy features of the model by Francis are:

1] The sediments were recently deposited and there was plenty of pore water to turn to steam and ease the passage of magma; and

2] The syn-sedimentary basinal form of the country rock is the cause of the basinal form of the intrusion. (See Figure 2.3).
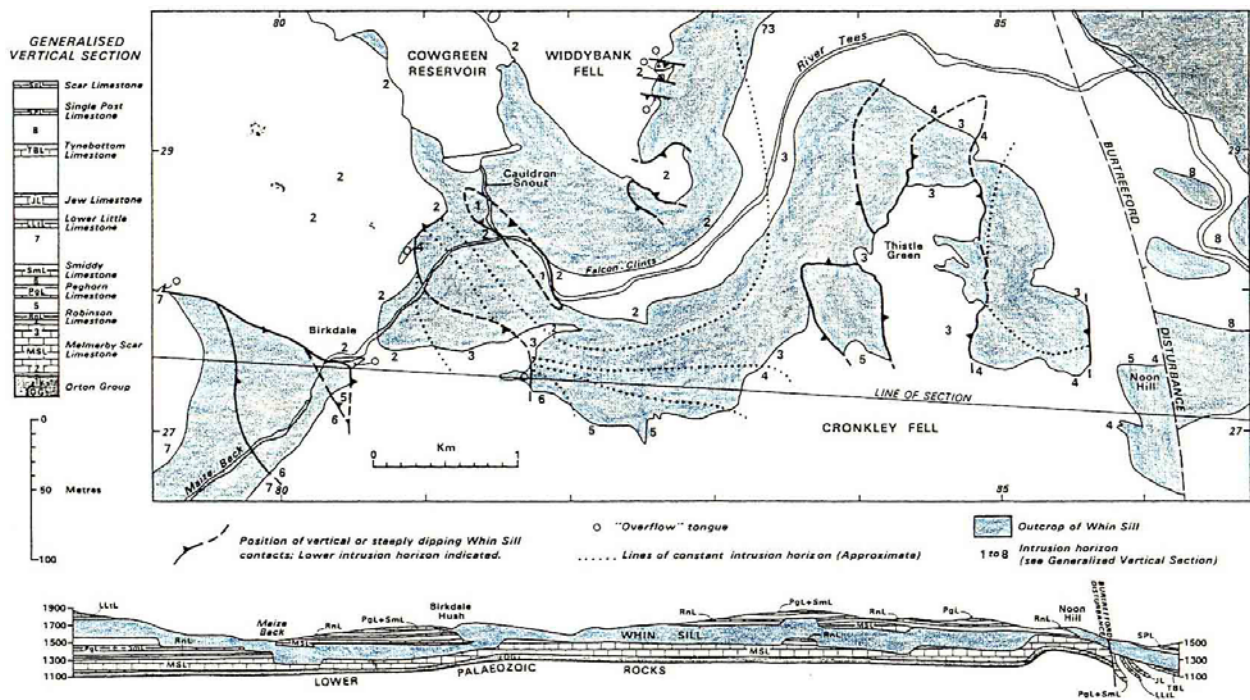
Figure 2.2: Sketch map of the Cronkley Fell area showing horizon changes made by the Whin Sill (Burgess and Holiday, 1979).

There is no obvious feeder for the Whin Sill and there is no good example of a dyke turning into the sill. "The combination of the greatest thickness and lowest stratigraphic horizon for the sill in upper Teesdale suggests that a feeder might me in the vicinity. However, it is not large enough to cause a significant magnetic anomaly such as might be expected over a dolerite plug." (Dunham (1970). Randall (1989) assumes that the magma was directed from the SE to the NW and that it was emplaced essentially in one episode to form a single unit.

The sill began to crystallize at approximately 1100 to 1150 °C and already contained microphenocrysts of plagioclase and pyroxene which began crystallizing at depth. By approximately 1025 °C the main part of the sill had completely solidified and the increased concentration of volatiles in the central and upper parts of the sill allowed the pegmatites to crystallize. Crystallization terminated in the final residual melt at approximately 750 °C and upon reaching 500 °C certain vertical joints and parts of the upper contact were mineralized with quartz and calcite, and also pectolite as exposed in the joints of both Force Garth and High Force quarries. (after Randall, 1989).
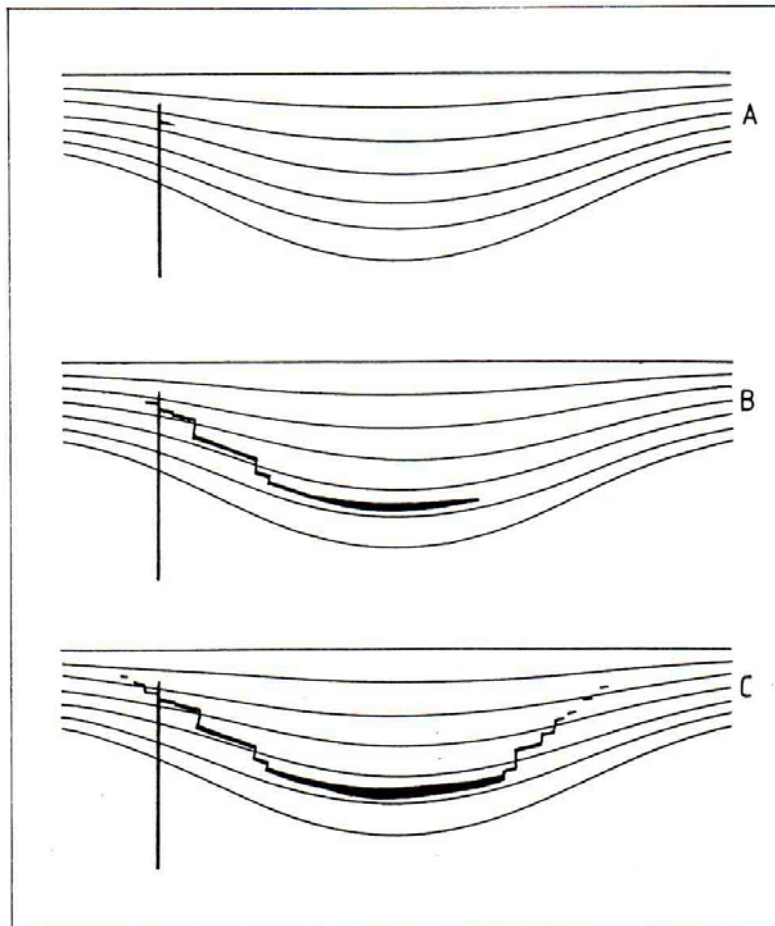
Figure 2.3: The mechanism of sill intrusion (after
Francis, 1982 In Hall, 1987). A: A dyke reaches within
1 km of the surface. B: Lateral intrusion under a head
leads to gravitational down-dip flow. C: Magma ascends
to achieve hydrostatic equilibrium.

3.0   FIELDWORK

The fieldwork for this project was undertaken during the period from the 12th September 1991 to the 21st September 1991, and a visit to Force Garth Quarry (permission to enter required) on Saturday 19th October with the British Geological Survey (Northern branch). The objective of the study was to take samples of the Whin Sill dolerite and surrounding country rock at measured intervals from the base or roof of the sill, so as to make comparative petrological studies of the samples. All nine of the locations studied can be seen labelled on the following ordinance survey map of Middleton-in-Teesdale (Figure 3.0). A detailed account of each location is presented on the following pages.
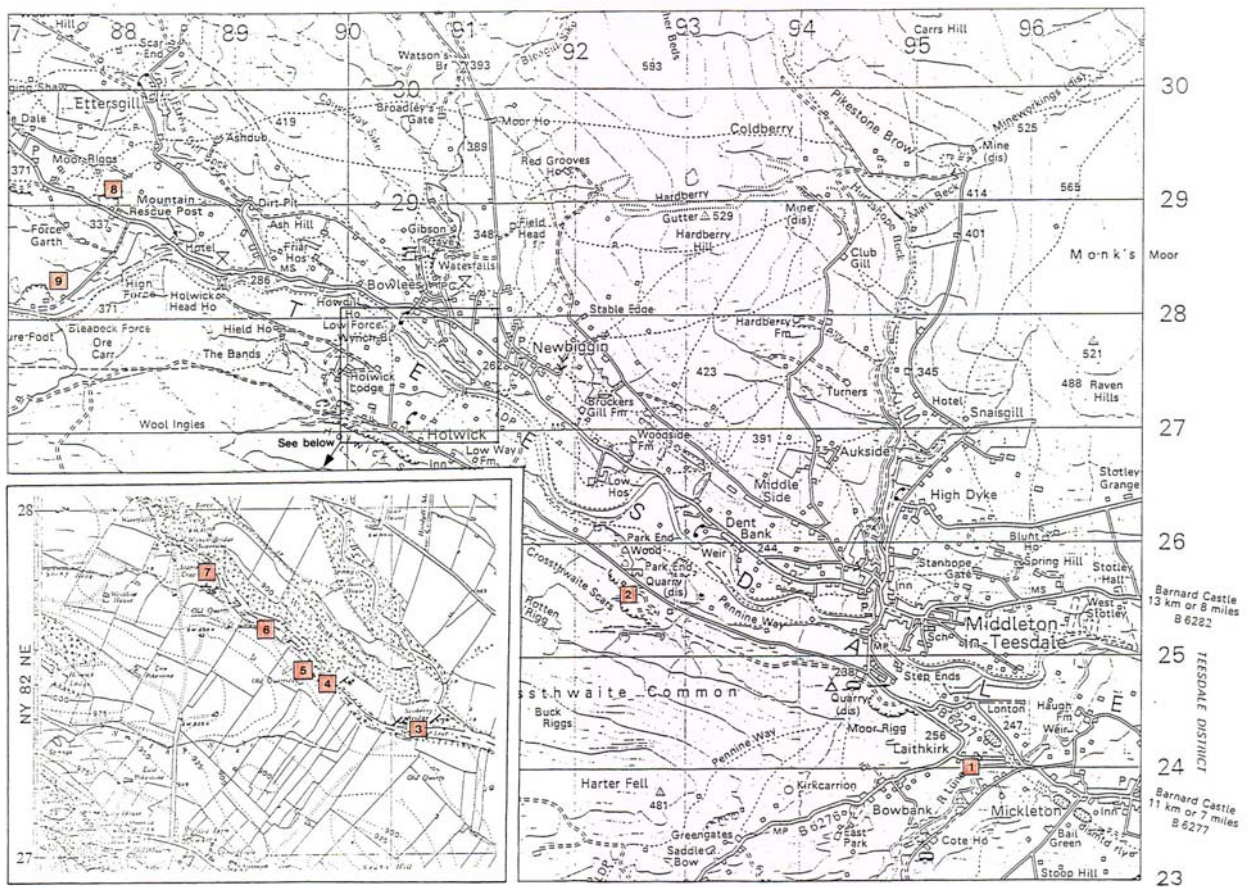
Figure 3.0: O.S. Map showing all of the
nine locations studied.

3.1 Lune River cutting at Laithkirk

Location number 1 ($_{NY}$ 950 240) is an exposure in the bank of the River Lune. The base of the Whin Sill has been exposed in contact with altered sandstone country rock. The outcrop contains a wedged block of sandstone which has been lifted out of the shallow dipping sandstone beds (average dip 6° SE) to a much steeper angle by the intrusion of the dolerite. This feature can be seen in Plate 3.0 below. Sample numbers 16, 17 and 18 were all taken from this location as indicated on the field sketch.
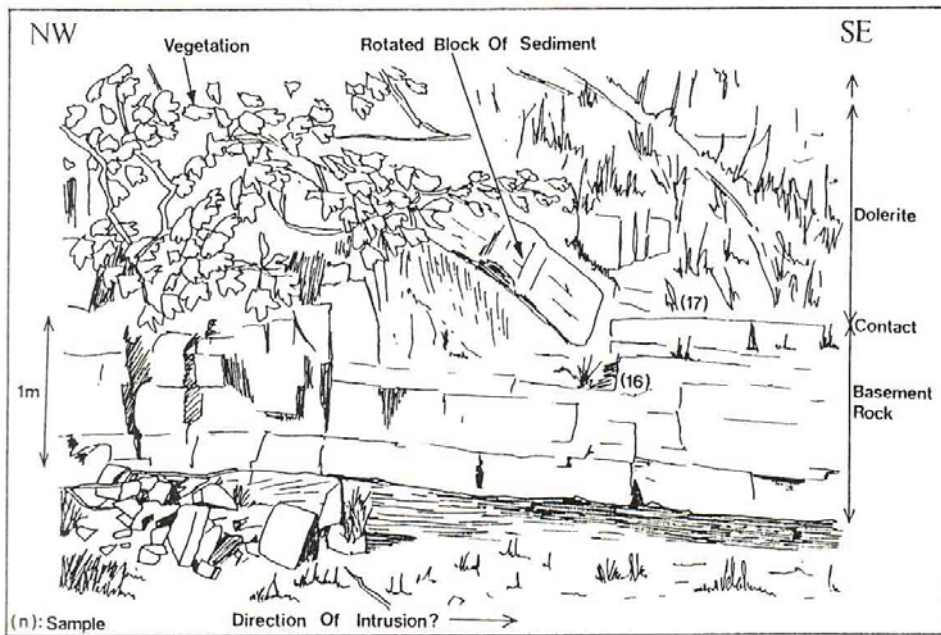
Plate 3.0: Photograph and field sketch from the River Lune, Laithkirk, showing a rotated raft of sediment in the basement of the Whin Sill dolerite.

3.2 Crossthwaite Quarry

Crossthwaite Quarry (NY 925 255), location 2, is a disused dolerite quarry at the base of the Whin Sill. The altered country rocks at the base of the sill have been exposed, although the true contact of the sill cannot be determined because of scree and vegetation cover. The photograph and field sketch in Plate 3.1 show the outcrop and the locations where sample numbers 1 – 5 were taken from. The altered strata was measured to be dipping at approximately 2° NW.
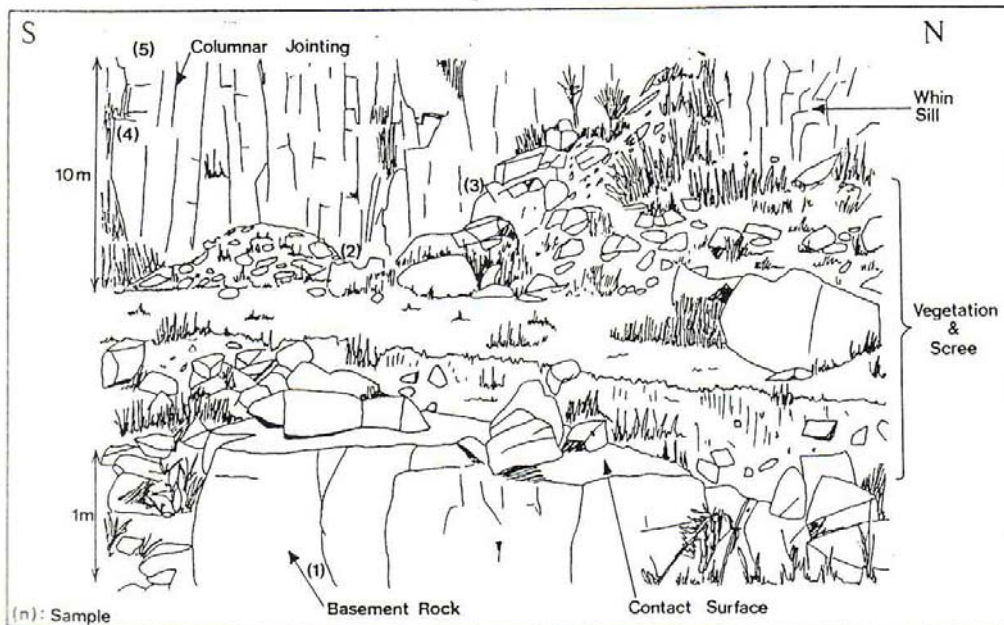
Plate 3.1: Photograph and field sketch from Crossthwaite
Quarry, showing the base of the Whin Sill.
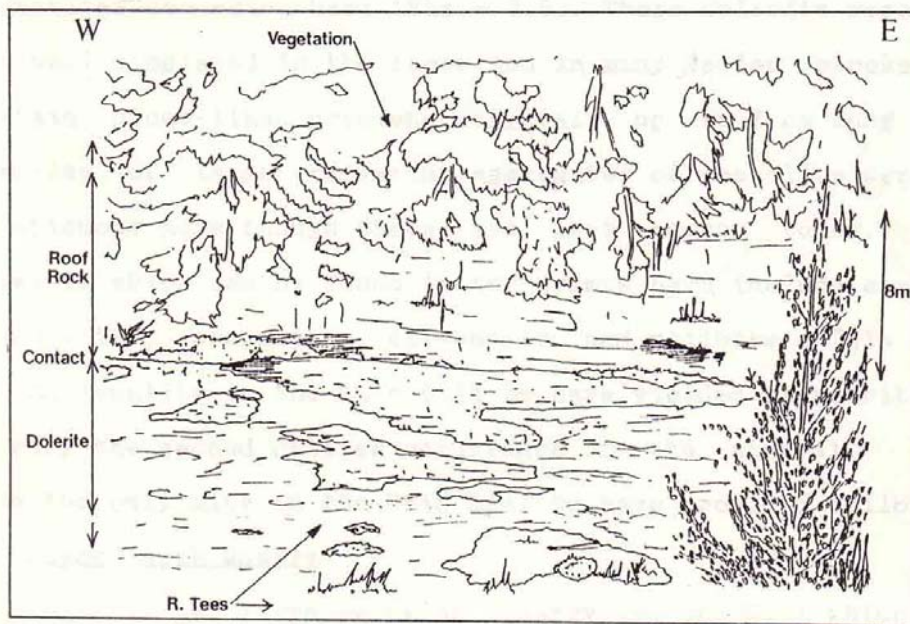
Plate 3.2: Photograph and field sketch from the south bank
of the River Tees, showing the top contact of the Whin Sill.

3.3 Scoberry Bridge

This outcrop ($_{NY}$ 911 274), location 3, consists of unaltered massive fossiliferous limestone dipping approximately 2° SE. The limestone is similar in colour to the dolerite of the sill (blue/grey), but is recognised easily as limestone because its surface is pitted with small solution holes, averaging 20 cm in diameter, and it has a large fossil content. Sample number 9 was taken from this location.

3.4 Edge of Wynch Bank Plantation

Location number 4 ($_{NY}$ 909 275) consists of an outcrop of altered country rocks, sandstone, limestone and shale dipping approximately 4° SE. Sample numbers 13a and 13b were taken from this location.

3.5 South bank of River Tees

Sample number 15 was taken from location 5 ($_{NY}$ 907 275) and consists of Whin Sill dolerite. This sample was taken as close to the top of the sill as was possible. The contact is not visible on the southern river bank, but can be seen on the opposite river bank as indicated in the photograph and sketch in Plate 3.2.

3.6 South bank of River Tees

Location 6 ($_{NY}$ 906 277) is similar to location 5 in that Whin Sill dolerite is exposed on the southern riverbank and country rock on the northern riverbank. Sample number 14 was taken from this location.

3.7 Wynch Bridge

At location 7 ($_{NY}$ 905 278) a rotated raft of baked sediments, presumably a fragment of the roof of the sill, can be seen engulfed in the dolerite. The raft was measured to be dipping 25° N, whereas most of the strata in the Middleton-in-Teesdale area is near horizontal. The base of the raft is not exposed, so the thickness of the raft is not known. Plates 3.3 and 3.4 show the contact clearly between the strata (bottom) and the Whin Sill (top).

3.8 High Force Quarry

Location number 8 is a large abandoned quarry ($_{NY}$ 879 290). The rather weathered faces exhibit very good columnar jointing, which is almost cubic due to the coarse grained dolerite pegmatites occurring here (Plate 3.5). These dolerite pegmatites are well displayed in the faces and in many fallen blocks, and contain plume-like pyroxene crystals up to 2 cm long. Good examples of large radiating aggregates of pectolite were once conspicuous here though these are less common today. Other minerals which can be found in the joints here include analcite, apophyllite, chabazite, stevensite and stilbite. This is the second locality in the Whin Sill to have yielded stevensite, and is only the second British occurrence of the mineral. It is also the only site in the Whin Sill to have provided stilbite.

3.9 Force Garth Quarry

This is a large working quarry in the sill which is at almost the same stratigraphic level as high Force Quarry. The sill is intruded here between the Tynebottom and Single Post limestones. The rock is a typical medium-grained dolerite exhibiting crude cuboidal columnar jointing (Plate 3.6). Dolerite pegmatites also occur in this quarry. Fine examples of radiating crystalline pectolite are exposed in the joints from time to time.

Plates 3.3, 3.4: Photographs showing the contact
between the Whin Sill (top) and the top of
a raft of tilted, baked sediments (bottom)
near Wynch Bridge.
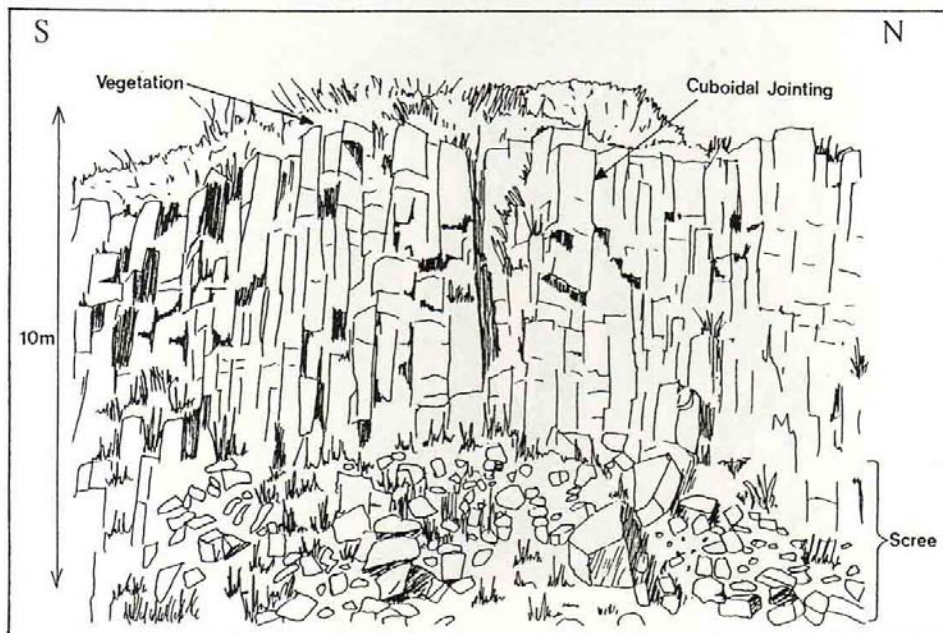
Plate 3.5: Photograph and field sketch showing
cubic columnar jointing in Whin Sill dolerite
and dolerite-pegmatite at High Force Quarry.
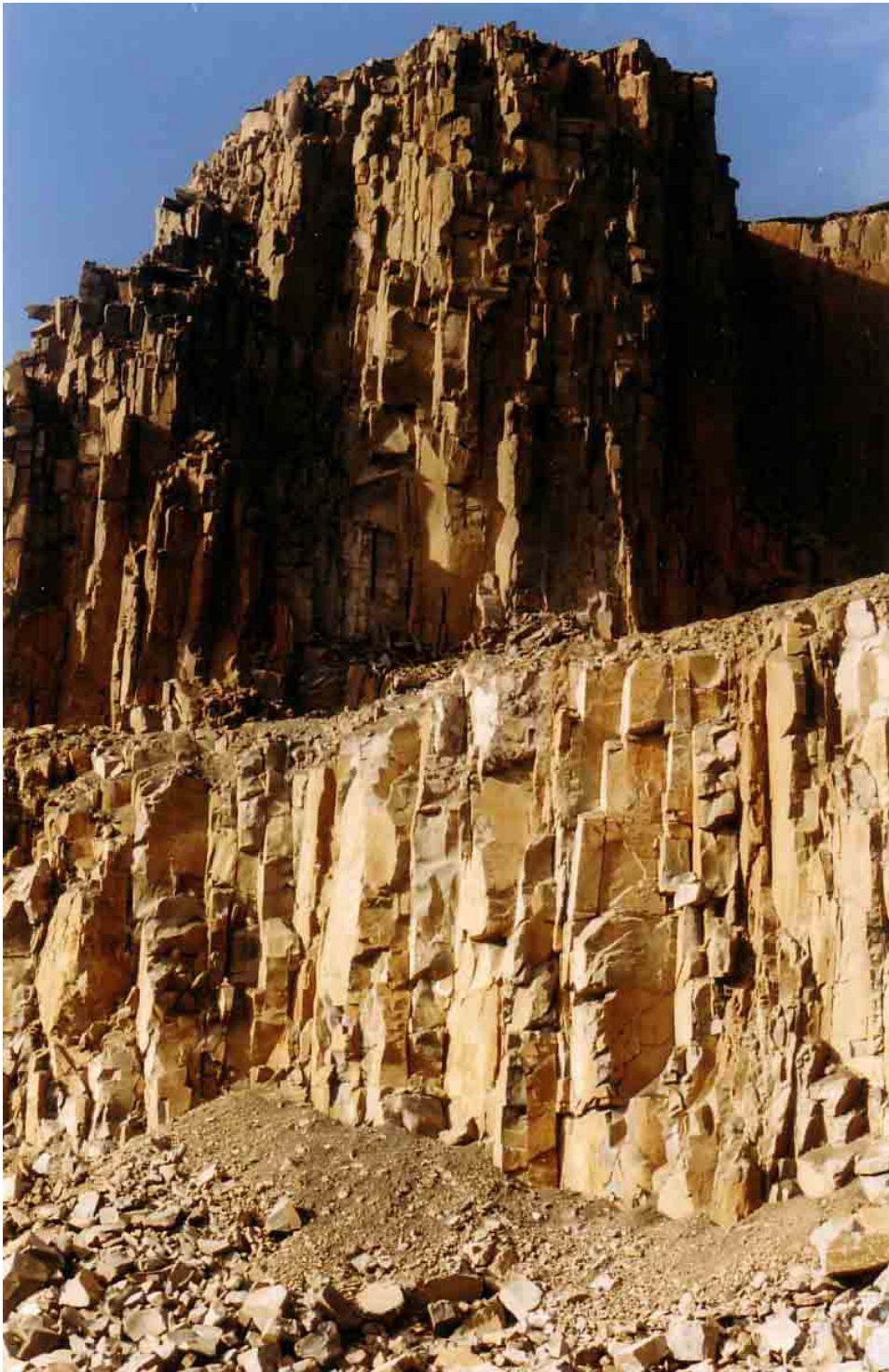
Plate 3.6: The working face of Force
Garth Quarry, showing crude cuboidal
columnar jointing.

Figure 3.1, overleaf, is a sketch section through the Whin Sill and contact rocks showing the vertical distribution of samples taken in the field. Table 3.0, is a detailed list of samples and locations.
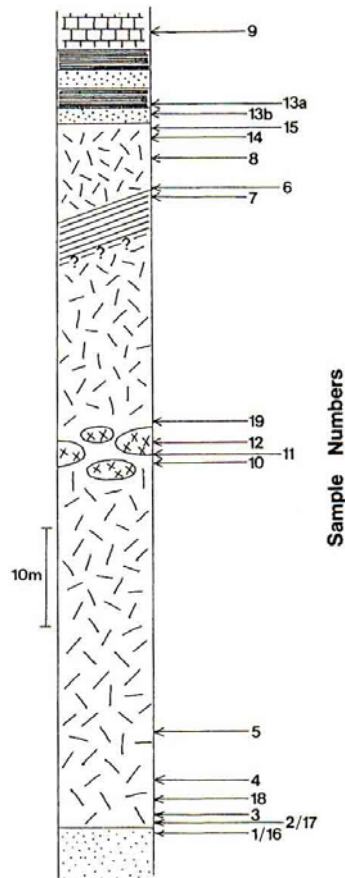
Figure 3.1: Sketch section through the
Whin Sill, showing sample locations.

Sample No.	Grid Ref.	Placement in Sill	Rock Type
1	925 255	0.5 m ⇓ from base	Basement rock
2	925 255	0.5 m ⇑ from base	Dolerite
3	925 255	1.5 m ⇑ from base	Dolerite
4	925 255	5.0 m ⇑ from base	Dolerite
5	925 255	10.0 m ⇑ from base	Dolerite
6	905 278	0.3 m ⇑ from raft	Dolerite
7	905 278	0.3 m ⇓ into raft	Baked Sediment
8	905 278	4.0 m ⇑ from raft	Dolerite
9	911 274	? m ⇑ from roof	Limestone
10	879 290	? m mid sill	Dolerite
11	879 290	? m mid sill	Dolerite / Pegmatite
12	879 290	? m mid sill	Pegmatite
13a	908 275	? m ⇑ from roof	Roof Sediment
13b	908 275	? m ⇑ from roof	Roof Sediment
14	906 277	? m ⇓from roof	Dolerite
15	907 275	? m ⇓ from roof	Dolerite
16	950 240	0.2 m ⇓ from base	Basement Rock
17	950 240	0.5 m ⇑ from base	Dolerite
18	950 240	3.0 m ⇑ from base	Dolerite
19	874 282	? m mid sill	Dolerite

Table 3.0.

| 4.0 | PETROGRAPHY |

The main mass of Whin Sill is a very hard, dark grey, medium grained quartz-dolerite, with sparse phenocrysts rarely exceeding 2 mm in length, and an average groundmass granularity ranging between 0.1 mm and 0.6 mm. It is typically composed of 55.3% plagioclase (zoned from An_{88} to An_{25}), 31.7% clinopyroxene (augite, subcalcic augite and pigeonite), 3.5% orthopyroxene, 6.5% Fe-Ti oxides, 1.5% quartz, 1.3% biotite and a small amount of secondary carbonate, pegmatite, apatite and hornblende (See Table 6.0). Specific gravity measurements throughout the sill have been made by Dunham and Strasser-King (1982) and give a mean value of 2.983 ± 0.009, although the following table of specific gravity measurements by Teall (1884), shows variations from 2.820 to 2.959.

Hot Bank near Craig Lough	2.924
Longhoughton near Alnwick	2.906
Greenhead Quarry near Haltwhistle	2.945
Barrasford Quarry, N.Tyne	2.945
Crags near Bourbovicus	2.944
Middleton-in-Teesdale	2.959
Tinkler's Syke	2.820
Teward's Bridge near Forest Church	2.840

Four major lithologies have been determined within the Whin Sill (Fitch and Miller, 1967).

1} Tachylitic chilled marginal facies – Black, very fine-grained rock in which the constituent minerals cannot be distinguished by the naked eye.

2} Fine-grained quartz-dolerite – Fine-grained, grey or greenish rock in which ferromagnesian minerals and feldspars are seen using a hand lens. (Samples 2,3,4,5,8,14,15,16,17,18.)

3} medium-grained quartz-dolerite – This is typical Whin Sill dolerite in which the constituent minerals are visible to the naked eye. (Samples 10,11,19.)

4} Dolerite pegmatites of two types:

    i.   Dark greenish or grey rocks, rich in large pyroxenes up to 20 mm long. (Samples 11,12.)

    ii.   Pink granophyric rocks with an average grain size of 2 mm to 3 mm.

4.1 <u>Plagioclase Feldspar</u>

Plagioclase is the most abundant mineral in the Whin Sill and forms an average of 55.3% of the rock. It occurs throughout the sill both as lath-shaped phenocrysts, commonly 2 mm or more in length and in the groundmass, similarly lath-shaped but only attaining the length of up to 1 mm. Petrographical evidence shows that only the plagioclase crystallized throughout almost the entire crystallization of the rock with compositional extinction zoning from cores of An_{88} to rims of An_{25} ($NaAlSi_3O_8$ (Albite) – $CaAl_2Si_2O_8$ (Anorthite)). This compositional zoning of the plagioclase suggests that the crystals were not in equilibrium with the liquid during its crystallization due to either the co-precipitation of clinopyroxene or to the cooling rate (Dunham and Strasser-King, 1981). 2V ranges between 74° and 90° depending upon the composition (An_{88} = high 2Vγ, An_{25} – low 2Vγ). Using figure 4.0, the refractive index variation can be determined as listed overleaf:

	An$_{25}$	An$_{88}$
nα	1.542	1.560
nβ	1.546	1.566
nγ	1.549	1.571
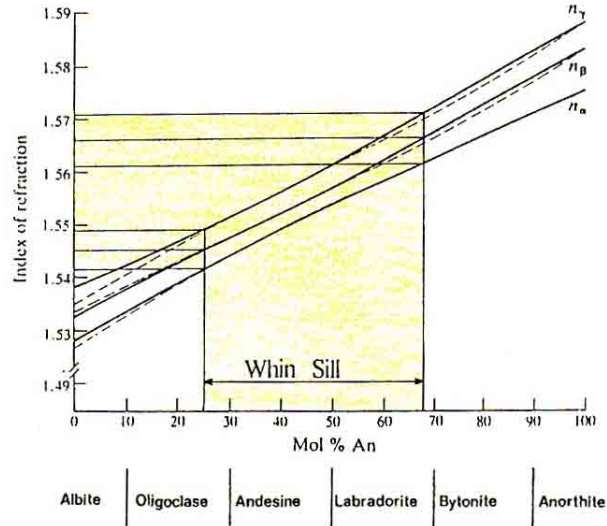
Figure 4.0: Refractive index variation in
Plagioclase feldspars of the Whin Sill.

The crystals have low relief, are colourless in P.P.L., and form subhedral to euhedral prisms with two perfect cleavages {001} and {010} meeting at right angles on the (100) plane. Figure 4.1 shows a typical labradorite (An$_{50}$) plagioclase feldspar (Gribble and Hall, 1985).

Figure 4.1: Labradorite (An$_{50}$) plagioclase
feldspar (Gribble and Hall, 1985).

The crystals have low birefringence, with interference colours varying from first order greys (Na-rich) to first order yellows (Ca-rich). Twinning is common in almost all the plagioclase feldspars and this is there characteristic feature. Most crystals are twinned according to the albite law but combined carlsbad-albite twins are not uncommon.

4.2 Plagioclase Determinations

The composition of the plagioclase feldspar laths in the Whin Sill have been determined using the Michel-Lévy method as follows:

1} A multiple-twinned plagioclase lath with sharply defined twin lamellae, in which both parts of the twin show the same shade of grey when the lamellae are placed parallel to the N-S crosswire in X.P.L., was selected.
2} The stage graduations in the N-S position were noted.
3} The stage was rotated clockwise until one set of twin lamellae was completely extinct. The new stage graduations were noted and the difference between readings in 2} and 3} taken.
4} The stage was then rotated anticlockwise until the other set of twin lamellae was in complete extinction. The stage graduations were taken again and the difference from the reading under }2 was noted. The mean of results 3} and 4} was used.

The final readings have all been plotted on figure 4.2 and show plagioclase crystals ranging in composition from Oligoclase (An_{29}) to Labradorite (An_{89}). These results are comparable to those of the refractive index variation shown in figure 4.0.
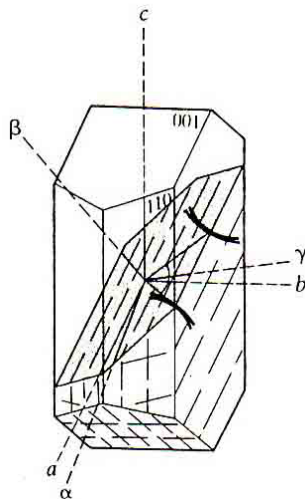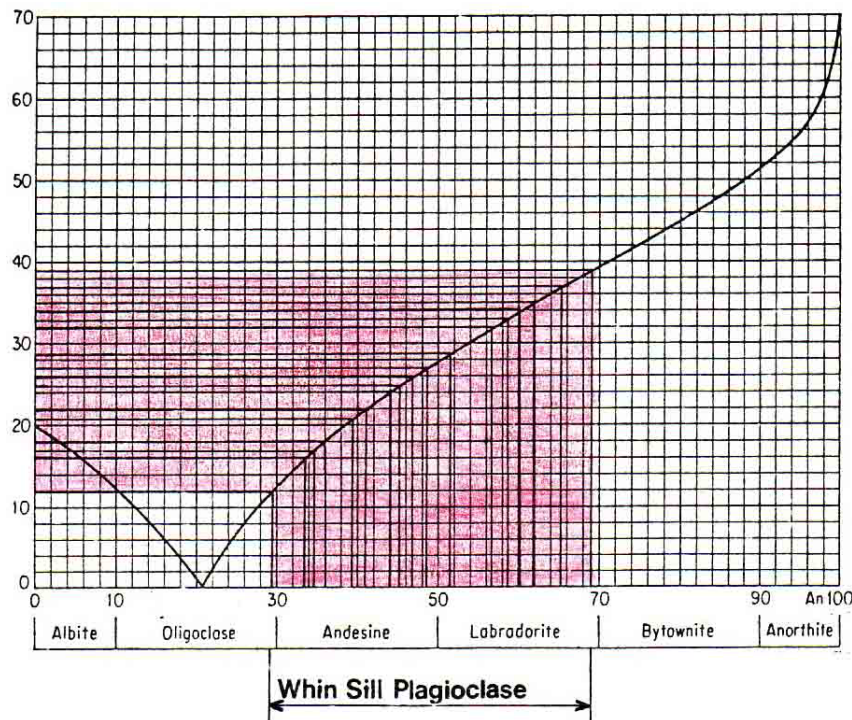

Figure 4.2: Plagioclase feldspar
compositional determinations.

4.3 Pyroxenes

Both clinopyroxene and orthopyroxene are present in the Whin Sill although in differing proportions. Holmes and Harwood (1928) noted that in some specimens, especially those from the northern occurrence of the sill, orthopyroxene is rare and very much altered, or may even be absent altogether,

i. Clinopyroxene

Clinopyroxene is the second most abundant mineral, consisting approximately 31.7% of the total rock mass. It occurs both as phenocrysts up to 2 mm long and in the groundmass as pale brown top pale

green, subhedral to euhedral individuals. The phenocrysts are not so elongate as the orthopyroxenes and may show twinning, some in two directions parallel to {100} and {001} producing a characteristic chequerboard appearance. Three groups of clinopyroxene phases have been recognised in the rock on the basis of 2V's and probe analysis by Dunham and Strasser-King (1981). Those with $2V\gamma$ around 0° are recognised as pigeonite whilst $2V\gamma$'s generally over 40° are augite. Those of intermediate $2V\gamma$ ($\approx$32°) are thought to be subcalcic augite. Pigeonite, $Ca(Mg,Fe)Si_2O_6$ is very similar to augite except for its small 2V, generally around 0°. Its refractive index varies between 1.682 to 1.722 ($n\alpha$) and 1.705 to 1.751 ($n\gamma$). Pigeonite shows an extinction angle between 35° and 45°. OAP is perpendicular to (010), interference colours are very low first order greys and two cleavages are present, meeting at an angle of less than 90°. Figure 4.3 shows a typical pigeonite crystal (Gribble and Hall, 1985).
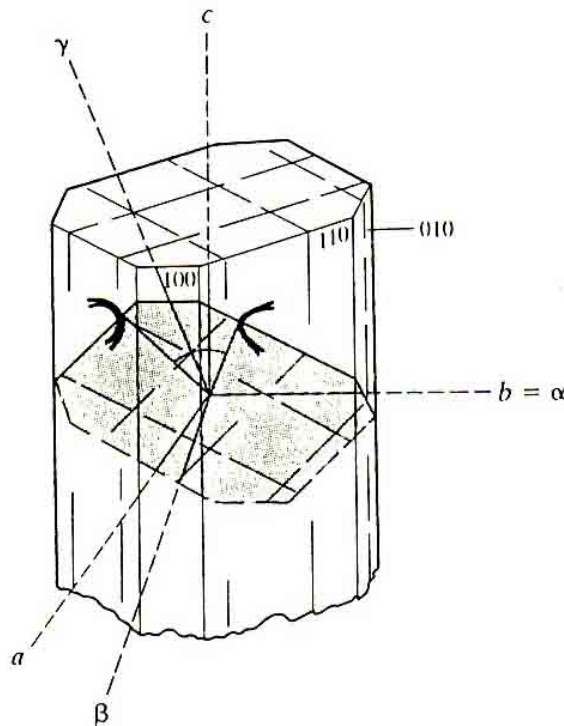
Figure 4.3: A typical pigeonite
clinopyroxene (Gribble and Hall, 1985).

Augite, $Ca(Mg,Fe^{2+})(Al,Fe^{3+}Ti)(Al,Si)^2O^6$ is the most dominant phase in the Whin Sill and shows a 2V angle generally over 40°. Its refractive index varies between 1.662 and 1.761 depending upon the Mg:Fe ratio. It is colourless to pale brown with moderate to high relief. Birefringence is moderate with maximum interface colours being low second order blues or greens. Twinning is both simple and multiple, occurring on {100} and {001} and cleavage shows good {110} and poor {100} and {001} partings. Augite typically shoes extinction angles between 31° and 50°. Figure 4.4 shows a typical augite crystal (Gribble and Hall, 1985).

Subcalcic augite is thought to be a metastable phase consisting of unmixing augite – pigeonite grains.
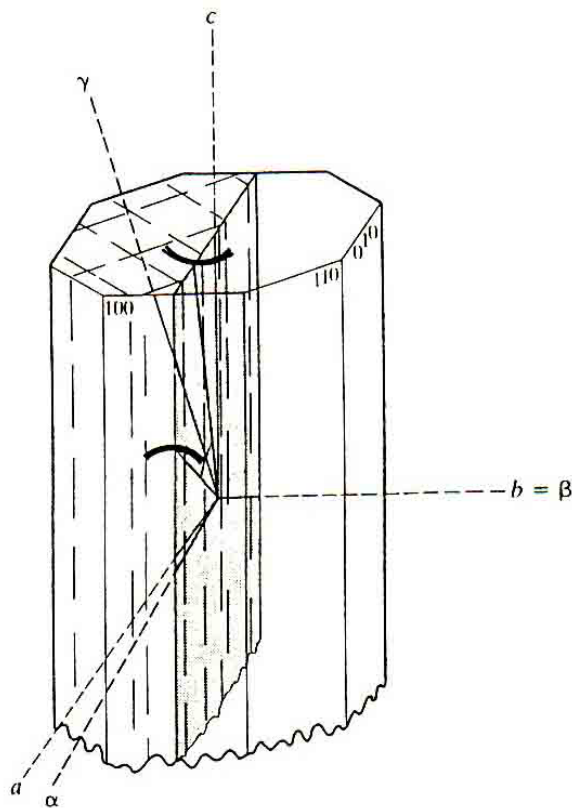
Figure 4.4: A typical augite clinopyroxene
Crystal (Gribble and Hall, 1985).

ii.   Orthopyroxene

Orthopyroxene occurs only as phenocrysts up to 3 mm long and is not recognised in the groundmass. The grains are elongate, poikolitically enclosing plagioclase laths and are rimmed with clinopyroxene. Only a small percentage (3.5%) of the rock is composed of orthopyroxene whose composition varies between Fs_{23} and Fs_{27} ($2V\alpha$ varying between 67.5° and 73°) (Dunham and Kaye, 1965). Twinning in the crystals is not common and the crystals are frequently bent or broken. Figure 4.5, overleaf, taken from Gribble and Hall (1985) shows the variation of 2V angles and refractive indices for the orthopyroxene sequence ($MgSiO_3$ to $FeSiO_3$). Shown also is the compositional variation of the Whin Sill orthopyroxenes (Bronzite). Using the graph of refractive indices we can determine that the Whin Sill orthopyroxenes have refractive indices varying from 1.668 to 1.682 ($n\alpha$) and 1.685 to 1.688 ($n\gamma$).

As the Whin Sill is magnesium rich the crystals are colourless and show no pleochrosim. They show two good prismatic {110} cleavages meeting at 88° on a basal section. {010} and {100} are poor cleavages or partings. They also have moderate to high relief and low birefringence with interference colours of first order greys or yellows. The main difference between the orthopyroxenes is that the orthopyroxenes show straight extinction. Figure 4.6 shows an orthopyroxene of composition Fs_{14} to Fs_{100} (Gribble and Hall, 1985).

Figure 4.5: Variation of 2V angle and
indices of refraction in the orthopyroxene
series (Gribble and Hall, 1985).

Figure 4.6: A typical orthopyroxene crystal
of composition Fs_{14} to Fs_{100}
(Gribble and Hall, 1985).

4.4 Iron-Titanium Oxides

Iron-Titanium oxides typically make up 6.5% of the Whin Sill. These occur as minute grains towards the margins of the sill and average grain sizes are approximately 0.1 mm to 0.4 mm acr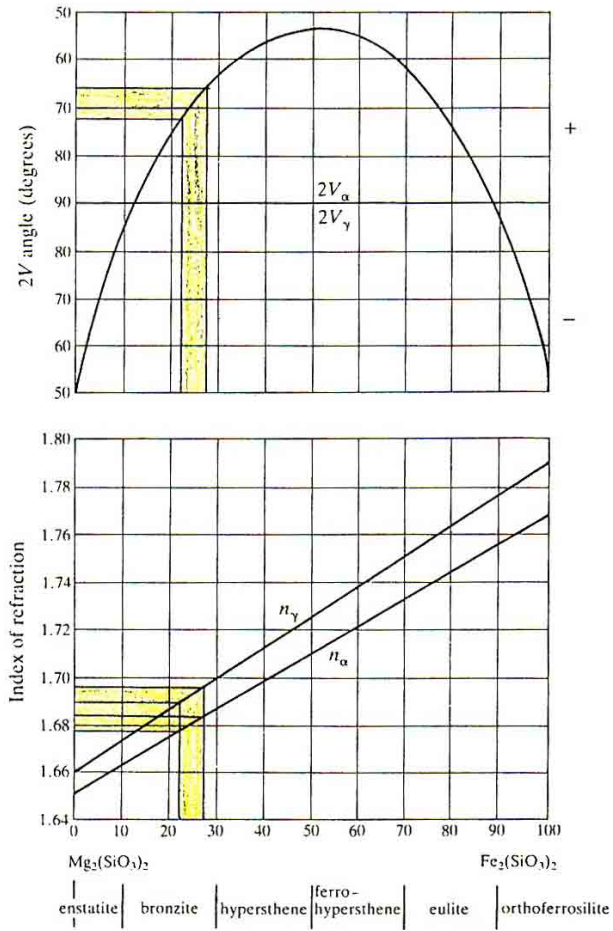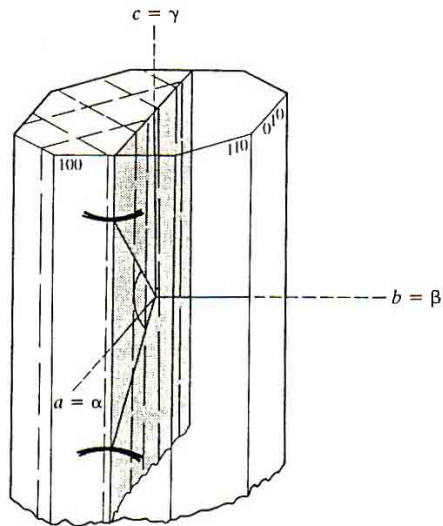oss. Towards the centre of the sill they occur both as phenocrysts, commonly enclosing silicates and in the groundmass. The dominant mineral is a magnetite-ulvöspinel solid solution with lamellae of ilmenite, but ilmenite-haematite solid solution can also be found.

4.5 Quartz

Quartz, SiO_2, occurs throughout the sill (1.5%) as discrete grains and as graphic intergrowth's with alkali feldspar in the pegmatite. The quartz sometimes exhibits radiating strain extinction (Dunham and Kaye, 1985) and are sometimes ringed by carbonate. There is an increase in size and abundance of quartz towards the centre of the sill.

4.8 Sulphides

Minor amounts of sulphides occur in the Whin Sill. The most common sulphide is pyrrhotite occurring generally with small amounts of chalcopyrite, pyrite and chalcopyrrhotite. They may have formed by early segregation of immiscible sulphide liquids within the Whin magma. The sulphides are generally denser than the magma in which they have formed, so that immiscible droplets of sulphide liquid may coalesce into globules of sufficient size to sink and accumulate at the base of the intrusion. (See Thin section DC 2.)

4.7 Other Minerals

Carbonate minerals are dispersed throughout the sill, decreasing towards the centre. They are usually found as very small grains making optical determination difficult. Apatite form elongate needles up to 0.3 mm long and are abundant in the pegmatite (Plate 4.0) and plagioclase, and increase in size and abundance towards the centre of the sill. Secondary biotite and hematite are also found in small quantities throughout the sill.

4.8 Pegmatite

The pegmatitic variety of the quartz-dolerite constitutes approximately 2.5% of the total Whin Sill. It is well exposed in both High Force and Force Garth quarries in flat-lying concordant sheets up to 150 mm thick. This contains prominent bladed augite crystals up to 50 mm in length, which are rather more iron-rich than those in the ordinary sill, strongly zoned plagioclase from labradorite to oligoclase (An_{65} to An_{20}) (Tomkeieff, 1929), quartz-alkali feldspar intergrowths, biotite, amphibole, areas of clear quartz, apatite and calcite.
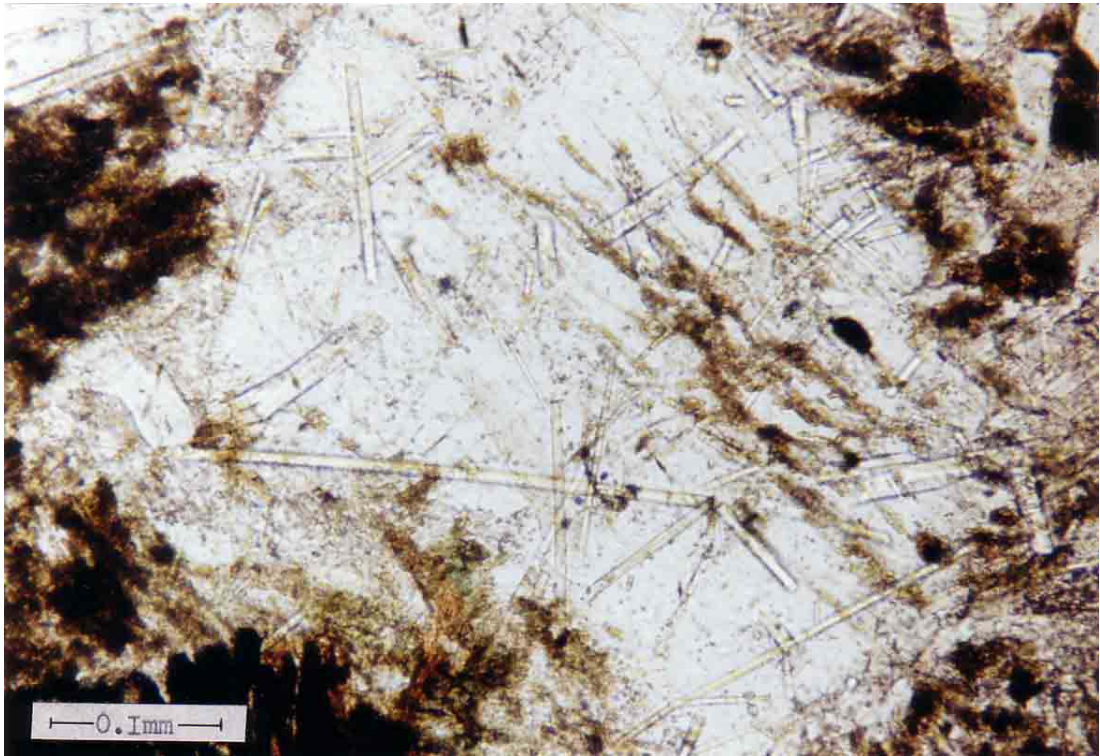
Plate 4.0: Elongate apatite needles
In sample DC 12 (Dolerite pegmatite).

5.0 THIN SECTIONS

   Thin sections were produced from all the samples taken in the field, so as to be studied in greater detail. Modal and grain size analyses have been carried out on the sections and are shown on page 42. Using the diagrams shown in figure 5.0, below, visual estimations of 2V angles have been made throughout the sections.
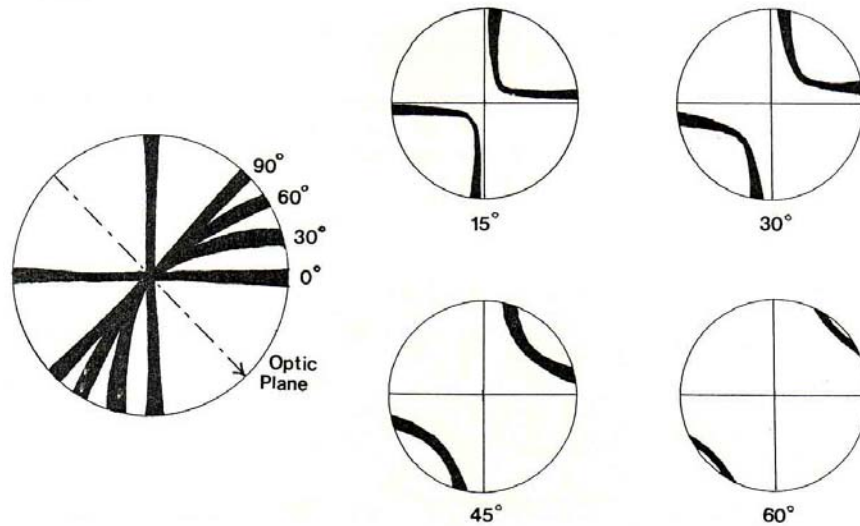
Figure 5.0: Visual estimation of 2V angle from an
optic axis figure (left) and an acute bisectrix
figure (right) (Phillips, 1971).

5.1 DC 2 (Plate 5.0)

TEXTURE:	Intergranular, Interstitial, Sub-ophitic.
GRAIN SIZE:	Fine grained.
PLAGIOCLASE:	Plagioclase constitutes 55.8% of the section and forms laths up to 0.5 mm long, often showing zoning and also albite and carlsbad twinning. They have low relief and are colourless in P.P.L.
CLINOPYROXENE:	Clinopyroxene constitutes 28.6% of the section and occurs as granular aggregates with individual crystals up to 0.1 mm in diameter. They have moderate relief and are pale brown in P.P.L. Under X.P.L. they show interference colours up to second order blues/greens and have inclined extinction. Figure 5.2 is an optic axis figure of augite obtained from the section.
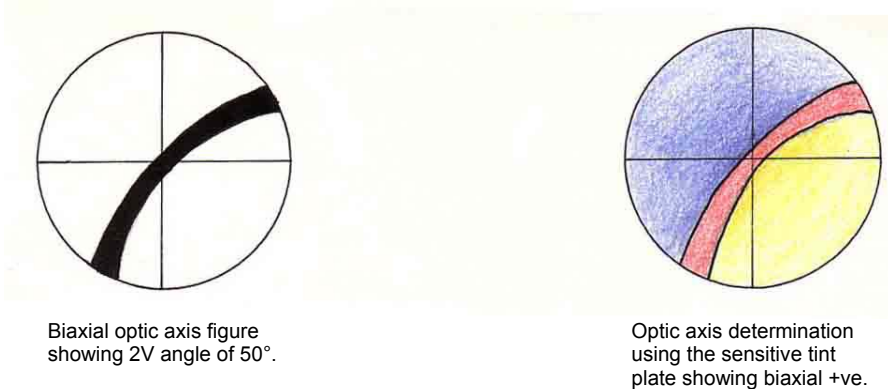
Biaxial optic axis figure
showing 2V angle of 50°.

Optic axis determination
using the sensitive tint
plate showing biaxial +ve.

Figure 5.2: Optic axis figure of augite obtained from slide DC2.

ORTHOPYROXENE: Orthopyroxene constitutes 4.5% of the section and occur as individual grains up to 0.3 mm in length. They show moderate – high relief and are pale – dark brown in P.P.L. In X.P.L. they show straight extinction and interference colours up to first order yellows. They often occur as sub-ophitic grains with plagioclase laths embedded in the crystal sides.
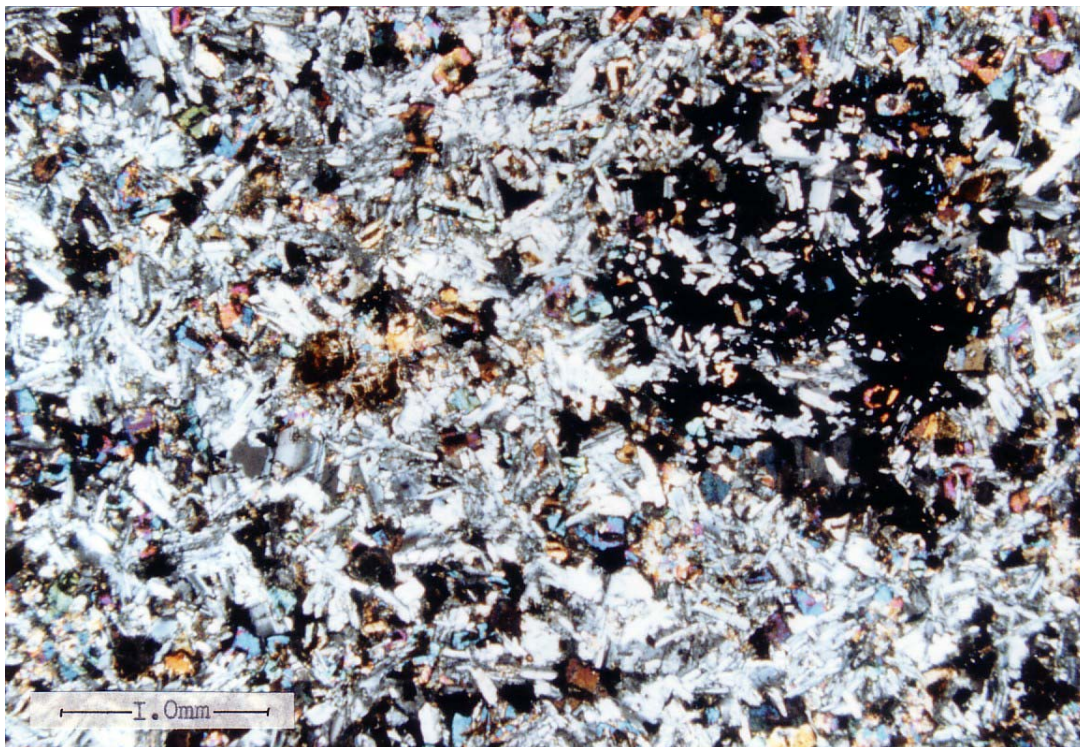
Plate 5.0: Photomicrograph of thin section
DC 2, in X.P.L., showing sulphide 'spot' in the
top right hand corner.

OPAQUES: Fe-Ti oxides occur as individual grains up to 0.2 mm in diameter, sometimes poikolitically enclosing plagioclase laths. Sulphides occur as composite grains up to 3.0 mm in diameter, see photograph 4, and enclose plagioclase and pyroxene crystals. Fe-Ti oxides constitute 5.9% of the section and Sulphides 2.8%.

OITHER MINERALS: Free quartz occurs throughout the slide as interstitial crystals up to 0.1 mm in diameter and constitutes 1.6% of the section. Biotite and apatite also occur as small amounts throughout the section.

5.2 <u>DC 3</u> (Plates 5.1, 5.2)

TEXTURE: Intergranular, Interstitial, Sub-ophitic.
GRAIN SIZE: Fine grained.
PLAGIOCLASE: Plagioclase constitutes 53.6% of the section and forms laths up to 0.6 mm long, often showing zoning and also albite and carlsbad twinning. They have low relief and are colourless in P.P.L.
CLINOPYROXENE: Clinopyroxene constitutes 33.6% of the section and occurs as individual grains up to 0.2 mm in diameter. They have moderate relief and are pale brown in P.P.L. Under X.P.L. they show interference colours up to second order blues/greens and have inclined extinction. Figure 5.2 is an acute bisectrix figure for augite which was obtained in this section.
ORTHOPYROXENE: Orthopyroxene constitutes 3.9% of the section and occurs as individual grains up to 1.0 mm in length. They show moderate – high relief and are pale – dark brown in P.P.L. In X.P.L. they show straight extinction and interference colours up to first

order yellows. Some crystals show signs of alteration to secondary biotite along cleavages.

Biaxial acute bisectrix figure
showing 2V angle of 50°.

Acute bisectrix determination
using the sensitive tint
plate showing biaxial +ve.
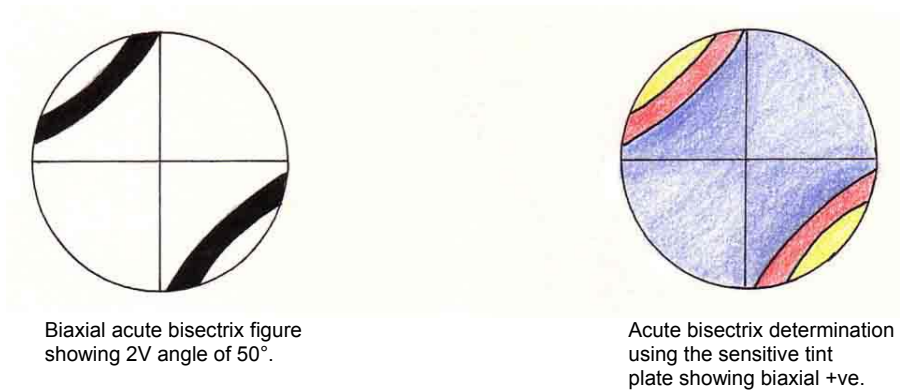
Figure 5.2: Acute bisectrix figure of augite
obtained from slide DC 3.

OPAQUES: Fe-Ti oxides constitute 6.6% of the section and form individual grains up to 0.4 mm in diameter.

OTHER MINERALS: A small amount of interstitial biotite can be observed in the slide, showing pleochrosim in P.P.L. from pale brown to dark brown (0.7%). Free quartz also occurs as interstitial grains and constitutes 1.4% of the section. Apatite needles can also be found throughout the slide.
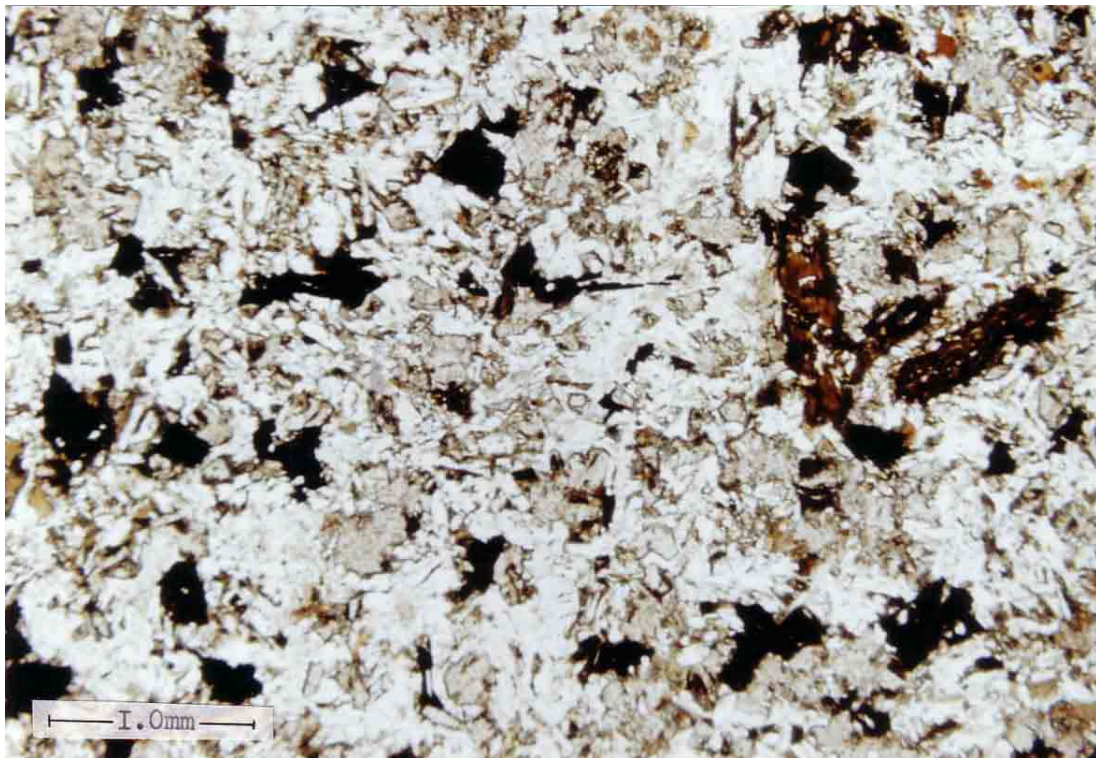
Plate 5.1: Photomicrograph of thin section DC 3, in P.P.L.

Plate 5.2: Photomicrograph of thin section DC 3, in X.P.L.

5.3 DC 4 (Plate 5.3)

TEXTURE:	Intergranular, Interstitial, Sub-ophitic.
GRAIN SIZE:	Fine – medium grained.
PLAGIOCLASE:	Plagioclase constitutes 51.5% of the section and forms laths up to 0.4 mm in length, often showing twinning. They have low relief and are colourless in P.P.L.
CLINOPYROXENE:	Clinopyroxene constitutes 33.4% of the section and occurs as granular aggregates up to 2.0 mm in diameter with individual grains up to 0.3 mm in diameter. They have moderate relief and are pale brown in P.P.L. In X.P.L. they show interference colours up to second order blues and inclined extinction. Figure 5.3 is an optic axis figure of augite obtained from the section.
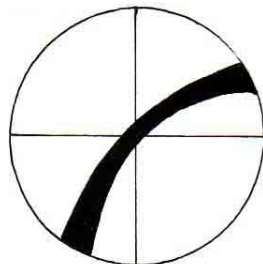
Biaxial optic axis figure
showing 2V angle of 50°.
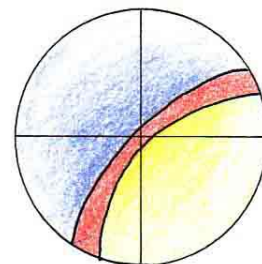
Optic axis determination
using the sensitive tint
plate showing biaxial +ve.

Figure 5.3: Optic axis figure of augite obtained from slide DC 4.

ORTHOPYROXENE:	Orthopyroxene constitutes 5.9% of the section and occurs as individual grains up to 0.8 mm long. They show moderate – high relief and are pale – dark brown in

P.P.L. In X.P.L. they show straight extinction and interference colours up to first order greys/yellows. Most crystals show alteration along cleavages to biotite.

OPAQUES: Fe-Ti oxides constitute 6.6% of the section and occur as individual grains up to 0.6 mm in diameter.

OTHER MINERALS: Free quartz occurs throughout the slide as interstitial grains up to 1.0 mm in diameter and constitutes 1.6% of the section. Biotite also occurs interstitially with grains up to 0.1 mm in diameter and apatite occurs throughout the slide.
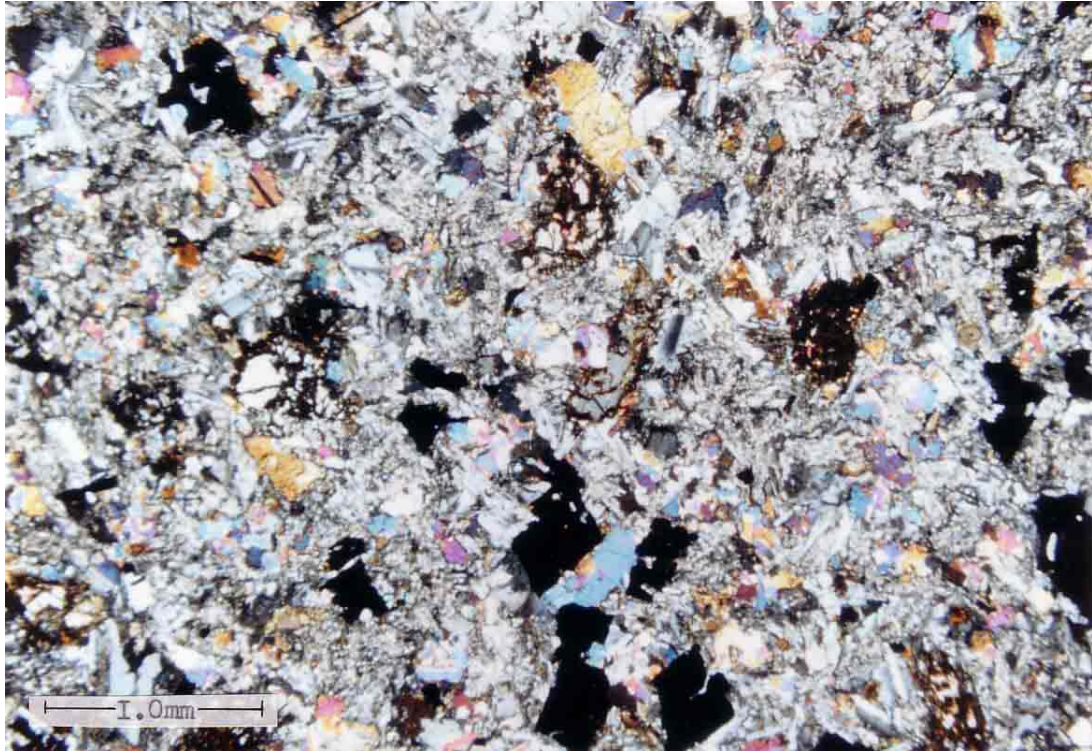

Plate 5.3: Photomicrograph of thin section DC 4 in X.P.L.

5.4 DC 5 (Plates 5.4, 5.5)

TEXTURE: Intergranular, Interstitial, Sub-ophitic.

GRAIN SIZE: Fine – medium grained.

PLAGIOCLASE: Plagioclase constitutes 54.3% of the section and forms laths up to 0.6 mm long. Twinning can be clearly seen, both albite and carlsbad being present. They have low relief and are colourless in P.P.L.

CLINOPYROXENE: Clinopyroxenes constitute 31.8% of the section and occur as individual grains up to 0.5 mm in diameter. They have moderate to high relief and are pale brown in P.P.L. In X.P.L. they show interference colours up to second order blues and show inclined extinction. Figure 5.4 is an optic axis figure obtained from the section showing a 2V angle of approximately 35-40° indicating a subcalcic augite.

ORTHOPYROXENE: Orthopyroxene constitutes 5.4% of the section and occurs as individual grains up to 0.9 mm in length. They have moderate – high relief and are dark brown in P.P.L. Under X.P.L. they show straight extinction and interference colour up to first order yellow.

OPAQUES: Fe-Ti oxides constitute 5.7% of the slide and occur as individual grains up to 0.5 mm in diameter and poikolitically enclose plagioclase.

OTHER MINERALS: Free quartz occurs interstitially as grains up to 0.1 mm in diameter and constitutes 1.9% of the section. Biotite and apatite also occur throughout the slide.

GROUNDMASS: The groundmass occurs as very distinct patches up to 5.0 mm in diameter throughout the slide (see Photographs 8,9). The patches are lacking large crystals and have distinct boundaries.
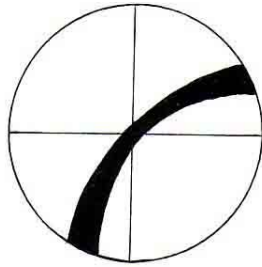
Biaxial optic axis figure
showing 2V angle of 35-40°.
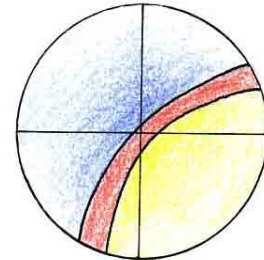
Optic axis determination
using the sensitive tint
plate showing biaxial +ve.

Figure 5.4: Optic axis determination of subcalcic augite from slide DC 5.
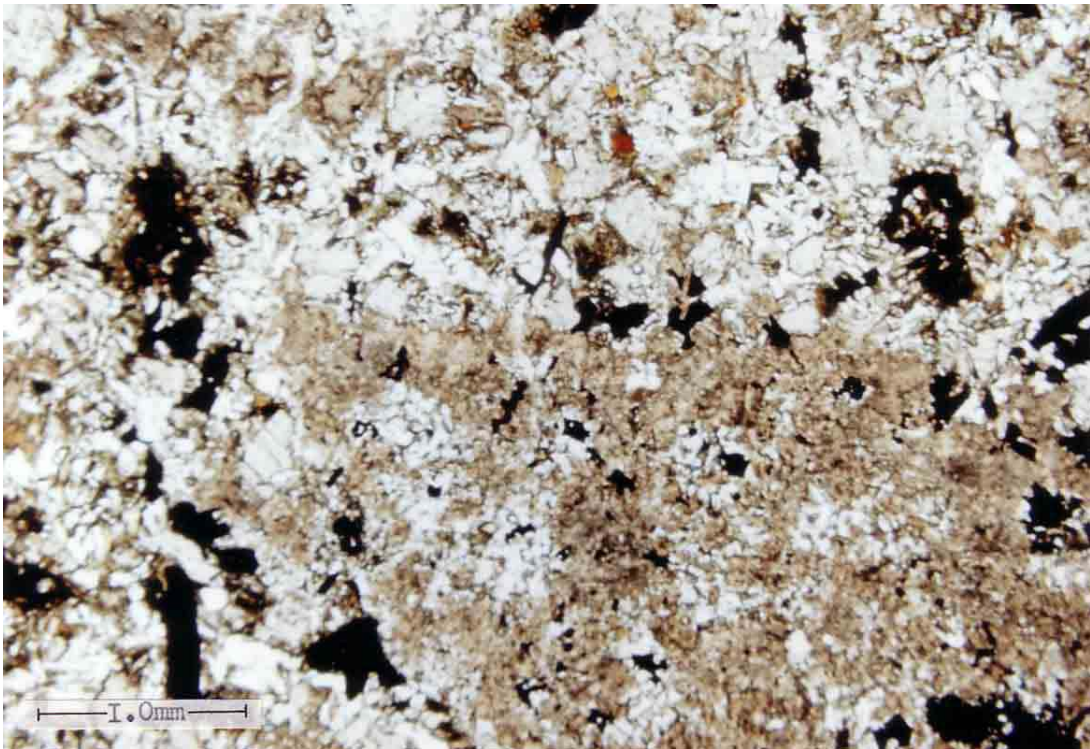
Plates 5.4: Photomicrograph of thin section DC 5, in P.P.L.
showing patch of groundmass (Bottom right of picture).

Plates 5.5: Photomicrograph of thin section DC 5, in X.P.L.
showing patch of groundmass (Bottom right of picture).

5.5 DC 6 (Plates 5.6, 5.7)

TEXTURE:	Porphyritic, Intergranular, Interstitial, Sub-ophitic.
GRAIN SIZE:	Fine grained (excluding phenocrysts).
PLAGIOCLASE:	Plagioclase constitutes 53.7% of the section and occurs both as laths up to 0.3 mm long and phenocrysts up to 3.0 mm long. They show albite twinning and compositional zoning. They have low relief and are colourless in P.P.L. The presence of phenocrysts indicates that crystals were present within the intrusive liquid before cooling.
CLINOPYROXENE:	Clinopyroxene constitutes 36.7% of the section and occurs as individual grains up to 0.2 mm in diameter and also as phenocrysts up to 1.0 mm in length. They have moderate relief and are pale brown in P.P.L. In X.P.L. they show interference colours up to second order blues and show inclined extinction.
ORTHOPYROXENE:	Orthopyroxene constitutes 3.2% of the section as individual grains up to 0.2 mm long. They show moderate – high relief and are pale – dark brown in P.P.L. They show straight extinction and interference colours up to first order yellow in X.P.L. They often show alteration to biotite along cleavages.
OPAQUES:	Fe-Ti oxides constitute 4.7% of the section and occur as individual grains up to 0.1mm in diameter.
OTHER MINERALS:	Free quartz occurs interstitially, as does biotite. Apatite occurs throughout the slide as fine needles.

5.6 DC 8 (Plate 5.8)

TEXTURE:	Glomeroporphyritic, Intergranular, Interstitial, Sub-ophitic.
GRAIN SIZE:	Fine grained (excluding phenocrysts).

Plates 5.6, 5.7: Photomicrographs of thin section
DC 6 in P.P.L. (top) and X.P.L. (bottom), showing
porphyritic texture and zoning/twinning in plagioclase.

PLAGIOCLASE: Plagioclase constitutes 57.6% of the section and forms as laths up to 0.2 mm in length and microphenocryst clusters up to 1.5 mm in length. They show albite twinning and zoning in X.P.L., and are colourless with low relief in P.P.L. The presence of clustered microphenocrysts in the section indicates that crystals were present in the liquid before final cooling took place, mobility allowing them to form into clusters.

CLINOPYROXENE: Clinopyroxene constitutes 30.9% of the section and occurs as grains up to 0.2 mm in diameter. They have moderate relief and are pale brown in P.P.L. In X.P.L. they show interference colours up to second order blues and have inclined extinction.

Plate 5.8: Photomicrograph of thin section
DC 8, showing clusters of microphenocrysts enclosed
by a fine grained intergranular, interstitial and
sub-ophitic groundmass (X.P.L.).

ORTHOPYROXENE: Orthopyroxene constitutes 1.2% of the section and occurs as individual grains up to 0.2 mm in length. They show moderate – high relief and are pale – dark brown in P.P.L. They show straight extinction and interference colours up to first order yellow and grey.

OPAQUES: Fe-Ti oxides constitute 8.6% of the section and occur as individual grains up to 0.1 mm in diameter.

OTHER MINERALS: Quartz and biotite occur interstitially in the groundmass, constituting 1.3% and 0.2% respectively.

5.7 DC 10 (Plates 5.9, 5.10)

TEXTURE: Intergranular, Interstitial, Sub-ophitic, Poikolitic.
GRAIN SIZE: Medium grained.
PLAGIOCLASE: Plagioclase constitutes 53.4% of this section and forms a sub-ophitic mesh of laths up to 1.0 mm in length. They show albite and carlsbad twinning and zoning, and are colourless with low relief in P.P.L.

CLINOPYROXENE: Clinopyroxene forms granular aggregates and constitutes 36.3% of the section with individual grains up to 1.0 mm in diameter. They have moderate relief and are pale brown in P.P.L. In X.P.L. they show interference colours up to second order b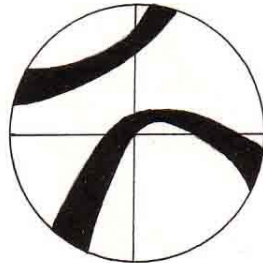lues and have inclined extinction. Some of the crystals show twinning as can clearly be seen in photograph 13. Figure 5.5 is an off-centred acute bisectrix figure, figures 5.6 and 5.7 are optic axis figures obtained from the section.

Off-centre biaxial acute
bisectrix showing
2V angle of 50°.
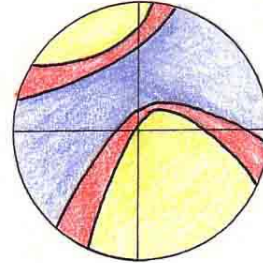
Off-centred acute bisectrix
determination using the
Sensitive tint plate, showing
biaxial +ve.

Figure 5.5: Off-centred acute bisectrix
figure of augite obtained from thin section DC 10.
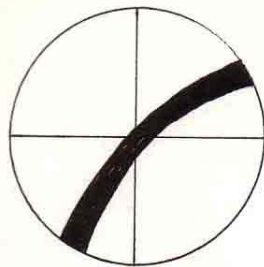
Biaxial optic axis figure
showing 2V angle of 50°.
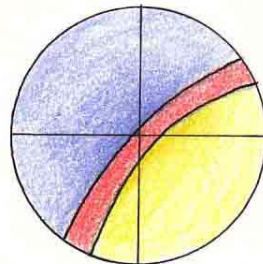
Optic axis determination
using the sensitive tint
plate showing biaxial +ve.

Figure 5.6: Optic axis figure of augite
obtained from thin section DC 10.
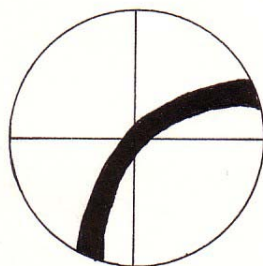
Biaxial optic axis figure
showing 2V angle of 35°.
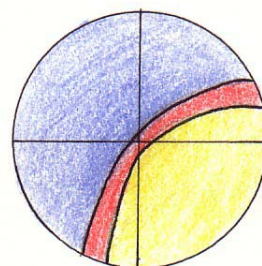
Optic axis determination
using the sensitive tint
plate showing biaxial +ve.

Figure 5.7: Optic axis figure of subcalcic
augite obtained from thin section DC 10.
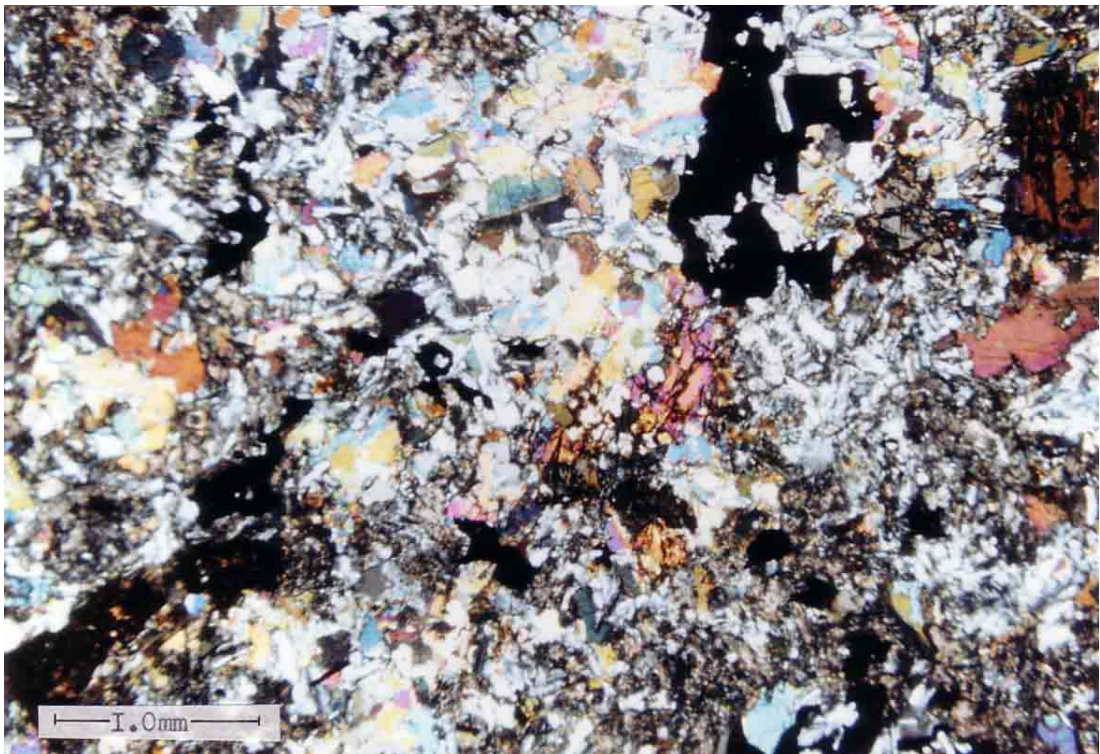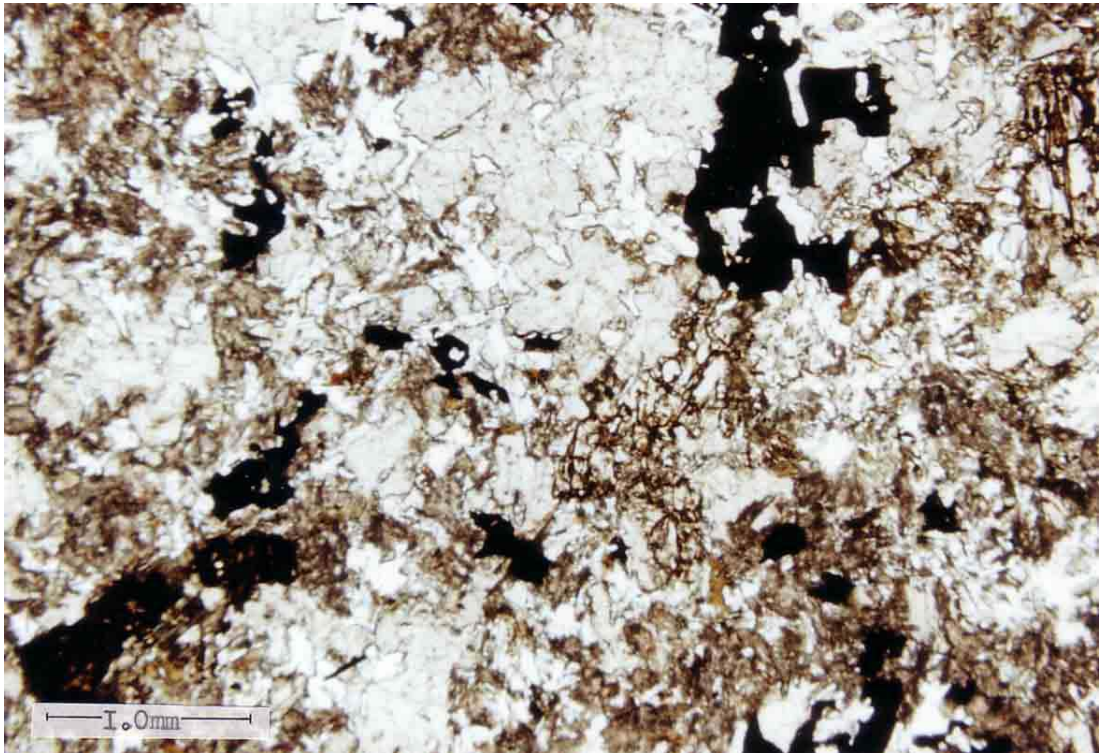
Plates 5.9, 5.10: Photomicrographs of thin section DC 10 (P.P.L. top, X.P.L. bottom).
The differences in relief between the plagioclase, clinopyroxene and orthopyroxene
can clearly be seen in the top (P.P.L.) picture.

ORTHOPYROXENE: Orthopyroxene constitutes 3.7% of the section and occurs as individual grains up to 1.0 mm in diameter and show alteration effects in various degrees. They have moderate – high relief and are pale – dark brown in P.P.L. They show straight extinction and interference colours up to first order yellows.

OPAQUES: Fe-Ti oxides occur as grains up to 1.5 mm in diameter and constitute 4.0% of the section. They commonly poikolitically enclose plagioclase laths.

OTHER MINERALS: Free quartz occurs interstitially and constitutes 1.6% of the section. Biotite can also be seen throughout the section and constitutes 0.7%. Elongate apatite needles occur throughout the slide.

5.8 DC 12 (Plates 5.11, 5.12)

TEXTURE: Intergranular, Interstitial, Sub-ophitic, Poikolitic, Granophyric.
GRAIN SIZE: Very coarse grained.
PLAGIOCLASE: Plagioclase feldspar constitutes 59.0% of this thin section and forms laths up to 3.0 mm in length and also occurs as a micrographic intergrowth with quartz (See photographs 15, 16 [centre]). It is colourless with low relief in P.P.L.
CLINOPYROXENE: Clinopyroxene constitutes 24.6% of the section and forms prominent bladed laths up to 6.0 mm in length (See photographs 15, 16 [top]). The laths have moderate relief and interference colours up to second order blues/reds, inclined extinction and simple twinning. Figure 5.8, below, is an optic axis figure of augite obtained from the thin section.
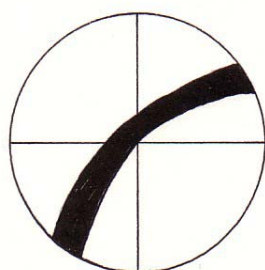
Biaxial optic axis figure
showing 2V angle of 40°.
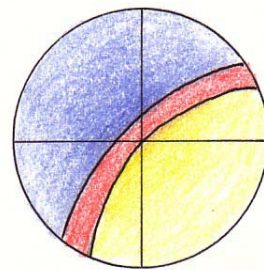
Optic axis determination
using the sensitive tint
plate showing biaxial +ve.

Figure 5.8: Optic axis figure of augite
obtained from thin section DC 12.

ORTHOPYROXENE: Orthopyroxene constitutes 4.3% of the thin section and occurs as small phenocrysts up to 2.0 mm in length which are altered, peripherally and along cleavage cracks to green or brown Fe-talc. They have moderate – high relief and are pale brown – green in P.P.L. They show straight extinction and interference colours up to first order yellow.

OPAQUES: Fe-Ti oxides constitute 5.9% of the section and occur as large dendritic crystals up to 3.0 mm in diameter, sometimes poikolitically enclosing plagioclase and quartz.

OTHER MINERALS: Quartz constitutes 4.4% of the section and also occurs as micrographic intergrowths with plagioclase and also interstitially. Biotite occurs as tiny fragments and elongate apatite needles occur throughout the section up to 0.3 mm in length (See photograph 3).

### 5.9 DC 14 (Plate 5.13)

TEXTURE: Intergranular, Interstitial, Sub-ophitic, Poikolitic.
GRAIN SIZE: Fine grained.
PLAGIOCLASE: Plagioclase constitutes 59.8% of the section and occurs as laths up to 0.3 mm in length. They are colourless and have low relief in P.P.L.
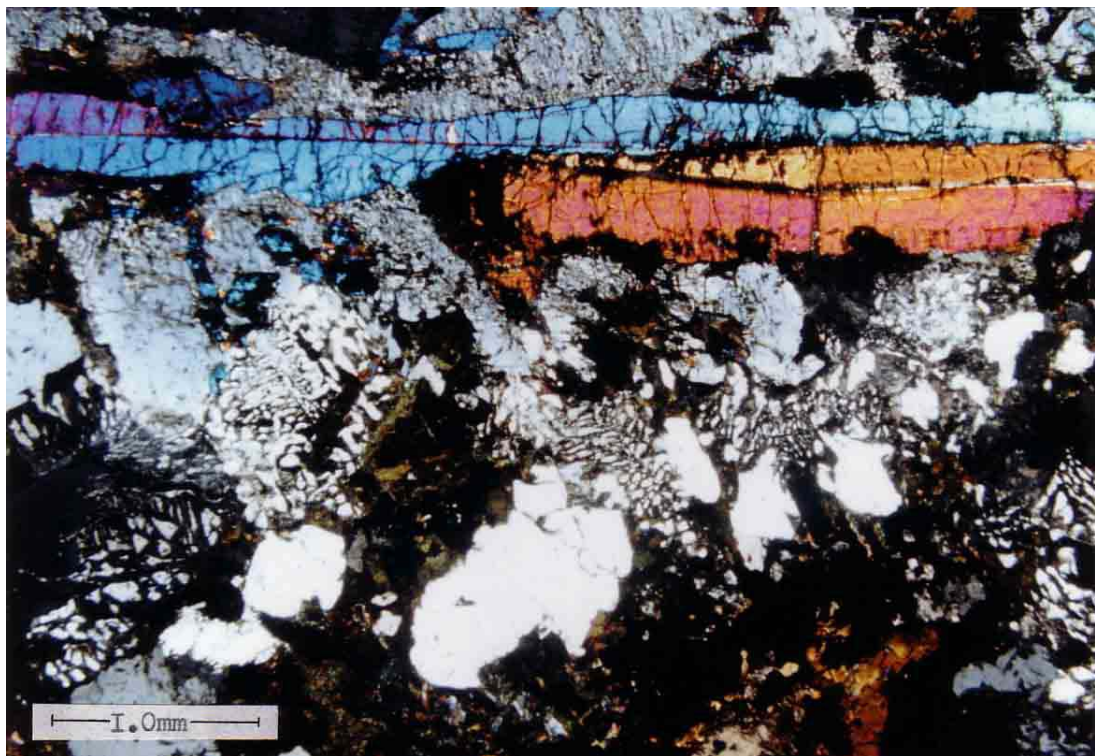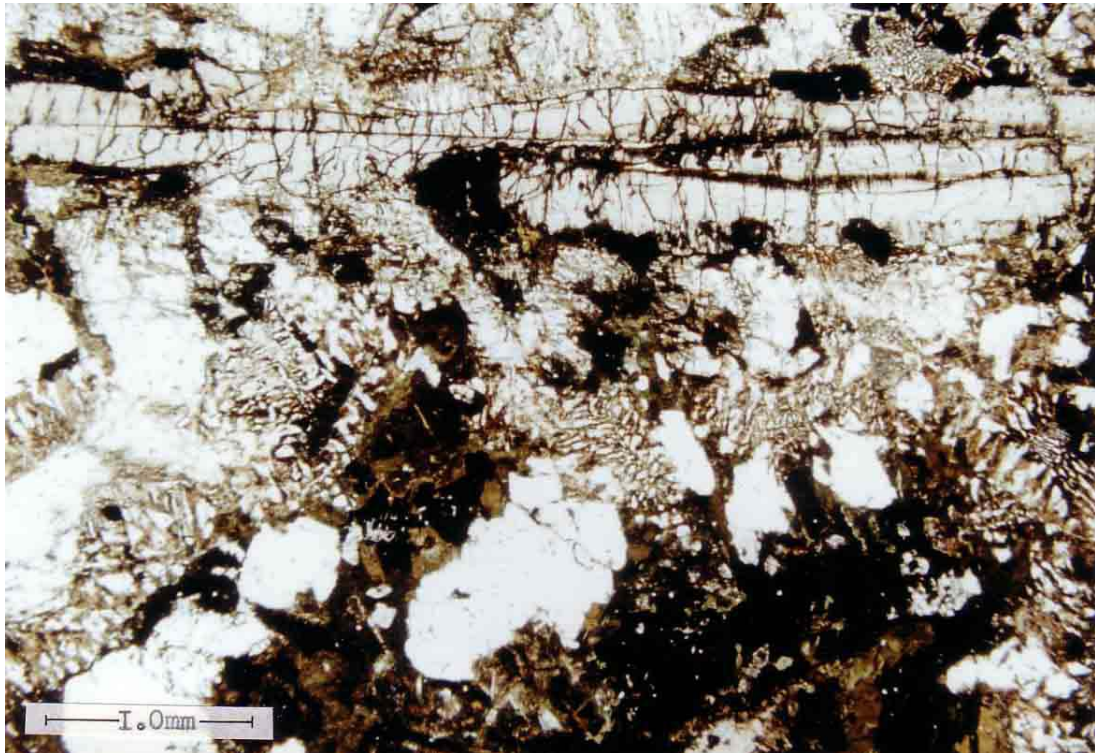
Plates 5.11, 5.12: Photomicrographs of thin section DC 12 (P.P.L. top, X.P.L. bottom).
The section is typical coarse grained dolerite pegmatite and shows a prominent bladed
clinopyroxene crystal (top) and micrographic intergrowths of plagioclase and quartz (centre).

CLINOPYROXENE:	Clinopyroxene occurs as grains up to 0.3 mm in diameter and constitutes 32.6% of the section. They have moderate relief and are pale brown in P.P.L. In X.P.L. they show interference colours up to second order blues and have inclined extinction.
ORTHOPYROXENE:	Orthopyroxene constitutes 1.2% of the thin section and occurs as rare phenocrysts up to 0.8 mm in length. They show moderate – high relief and are pale – dark brown in P.P.L. In X.P.L. they show straight extinction and interference colours up to first order yellow.
OPAQUES:	Fe-Ti oxides occur as poikilitic grains up to 0.7 mm in diameter and individual grains up to 0.3 mm in diameter.
OTHER MINERALS:	Quartz and biotite both occur in small amounts throughout the section as interstitial crystals and apatite needles also occur throughout the section.

Plate 5.13: Photomicrograph of thin section DC 14 in X.P.L.

5.10 DC 15 (Plate 5.14)

TEXTURE:	Intergranular, Interstitial, Sub-ophitic.
GRAIN SIZE:	Fine grained.
PLAGIOCLASE:	Plagioclase constitutes 59.3% of the section and occurs as laths up to 0.2 mm in length which are colourless and show low relief in P.P.L. In X.P.L. they show simple twinning.
CLINOPYROXENE:	Clinopyroxene constitutes 29.0% of the section and occurs as interstitial grains up to 0.2 mm in diameter. In X.P.L. hey show interference colours up to second order blue.
ORTHOPYROXENE:	Orthopyroxene constitutes 2.7% of the section and occurs as individual crystals up to 0.2 mm in length. In X.P.L. they show straight extinction and interference colours up to first order yellow.
OPAQUES:	Fe-Ti oxides occur as individual interstitial grains up to 0.2 mm in diameter and constitute 6.9% of the section.
OTHER MINERALS:	Quartz, biotite and apatite occur in small amounts throughout the section.

Plate 5.14: Photomicrograph of thin section DC 15 in X.P.L.

5.11 <u>DC 17</u> (Plates 5.15, 5.16)

TEXTURE:	Intergranular, Interstitial, Sub-ophitic.
GRAIN SIZE:	Fine grained.
PLAGIOCLASE:	Plagioclase constitutes 54.9% of the thin section and occurs as laths up to 0.5 mm in length. They often show twinning and zoning in X.P.L. and occur as colourless crystals with low relief in P.P.L.
CLINOPYROXENE:	Clinopyroxene occurs as individual grains up to 0.3 mm in diameter and constitutes 31.8% of the section. They have moderate relief and are pale brown in P.P.L. In X.P.L. they show interference colours up to second order blues and inclined extinction.
ORTHOPYROXENE:	Orthopyroxene constitutes 2.4% of the thin section and occurs as grains up to 0.2 mm in length. They show moderate – high relief and are pale – dark brown in colour in P.P.L. In X.P.L. they show straight extinction and interference colours up to first order yellows.
OPAQUES:	Fe-Ti oxides constitute 6.7% of the section and occur as individual grains up to 0.2 mm in diameter, sometimes poikolitically enclosing plagioclase laths.
OTHER MINERALS:	Free quartz occurs interstitially and constitutes 2.7% of the section. Biotite occurs in small mounts as fine grains and as an alteration product of orthopyroxene. Very fine apatite needles occur throughout the section.

5.12 <u>DC 18</u> (Plate 5.17)

TEXTURE:	Intergranular, Interstitial, Sub-ophitic, Porphyritic.
GRAIN SIZE:	Fine – medium grained.
PLAGIOCLASE:	Plagioclase constitutes 51.7% of the thin section and occurs both as laths up to 0.5 mm in length and as phenocrysts up to 1.0 mm in length. They show albite twinning and compositional zoning in X.P.L. The presence of these phenocrysts indicates that crystals were present in the intrusive liquid before final cooling took place.

Plates 5.15, 5.16: Photomicrographs of thin section
DC 17, in P.P.L. (top) and X.P.L. (bottom).

CLINOPYROXENE: Clinopyroxene constitutes 32.2% of the thin section and occurs as individual grains up to 0.1 mm in diameter. They have moderate relief and are pale brown in P.P.L. In X.P.L. they show interference colours up to second order blues and have inclined extinction.

ORTHOPYROXENE: Orthopyroxene constitutes 2.8% of the section and occurs as individual grains up to 0.1 mm in length. They show moderate – high relief and are pale – dark brown in P.P.L. In X.P.L. they show interference colours up to first order yellow with straight extinction.
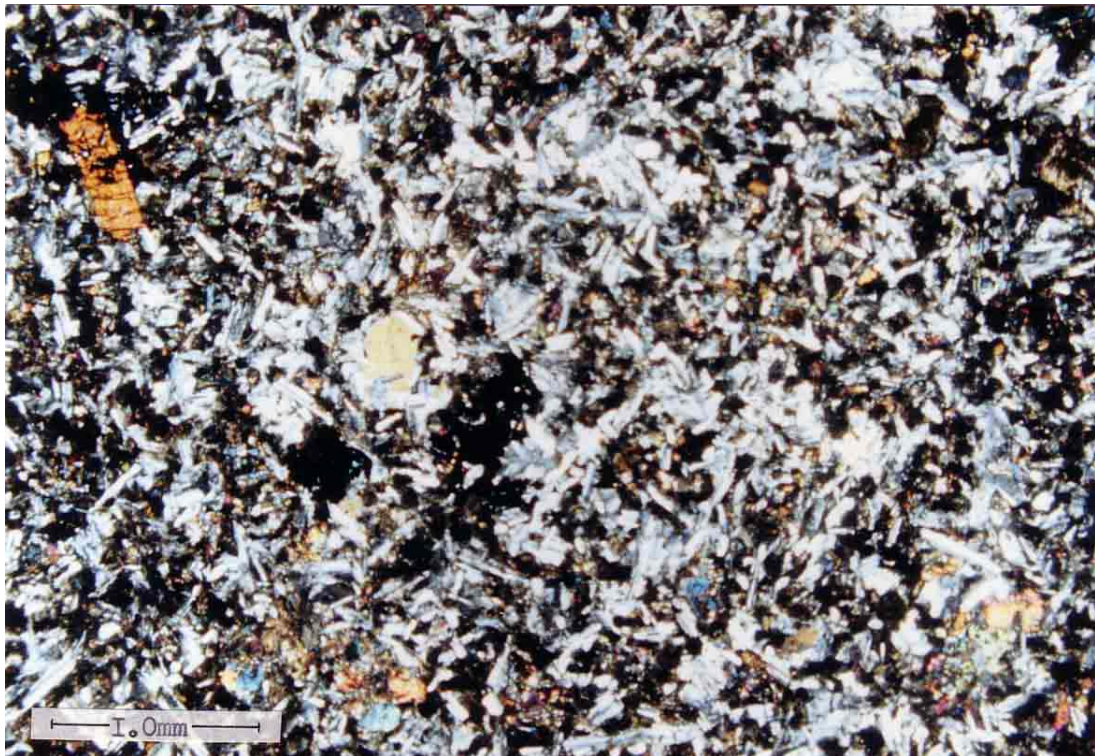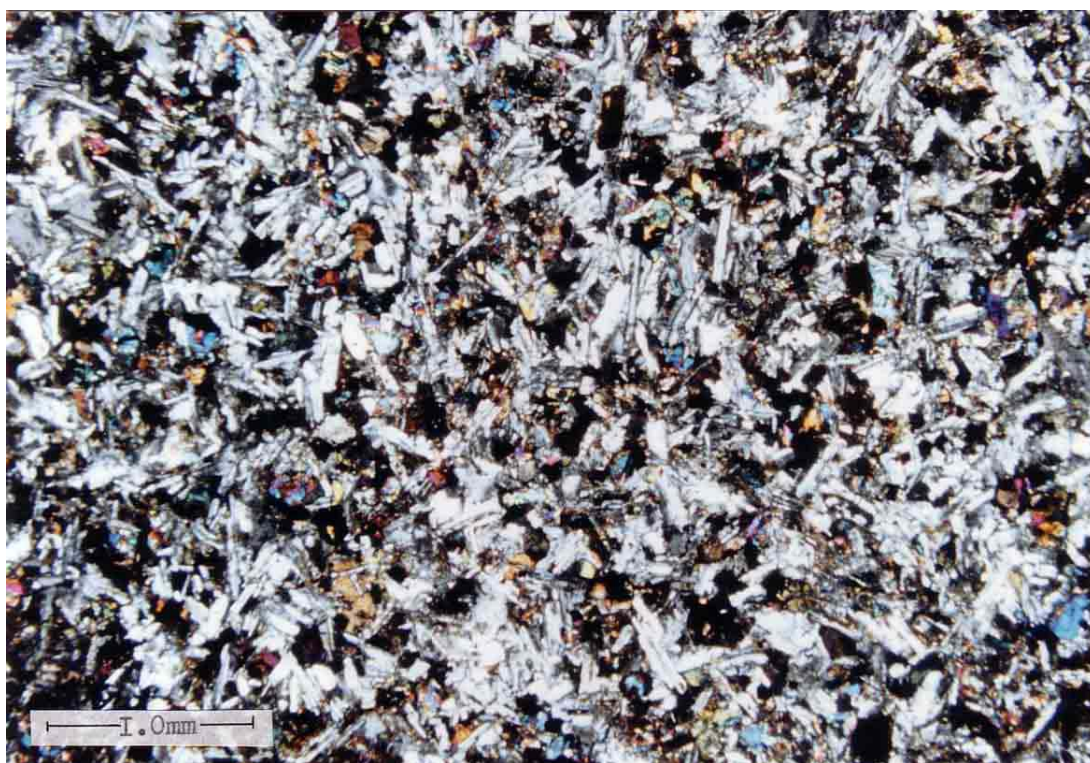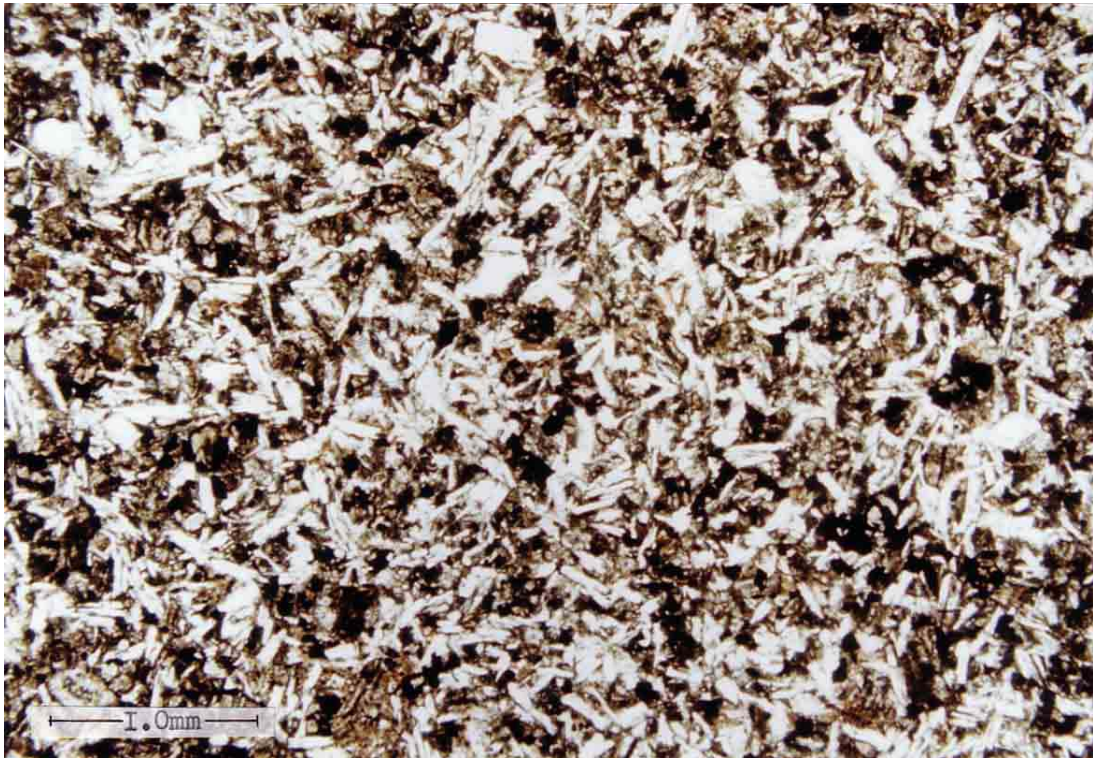

Plate 5.17: Photomicrograph of thin section DC 18 in X.P.L.

5.13 DC 19 (Plates 5.18, 5.19)

TEXTURE: Intergranular, Interstitial, Sub-ophitic, Poikolitic.
GRAIN SIZE: Medium grained.
PLAGIOCLASE: Plagioclase constitutes 55.0% of this section and forms as sub-ophitic laths up to 0.9 mm in length. They show both carlsbad and albite twinning and also compositional zoning in X.P.L. In P.P.L. they are colourless with low relief.
CLINOPYROXENE: Clinopyroxene constitutes 32.1% of the section and occurs as granular aggregates with individual grains up to 0.8 mm in diameter. They have moderate relief and are pale brown in P.P.L. In X.P.L. they show interference colours up to second order blue and exhibit inclined extinction and simple twinning.
ORTHOPYROXENE: Orthopyroxene constitutes 4.6% of the section and occurs as individual crystals up to 1.0 mm in length, partially enclosing plagioclase laths. They have moderate – high relief and are pale – dark brown in P.P.L. they show straight extinction and interference colours up to first order yellow in X.P.L.
OPAQUES: Fe-Ti oxides constitute 6.5% of the section and occur as interstitial grains up to 1.0 mm in diameter.
OTHER MINERALS: Free quartz occurs interstitially and constitutes 1.1% of the section. Biotite also occurs as an alteration product of orthopyroxene and fine apatite needles occur throughout the section.
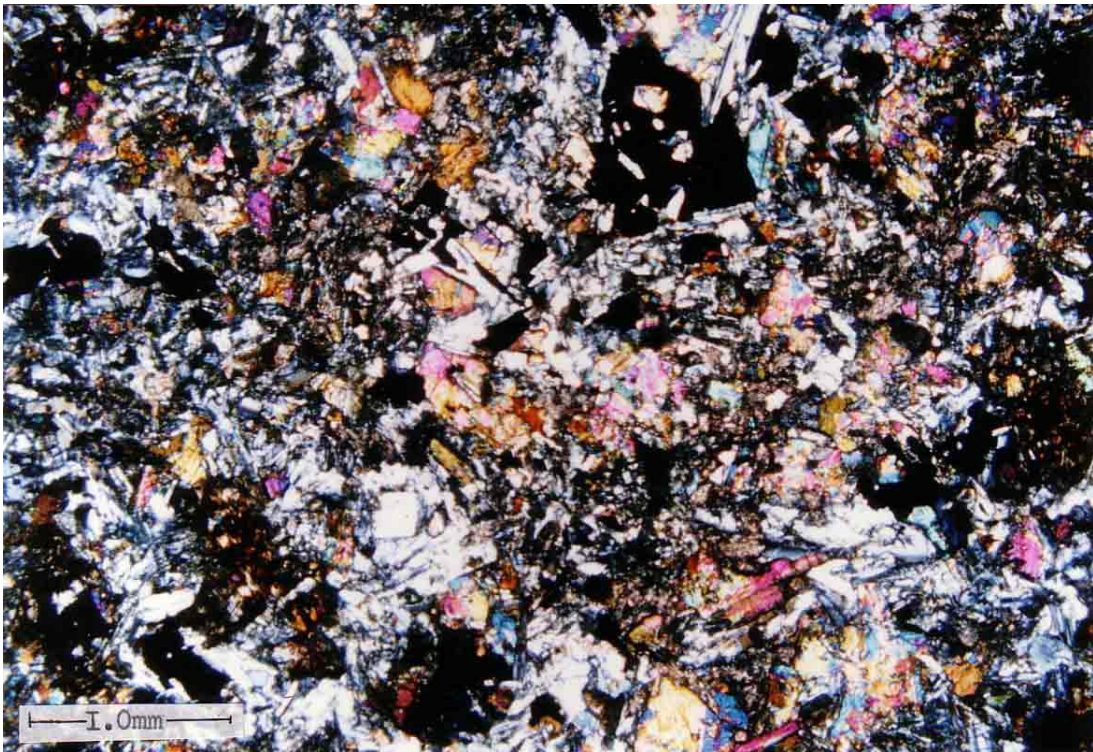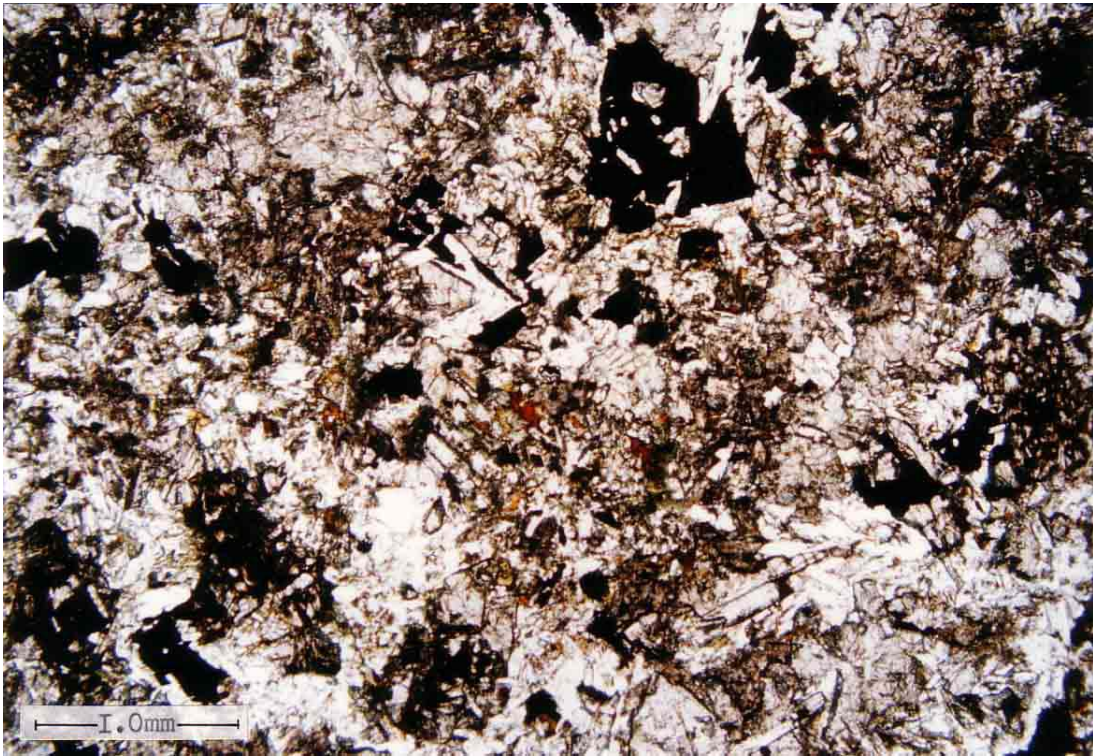
Plates 5.18, 5.19: Photomicrographs of thin section
DC 19 in P.P.L. (top) and X.P.L. (bottom).

6.0   ANALYSES

6.1 Grain Size Analysis

Grain size data, shown in Table 6.0, has been taken from each thin section and consists of average crystal grain size (mm) and average microphenocryst grain size (where applicable). For both plagioclase laths and orthopyroxene crystals the grain size is determined from the long axis of the grain, whereas clinopyroxene grain size is determined from the average diameter of the grain.

Table 6.0

Sample	Plagioclase		Clinopyroxene		Orthopyroxene		Opaques
	Average Grain Size (mm)	Micro-phenol-crysts (mm)	Average Grain Size (mm)	Micro-phenol-crysts (mm)	Average Grain Size (mm)	Micro-phenol-crysts (mm)	Average Grain Size (mm)
DC 2	0.4	-	0.1	-	0.2	-	0.2
DC 3	0.5	-	0.2	-	0.4	1.0	0.4
DC 4	0.4	-	0.3	-	0.8	-	0.5
DC 5	0.5	-	0.5	-	0.8	-	0.5
DC 6	0.2	3.0	0.2	1.0	0.2	-	0.1
DC 8	0.2	1.0	0.2	-	0.2	-	0.1
DC 10	0.6	-	0.8	-	1.0	-	1.0
DC 12	3.0	-	6.0	-	2.0	-	3.0
DC 14	0.3	-	0.3	-	0.2	0.8	0.2
DC 15	0.2	-	0.2	-	0.2	-	0.2
DC 17	0.4	-	0.3	-	0.2	-	0.2
DC 18	0.4	1.0	0.1	-	0.1	-	0.2
DC 19	0.6	-	0.8	-	1.0	-	1.0

For plagioclase, clinopyroxene, orthopyroxene and opaque minerals, vertical profiles of average grain sizes have been plotted against the section of the Whin Sill and are shown in figure 6.0, overleaf.

As can be seen from the vertical profiles, average grain sizes of all the minerals measured show slight variations, clinopyroxenes varying from0.1 mm to 0.8 mm, plagioclase from 0.2 mm to 0.6 mm, orthopyroxenes from 0.2 mm to 1.0 mm and opaque oxides from 0.1 mm to 1.0 mm. As would be expected all of the grin size data increases towards the centre of the sill due to chilling along the margins and residual liquid at the centre of the sill crystallizing to form coarse grained pegmatite. The 'kinks' produced in all the profiles are from samples taken in the River Lune exposure (See section 3.1). The consistently finer nature of these samples is possibly due to the thinning of the Whin Sill as it nears the Lunedale Fault.

6.2 Modal Analysis

Modal data, shown in Table 6.1, are based on 2000 points in each thin section. Because the rock is fine to medium-grained and fairly homogenous, this number is considered satisfactory to give a reasonable estimate of the mineral proportions.

Figure 6.1 shows a sketch section through the Whin Sill and vertical profiles for the modal analysis of plagioclase, pyroxenes, ore minerals, quartz and biotite at the sample locations.
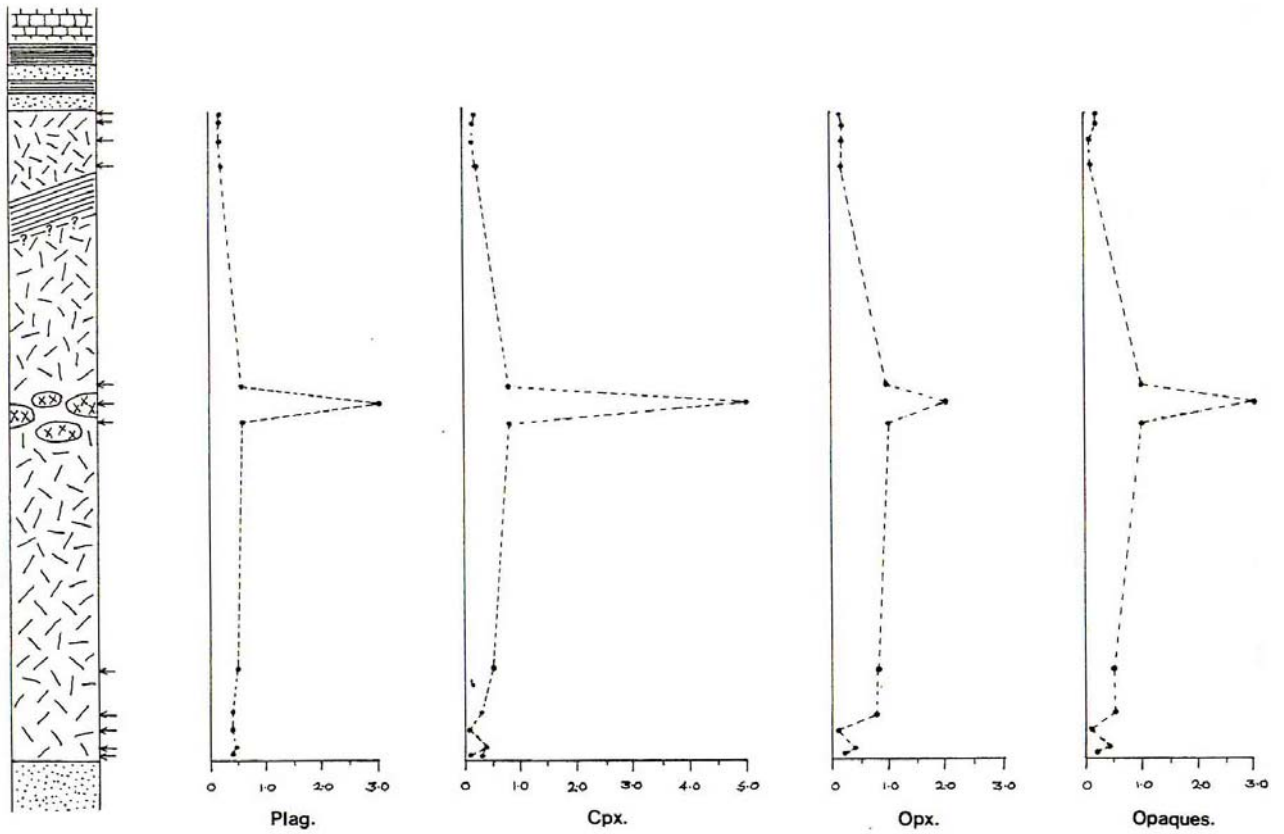
Figure 6.0: Vertical profiles for average grain sizes of
Plagioclase, clinopyroxene, orthopyroxene and opaque minerals.

Table 6.1

Sample	Plagioclase	Clinopyroxene	Orthopyroxene	Ore Minerals	Quartz	Biotite
DC 2	55.8%	28.6%	4.5%	8.7% *	1.6%	0.5%
DC 3	53.6%	33.6%	3.9%	6.6%	1.4%	0.7%
DC 4	51.5%	33.4%	5.9%	6.6%	1.6%	0.8%
DC 5	53.4%	31.8%	5.4%	5.7%	1.9%	1.6%
DC 6	53.7%	36.7%	3.2%	4.7%	0.5%	1.1%
DC 8	57.6%	30.9%	1.2%	8.6%	1.3%	0.2%
DC 10	53.4%	36.3%	3.7%	4.0%	1.6%	0.7%
DC 12	59.0%	24.6%	4.3%	4.9%	4.4%	1.7%
DC 14	59.8%	32.6%	1.2%	4.8%	0.9%	0.5%
DC 15	59.3%	29.0%	2.7%	6.9%	1.2%	0.8%
DC 17	54.9%	31.8%	2.4%	6.7%	2.7%	1.2%
DC 18	51.7%	32.2%	2.8%	11.6%	1.0%	0.7%
DC 19	55.0%	32.1%	4.6%	6.5%	1.1%	0.7%
Average	55.3%	31.7%	3.5%	6.7%	1.5%	1.3%

* 2.8% were determined as Sulphides, 5.9% as Fe-Ti Oxides.
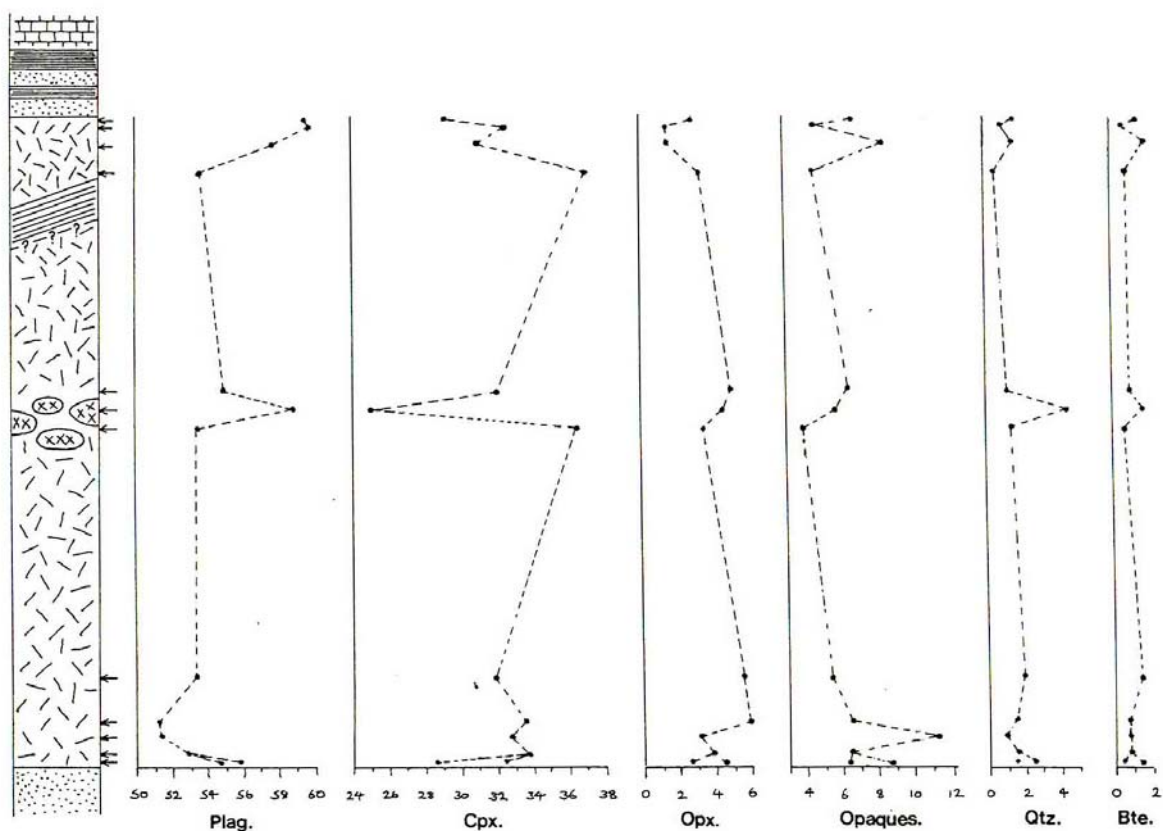
Figure 6.1: Vertical profiles for the mineral proportions of plagioclase,
pyroxenes, ore minerals, quartz and biotite.

The vertical profiles of mineral proportions show distinct trends towards both upper and lower contacts. The increase in the percentage of plagioclase present may be due to crystal settling towards the lower contact or crystals floating towards the upper contact. The idea of crystal settling of sulphides has been discussed earlier (See section 4.5) and this may account for the increase in opaques towards the base of the sill, this result is consistent with Dunham and Strasser-King (1981). The percentage of quartz present does not vary markedly although slight increases towards the contacts may be due to contamination from the surrounding metaquartzite contact rocks. Biotite shows no real systematic variation with placement in the sill as it occurs in such small quantities (<2%) and often as a secondary product of orthopyroxene.

6.3 Major Chemical Analyses

Major and trace element analyses were produced by atomic absorption spectrophotometry and colorimetry from samples DC 2, DC 3, DC 4, DC 5, DC 6, DC 8, DC 12, DC 14, DC 18 and DC 19 as these samples produced the most consistent results from the modal and grain size analyses.

The sample is firstly cut into thin pieces, taking care to ensure that all the pieces are fresh and unaltered, using a diamond saw. The pieces are broken into fragments using a hammer and then reduced to small chips using a jaw crusher. The chips are then sieved and cleaned using acetone and upon drying are ground to a very fine powder using a Fritsch Pulverisette grinder. To avoid any contamination between samples all of the equipment is thoroughly cleaned using acetone.

The major element analyses are produced from a solution of 100 mg of rock dissolved in 200 ml of solution. SiO_2, Al_2O_3 and MnO are determined directly from the solution by atomic absorption (AA) and TiO_2 and P_2O_5 by colorimetry, whereas CaO, MgO, Na_2O, K_2O, Fe_2O_3 and FeO are determined by AA from diluted solution. The AA is calibrated using 'synthetic standard solutions' and errors are detected by the use of 'international standard rocks'. The elements are then converted to weight percent in one sample. A carefully weighed 1 g sample is ignited at 1000°C for one hour and the weight change is represented as total loss of ignition (tot. LOI).

The results obtained by major chemical analyses are shown in Table 6.2, and vertical profiles for all of the elements have been plotted and can be seen in figures 6.2, 6.3 and 6.4.

Table 6.2

	DC 2	DC 3	DC 4	DC 5	DC 6	DC 8	DC 12	DC 14	DC 18	DC 19
SiO_2	52.27	51.12	51.37	50.75	50.87	51.33	54.07	50.48	51.30	49.91
Al_2O_3	14.48	13.45	14.10	14.06	14.36	14.50	13.20	14.27	13.69	14.45
Fe_2O_3	3.27	4.04	4.15	4.60	4.19	3.31	3.84	3.50	3.10	4.23
FeO	9.15	8.66	8.40	8.20	8.46	8.98	9.75	8.92	9.13	8.60
MgO	4.91	5.57	4.91	5.43	5.47	4.75	2.40	5.55	5.80	6.04
CaO	8.07	8.83	6.69	7.74	8.74	7.93	6.16	8.36	8.37	8.32
Na_2O	2.16	2.27	2.41	2.60	2.38	2.43	3.29	2.33	2.48	2.52
K_2O	0.54	0.93	2.20	1.89	0.90	0.76	1.61	0.76	0.81	1.25
TiO_2	2.60	2.66	2.61	2.55	2.58	2.49	2.29	2.54	2.53	2.57
MnO	0.17	0.15	0.16	0.15	0.14	0.16	0.15	0.15	0.15	0.15
P_2O_5	0.29	0.28	0.28	0.29	0.29	0.29	0.80	0.28	0.30	0.29
Tot LOI	2.54	2.13	2.30	2.31	2.13	2.54	2.64	2.60	2.61	1.81
Total %	+0.44	+0.07	-0.02	+0.56	+0.56	-0.54	+0.19	-0.25	+0.28	+0.12

Although the differences in the major chemical element data between the samples is very small, it is interesting to note the almost symmetrical array of the contact data around the normal Whin Sill values recorded from sample DC 19. The increase in SiO_2 towards the contacts confirms with the modal increase of quartz grains towards the contacts that there may have been some form of contamination on intrusion from the surrounding country rock. Na_2O and K_2O both decrease towards the contacts whilst total loss on ignition increases away from the centre. There is thus, perhaps, some slight indication of magmatic differentiation, with separation towards both upper and lower contacts of a more acidic magma, or some form of contamination from the contact rocks.

The coarse-grained, patchy dolerite pegmatite (DC 12) shows markedly different chemical compositions to that of the surrounding medium grained normal dolerite (DC 19) and may have been formed by a function of volatile concentration in the last stages of crystallization. The boundary line between the coarse- and medium-grained rock is always sharp and well defined, as shown in plates 6.0 and 6.1 taken from sample DC 11, the transition from one variety into the other being perfectly continuous.

Magmatic differentiation can be illustrated by the use of the triangular A.F.M diagram, Na_2O+K_2O – $FeO+Fe_2O_3+MnO$ – MgO. As can be seen on the diagram (Figure 6.5) the points for the Whin Sill fall into a small cluster showing a degree of iron enrichment. Dunham and Kaye (1965) state that 'The bulk of the Whin Sill analyses show a degree of iron enrichment similar to thick sills, though less extreme than large layered intrusions.
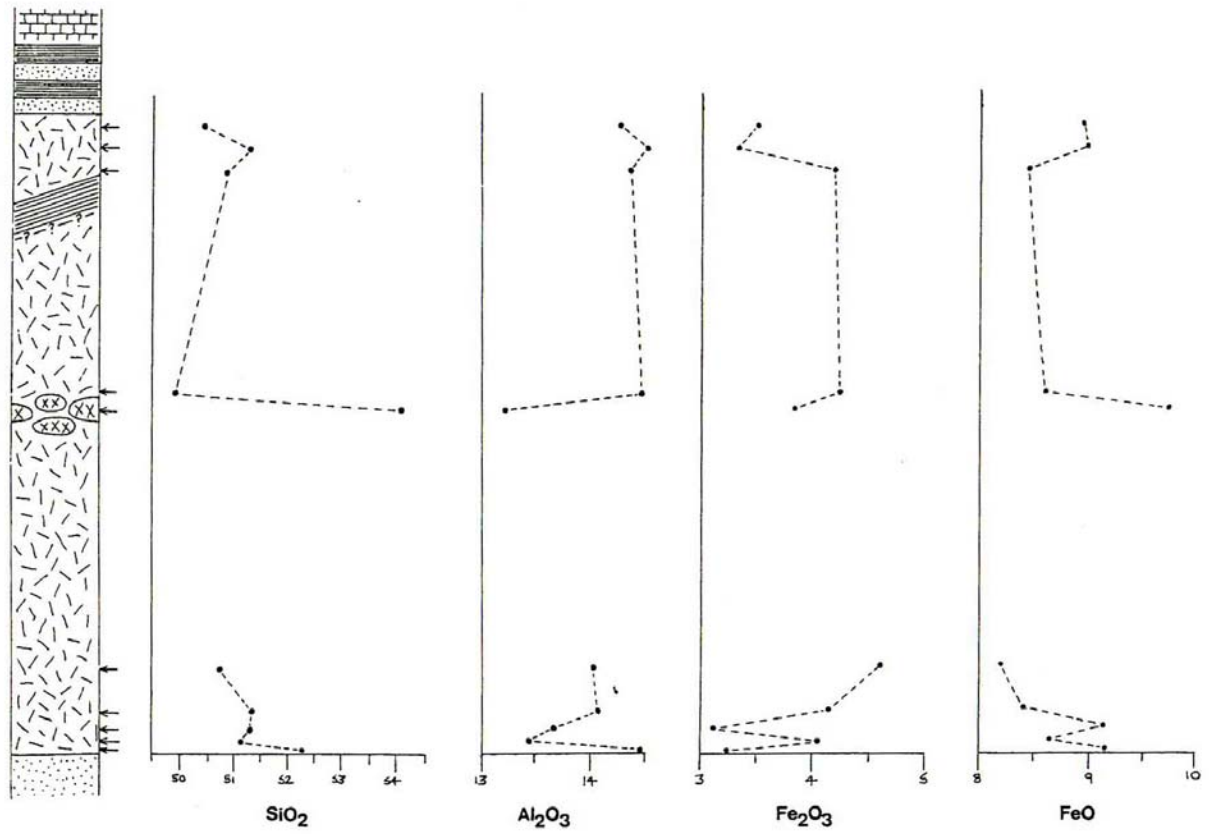
Figure 6.2: Vertical profiles of major chemical elements
SiO_2, Al_2O_3, Fe_2O_3 and FeO.
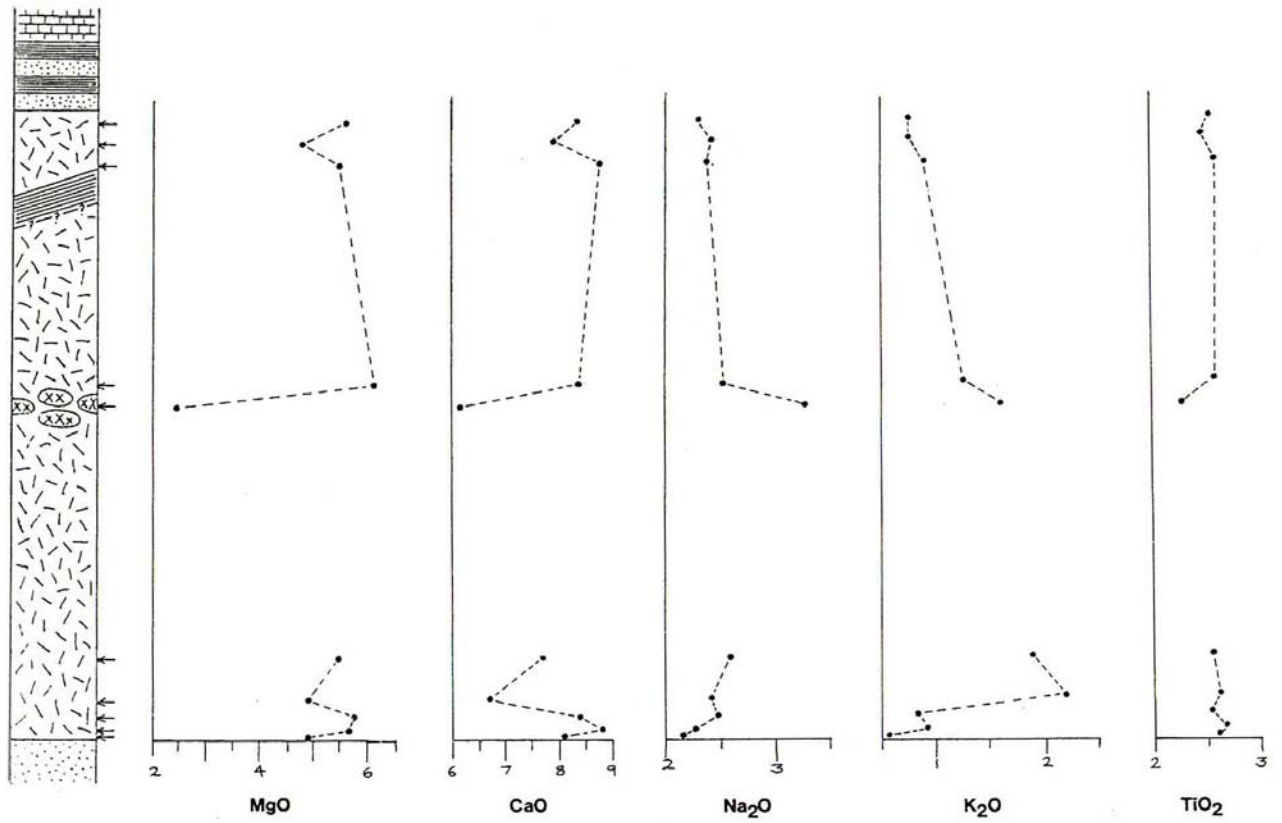
Figure 6.3: Vertical profiles of major chemical elements
MgO, CaO, Na_2O, K_2O and TiO_2.
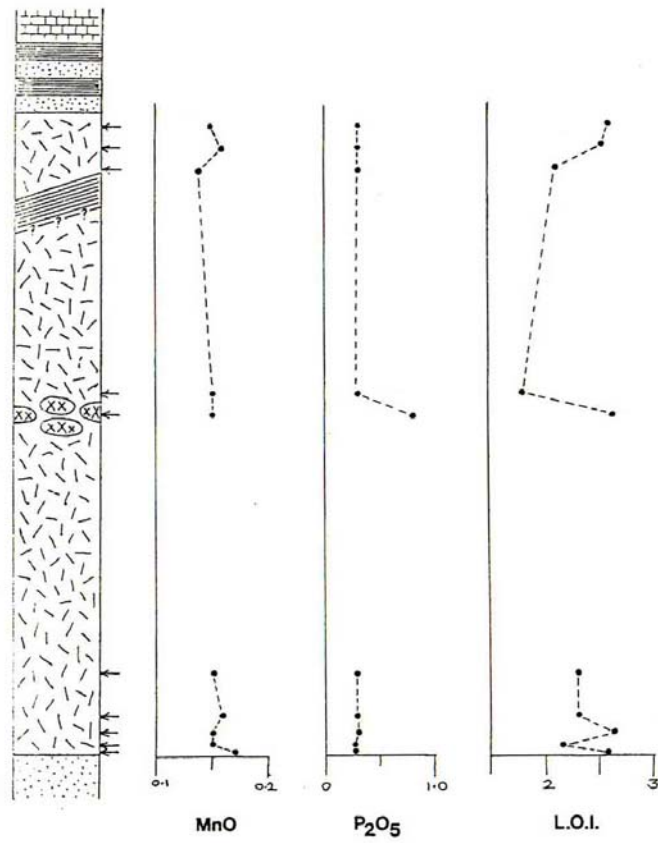
Figure 6.4: Vertical profiles of major chemical elements
MnO, P_2O_5 and total loss on ignition.
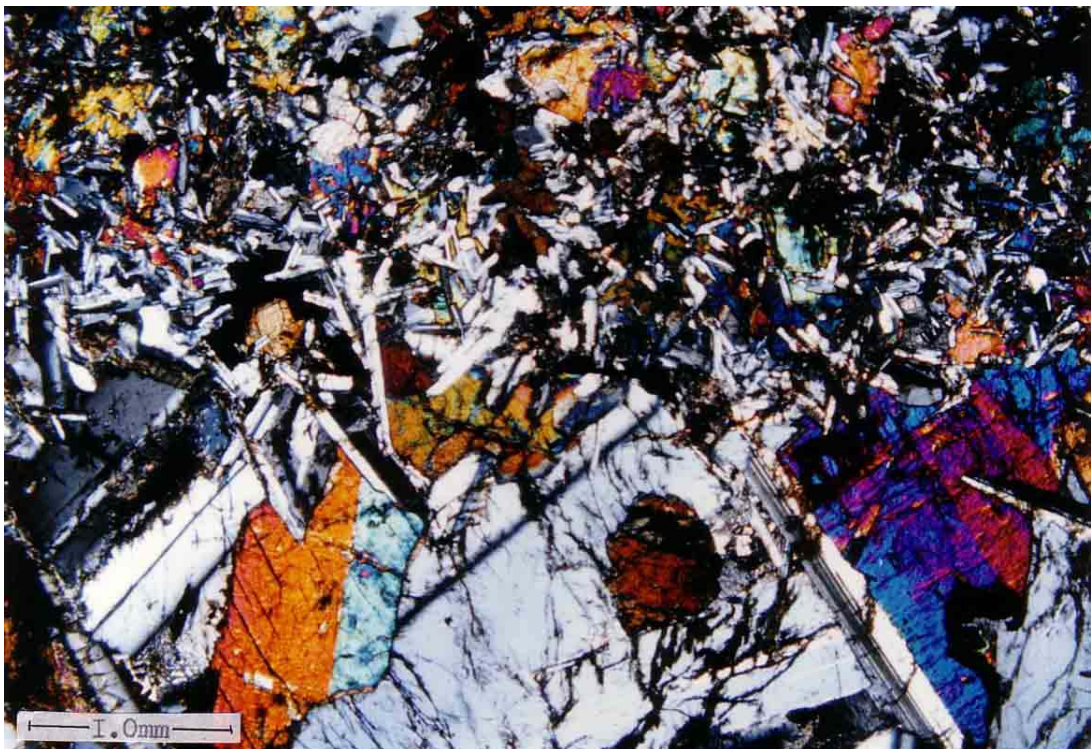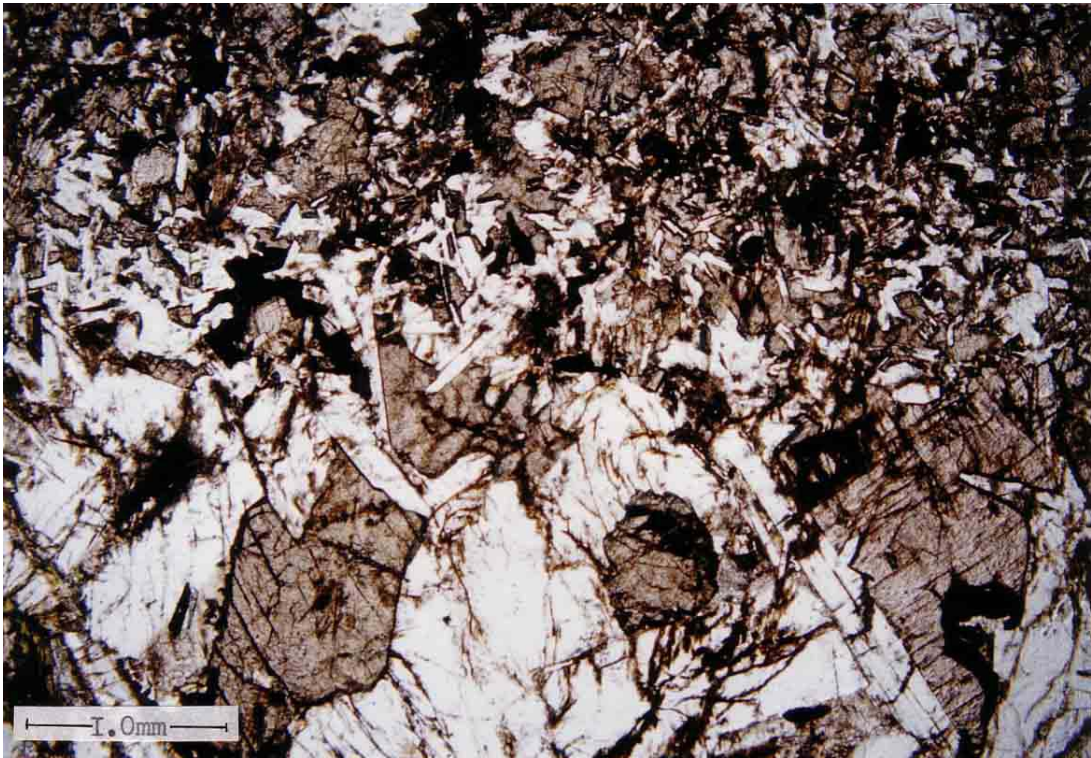
Plates 6.0, 6.1: Photomicrographs of thin section DC 11 in P.P.L. (top) and
X.P.L. (bottom), showing the well defined boundary between quartz-dolerite
(top of pictures) and dolerite pegmatite (bottom of pictures).
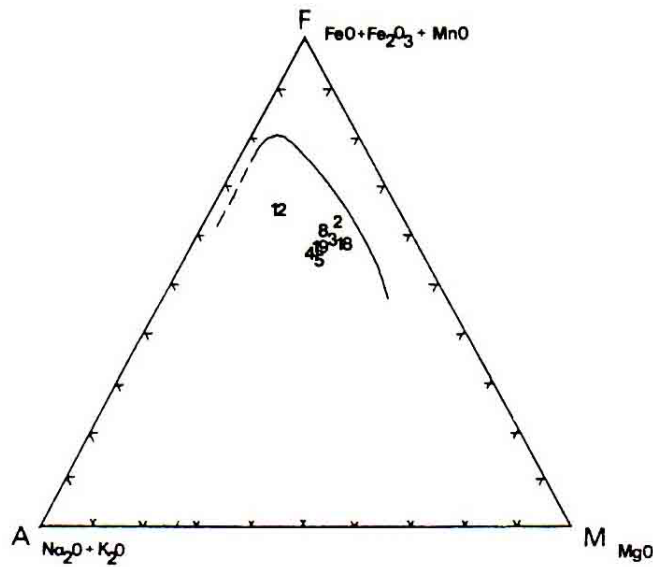
Figure 6.5: A.F.M diagram for the Whin Sill.
Skaergaard trend indicated by line.

Another diagram which illustrates the iron-rich nature of the magma is that of plotting the mafic index against the felsic index as shown in figure 6.6. The mafic index of the Whin Sill lies between 70 and 75 as compared with 40 to 45 for the initial rocks of the Skaergaard intrusion (Dunham and Kaye, 1965).

$$\text{Mafic Index} = \left(\frac{FeO + Fe_2O_3 \times 100}{FeO + Fe_2O_3 + MgO} \right)$$

$$\text{Felsic Index} = \left(\frac{Na_2O + K_2O \times 100}{Na_2O + K_2O + CaO} \right)$$

	DC 2	DC 3	DC 4	DC 5	DC 6	DC 8	DC 12	DC 14	DC 18	DC 19
Mafic	72	70	72	70	70	72	85	69	68	68
Felsic	25	27	41	37	27	29	42	27	28	31
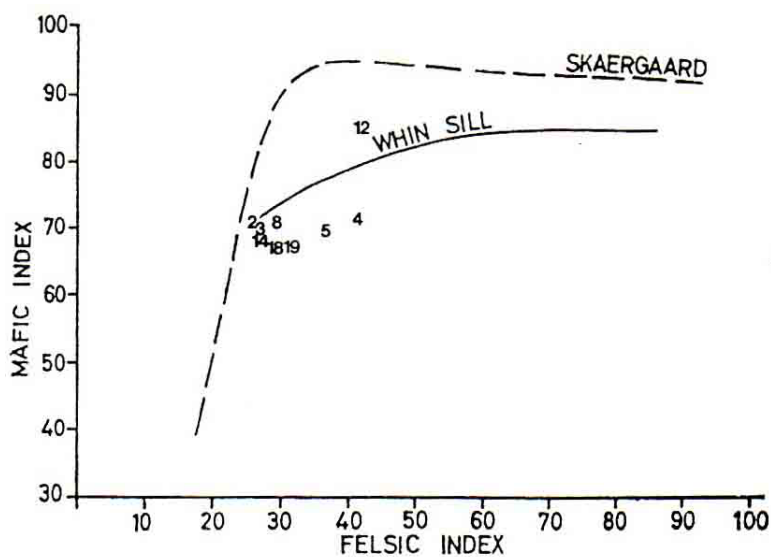
Figure 6.6: Plot of mafic index versus felsic index,
based on Dunham and Kaye (1965).

Petrographical and mineralogical evidence suggests that the Whin Sill is a tholeiite but if we plot total alkalis against silica as shown in figure 6.7, the majority of samples are classed as high-alumina basalts.
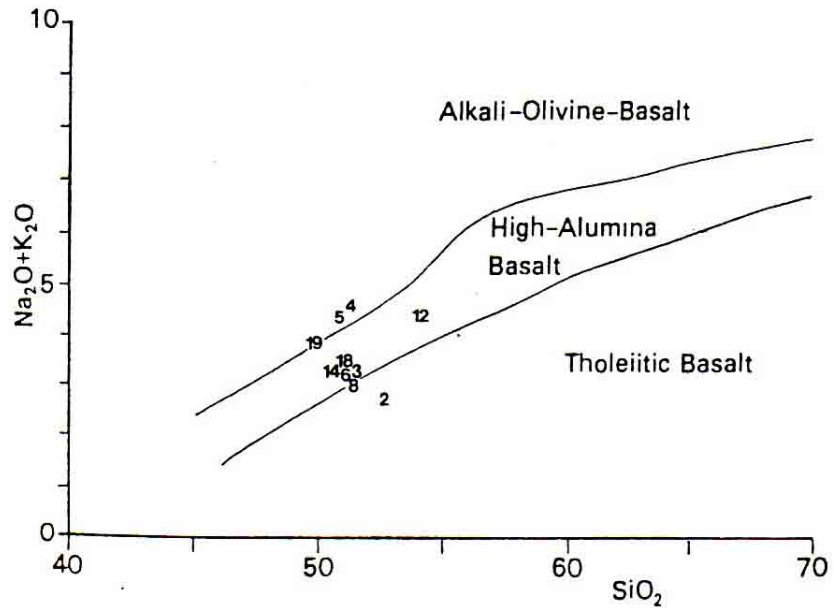
Figure 6.7: Plot of $Na_2O + K_2O$ versus SiO_2,
based on Dunham and Strasser-King (1981).

However, with an Al_2O_3 content of less than 15% the Whin Sill does not justify being classified as a high alumina basalt. By plotting Al_2O_3 against $Na_2O + K_2O$ (Figure 6.8) most points fall into the tholeiitic field, including the pegmatite (12), although the typical Whin Sill sample (19) intersects the tholeiitic/alkaline boundary.
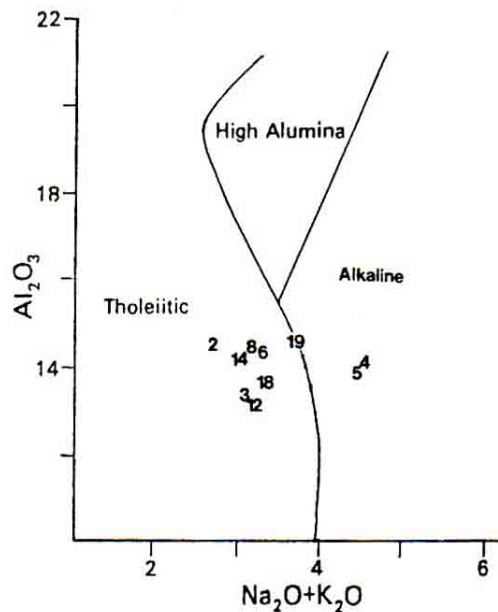
Figure 6.8: Plot of Al_2O_3 versus $Na_2O + K_2O$,
based on Dunham and Strasser-King (1981).

It is therefore of interest that chemical evidence suggests that the Whin Sill displays characteristics intermediate between tholeiitic and alkaline basalts though petrographical and mineralogical characteristics are mostly tholeiitic.

6.4 <u>Trace Element Analyses</u>

Trace element analyses were obtained using a solution of 1 g of powdered rock in 100 ml of solution and the results are given as ppm of each element in the rock. Cr, Pb, Zn, Sc, Cu, V, Ni and S are determined by polychromator, Ba and Sr by monochromator and Rb, Zr, Y and Nd by AA. The results for all of these elements are shown in table 6.3, below.

Table 6.3

|	DC 2	DC 3	DC 4	DC 5	DC 6	DC 8	DC 12	DC 14	DC 18	DC 19
Cr	52	47	53	56	56	53	3	59	54	67
Ni	58	55	55	58	58	57	17	59	60	58
Zn	118	118	120	121	128	118	168	129	124	122
Cu	59	59	57	60	61	61	54	59	61	56
Pb	7	6	6	7	7	7	7	7	7	7
Sr	382	412	589	428	389	378	400	378	381	420
Rb	33	44	66	48	37	37	57	39	50	68
Ba	249	389	402	306	304	290	487	297	332	276
Y	25	25	23	23	23	27	50	24	22	20
Zr	146	138	138	143	99	63	222	145	150	116
Nb	26	26	23	25	25	22	25	26	17	12
V	402	395	394	410	411	392	200	414	411	388
Sc	24	24	24	24	24	24	19	25	25	25
S	1179	1115	1127	1377	1164	1213	2366	1551	2866	1155

Vertical profiles have again been plotted for all of the trace elements analysed and can be seen in figures 6.9, 6.10, 6.11 and 6.12, overleaf.

As can be seen, the majority of the trace elements are similar throughout the profile except for the pegmatite which, as would be expected, shows marked changes in Cr, Zn, Ni, V, S, Y, Zr and Ba. Again, as with the major elements, there is a slightly symmetrical variation about the normal dolerite (DC 19) towards both upper and lower sill contacts in some of the elements e.g, Cr, Ni and V.
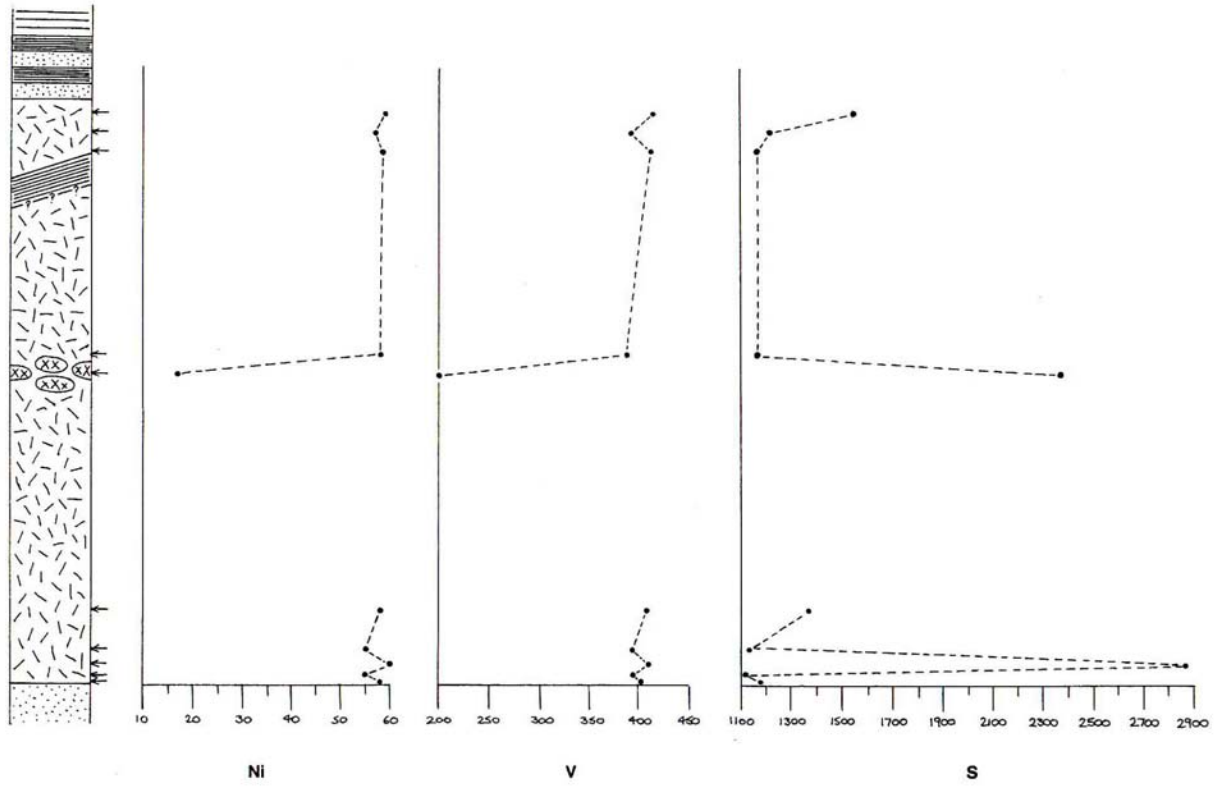
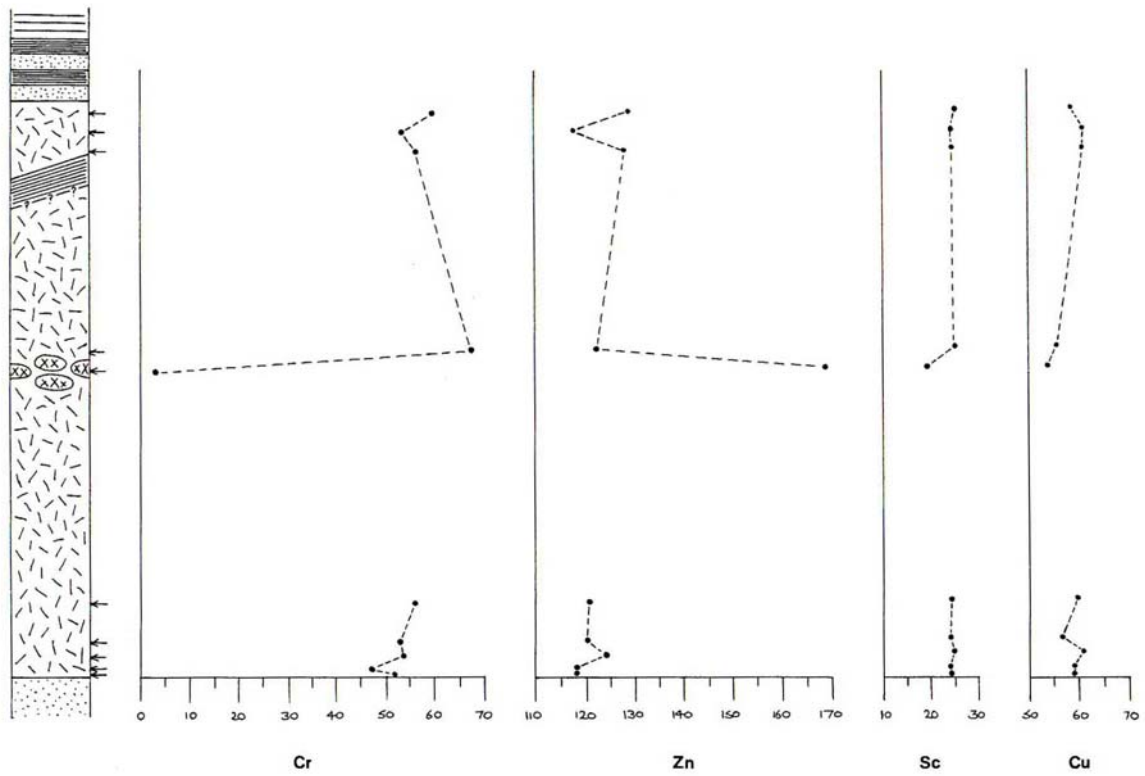Figure 6.9: Vertical profiles of trace elements Ni, V and S.

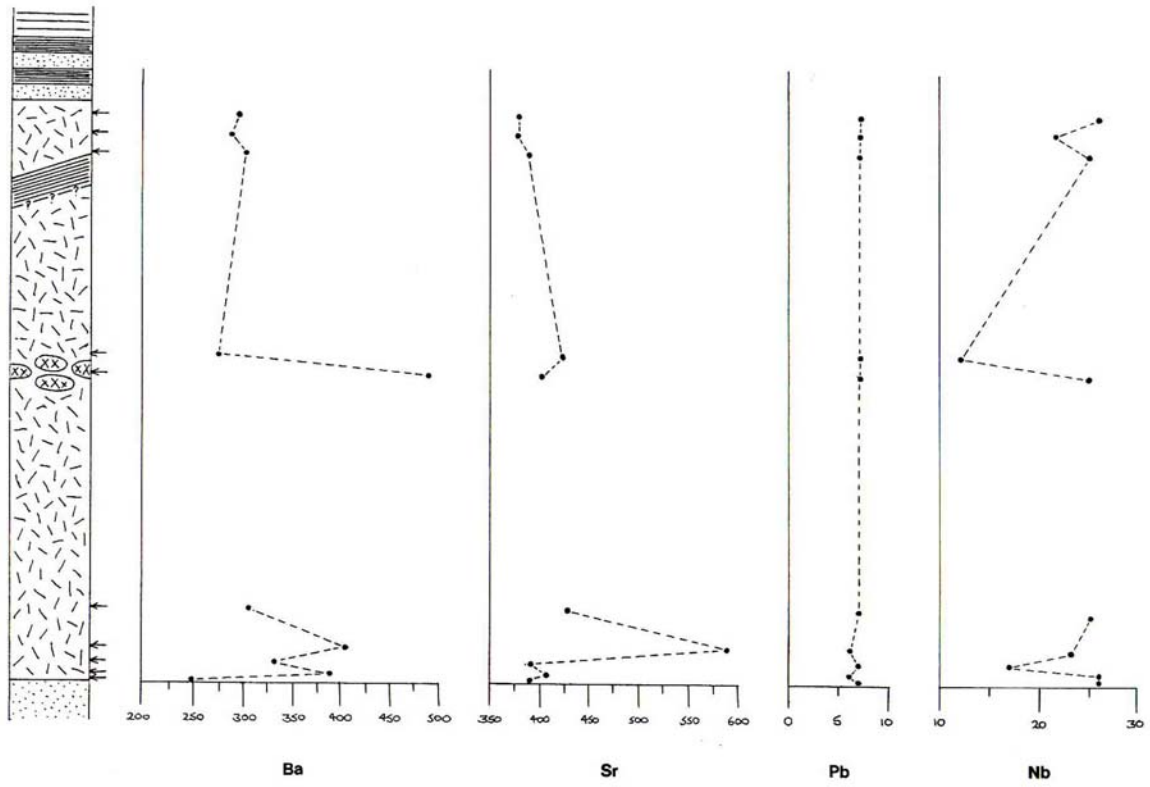Figure 6.10: Vertical profiles of trace elements Cr, Zn, Sc and Cu.

Figure 6.11: Vertical profiles of trace elements Ba, Sr, Pb and Nb.
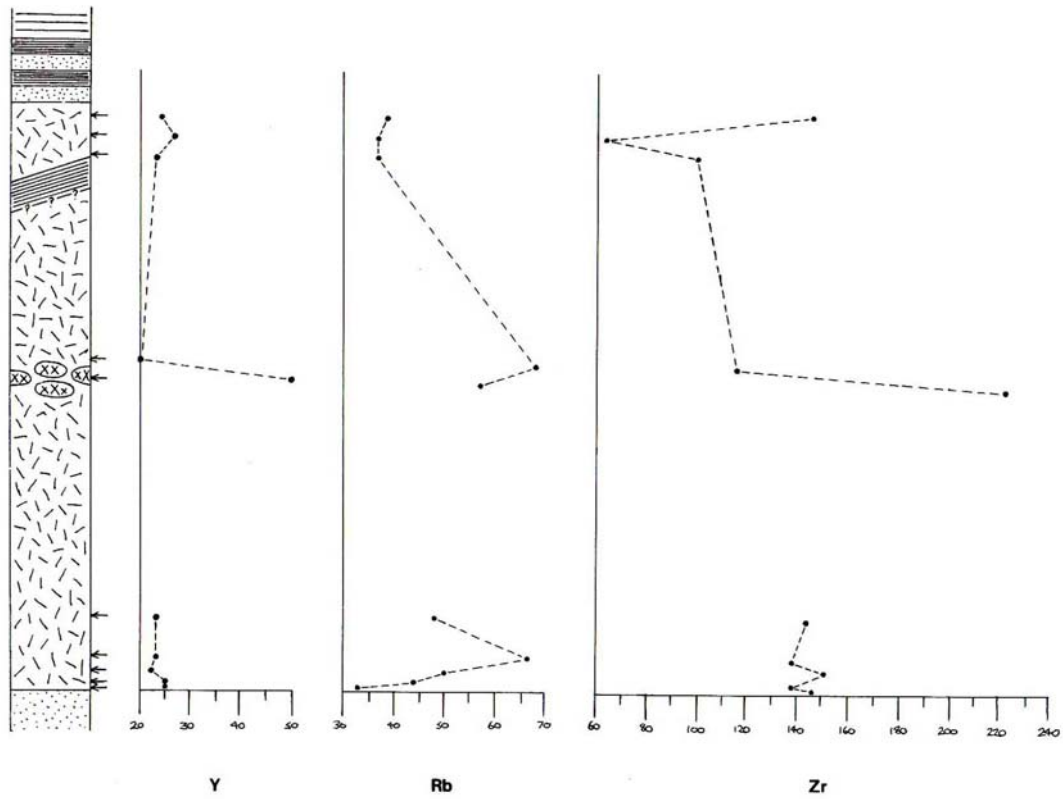

Figure 6.12: Vertical profiles of trace elements Y, Rb and Zr.

Clearly one factor that limits the potentiality for differentiation within an intrusive sheet of basaltic magma, such as the Whin Sill, is the time interval between intrusion and complete solidification. The most important controlling parameter in this connection is the thickness, since the time factor in solidification and cooling by outward conduction is proportional to the thickness squared. Time for complete solidification of a sheet t_s (in years), is related to the thickness D (in metres) by:

$$t_s = 0.014 \, D^2$$

$$\text{Whin Sill: } t_s = 0.014 \times 73^2$$

$$t_s = 74.6 \text{ years.}$$

Carmichael *et al* (1974)

In the simplest possible model, there is no internal motion, such as convection, within the magma body after intrusion. As cooling proceeds the magma solidifies inwards from the floor and roof. Carmichael *et al* (1974) states that 'for cover thicknesses of a kilometre or two the rate of cooling is the same at both surfaces.' Differentiation effects must therefore be symmetrical about the median horizontal plane of the intrusion and this can be seen in the modal and chemical sections through the sill. Convection and gravity controlled crystal sinking within many sills would lead to vertical asymmetry in the differential profile, but this is not the case in the sections of the Whin Sill and would therefore lead to the general conclusion that within the Whin Sill differentiation effects are controlled by temperature gradients falling off towards both upper and lower contacts.

When large bodies of basaltic magma, such as the Whin Sill are first intruded, they suffer chilling against the floor and roof of the intrusion. At the same time, the heat of the magma and the emitted volatiles also cause a certain amount of metamorphism with the enclosing country rocks (See Chapter 7.0). The chilling in the outer shell of magma is usually adequate to lower the temperature below the solidus range so that a rather fine-grained sample of rock approaching the bulk composition of the initial magma is formed. When the initial chilling against the wall rock has terminated and the steep temperature gradients have been much reduced, slow cooling of the main body of the magma continues.

6.5 Geochemical Variation Diagrams

Figure 6.13 (page 56) shows geochemical variations for all of the major elements against SiO_2. As can be seen from the figure, the majority of the elements form linear trends with very little scatter. The decrease in CaO and Al_2O_3, and increase in Na_2O and K_2O are due to the fractionation of plagioclase and clinopyroxene, whilst the sharp decrease in MgO most likely represents the fractionation of orthopyroxene. Apatite is found throughout the sill and can be represented by the consistent nature of P_2O_5 with SiO_2. The fractionation of iron-titanium oxides such as magnetite-ulvöspinel, ilmenite and haematite account mainly for the changes in the fractionation of FeO, Fe_2O_3 and TiO_2.

The incorporation of certain trace elements into the crystal lattice of major minerals is known as 'isomorphous substitution'. Isomorphous substitution is controlled by two main factors, firstly, the ionic radius of the substituting element must be very similar and secondly, the charge of the elements must be identical.

The trace element variation diagram (Figure 6.14) shows no significant correlation between Pb, Cu, Nb and Sc against SiO_2, as these elements remain of a similar quantity throughout the sill (See trace element

vertical profiles, pages 53 & 54). Cr shows a good negative correlation (Figure 6.15) as Cr typically replaces Al in clinopyroxenes. The fractionation of ferro-magnesian minerals from the Whin magma can be seen by the similar compatible relationships between Cr and Ni versus MgO (Figure 6.16).
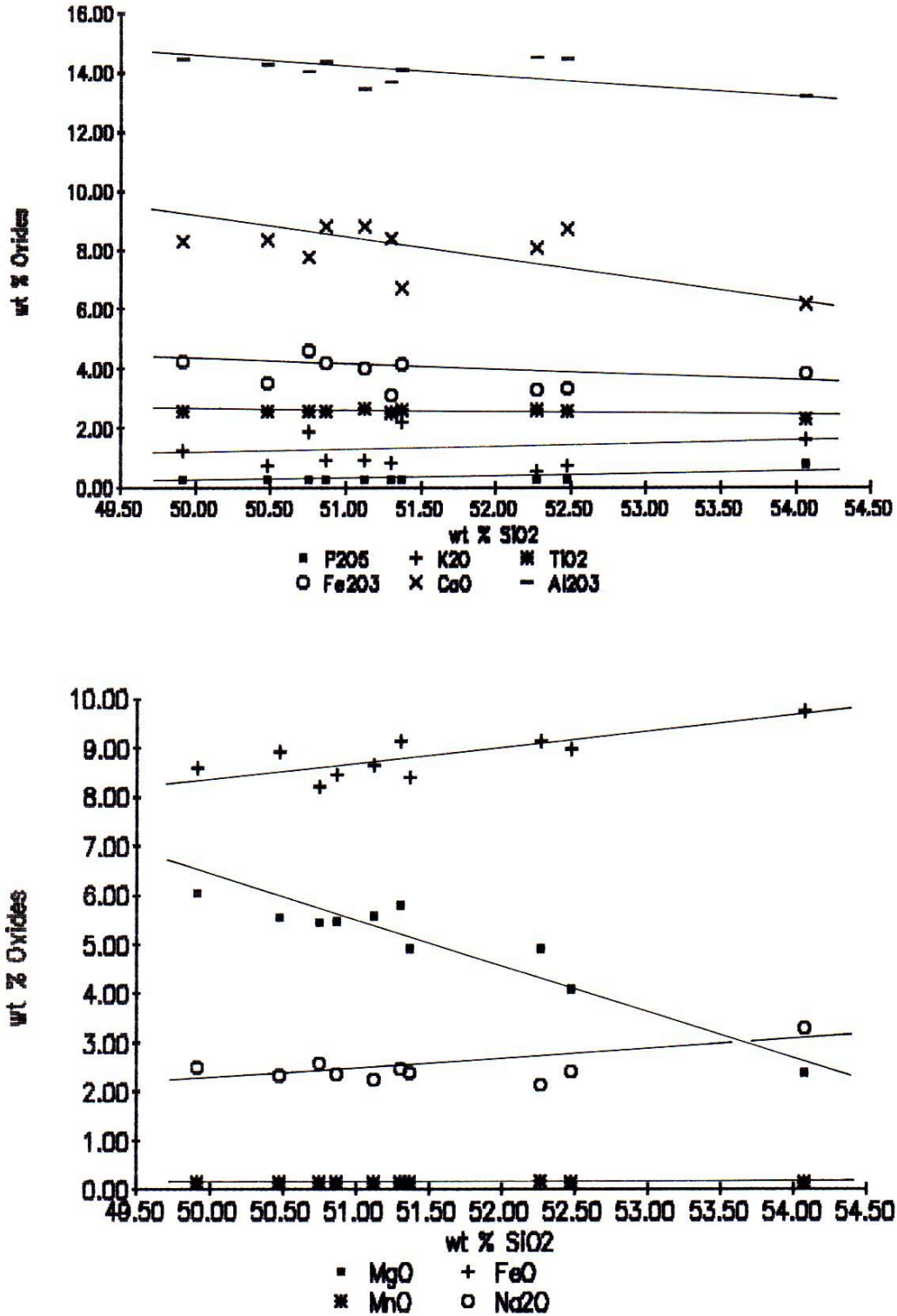

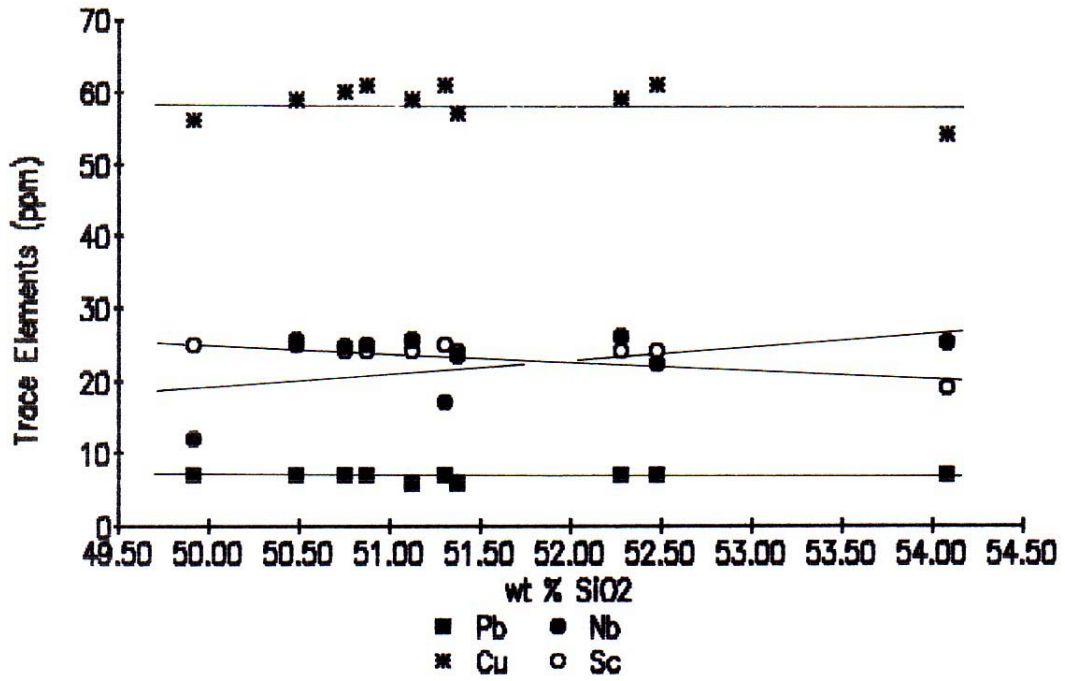Figure 6.13: Plot of Major Elements versus SiO_2
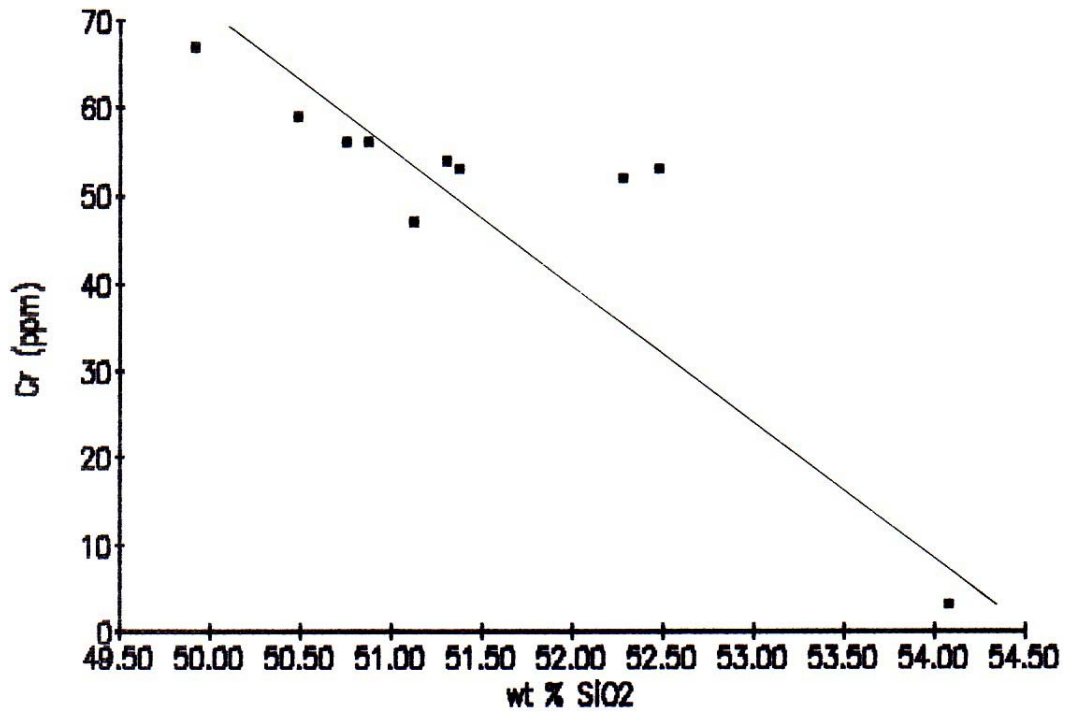
Figure 6.14: Plot of Pb, Nb, Cu and S versus SiO_2

Figure 6.15: Plot of Cr versus SiO_2
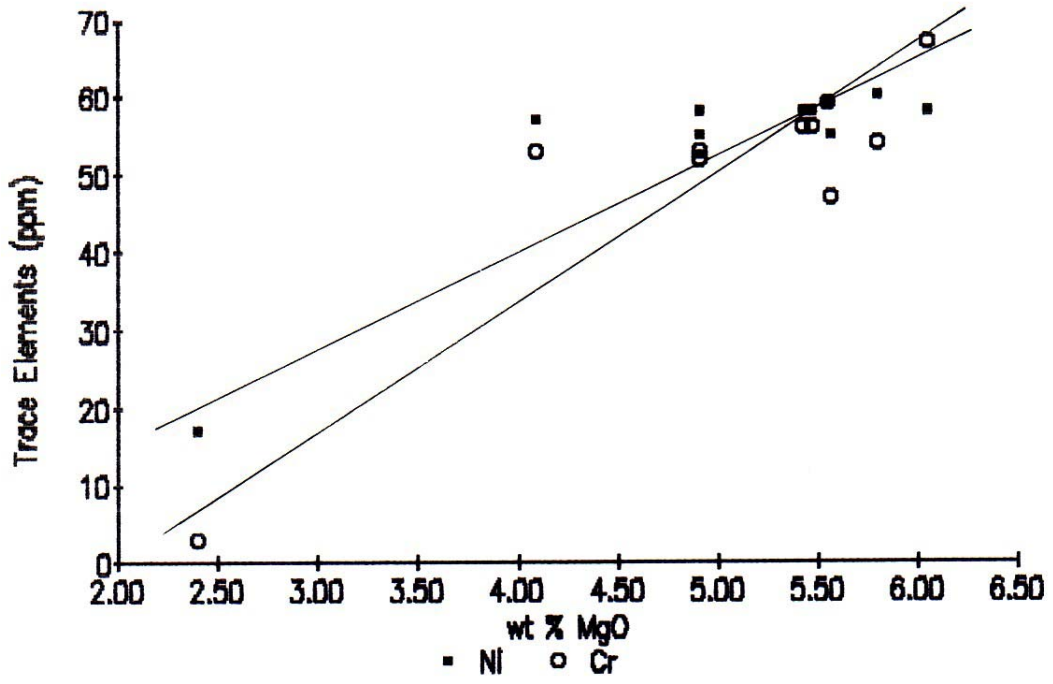
Figure 6.16: Plot of Cr and Ni versus MgO.
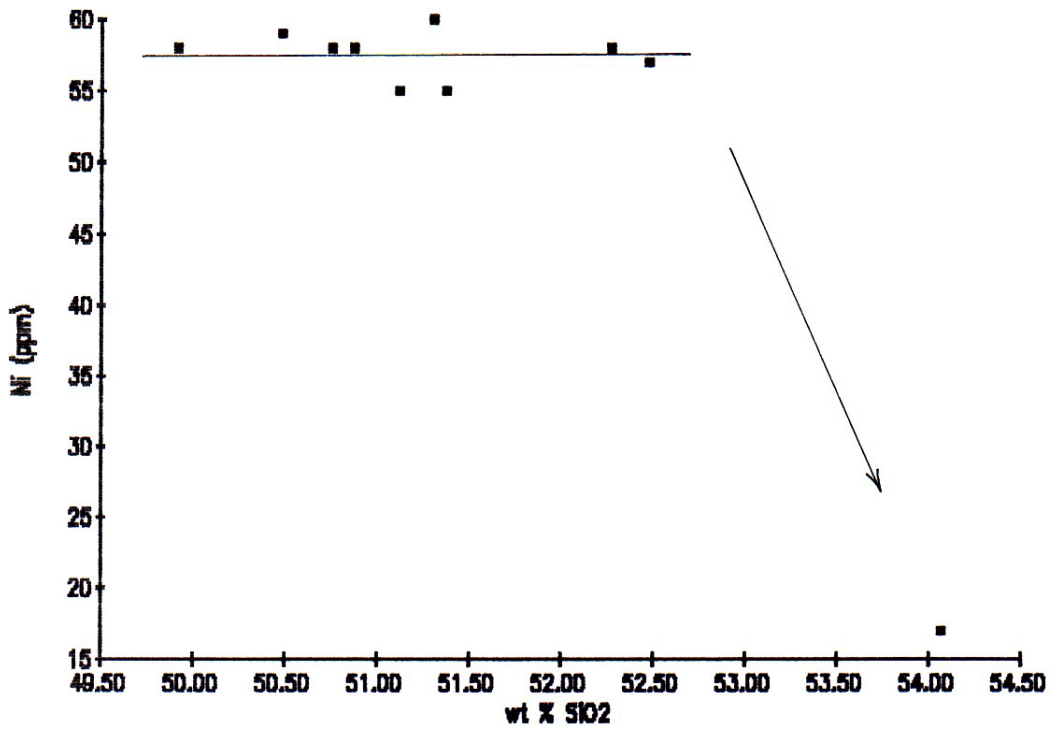
Figure 6.17: Plot of Ni versus SiO$_2$

A correlation between Ni and SiO$_2$ would typically represent the fractionation of olivine from a basaltic magma but this does not show in figure 6.17 and is due to there being little or no olivine in the Whin Sill (None was encountered during inspection of the sections). Fresh olivine has been found only in the chilled margins by Dunham and Kaye 91965) and as olivine pseudomorphs by Harrison (1966). It is interesting to note that Ni decreases markedly in the pegmatic version of the Whin Sill dolerite (Seen in both figures 6.17 and 6.9).

The use of Sr/Ca versus Ba/Ca or Onuma's SB Diagram (Figure 6.18) helps us to determine the crystal fractionation trend of basaltic magmas. The partial melt line shown in the diagram, with a slope of 45°, implies the addition or subtraction of Ca from a melt with a constant Sr/Ba ratio. The crystallization of plagioclase and clinopyroxene from the magma changes the Sr/Ca and Ba/Ca ratios and forms evolved melts. Onuma *et al* (1983) state that 'In the case of plagioclase crystallization, the Sr/Ca ratio in the melt hardly changes, whilst the Ba/Ca ratio in the evolved melt increases greatly, since plagioclase accepts both Ca and Sr with a similar degree but excludes Ba. In the case of clinopyroxene crystallization, both the Sr/Ca and Ba/Ca ratio is much greater than that of the Sr/Ca ratio, since Ca enters, whilst Sr is hard to enter and Ba does not enter into the clinopyroxene.' As can be seen in figure 8.18, there are two systematic upward concave shapes indicating that plagioclase crystallization prevailed in the early stages whilst clinopyroxene prevailed in the later stages of the crystal fractionation process in the Whin Sill. The two upwardly concave trends indicate that there were possibly two liquids fractionating within the Whin Sill, from an initial partial melt of composition X.
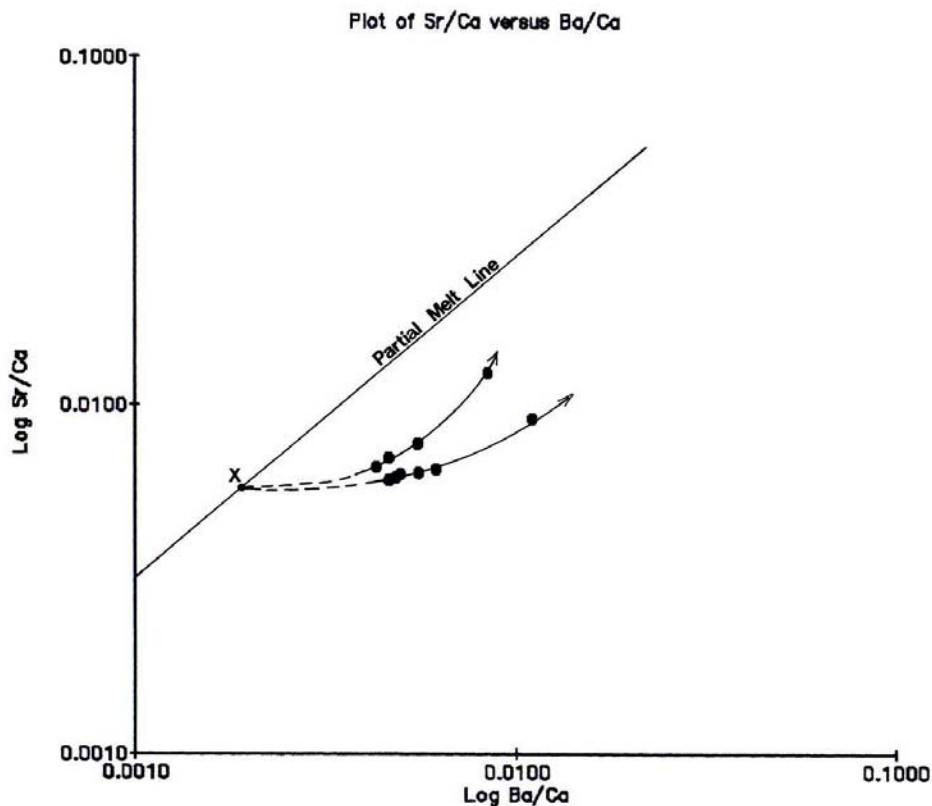
Figure 8.18: Onuma's SB Diagram showing crystal fractionation
trends from the Whin Sill, Teesdale.

The tectonic setting and discrimination between oceanic and continental type basalts can be undertaken using the Pearce and Cann diagram (Ti/100 – Zr – 3.Y). As can be seen from figure 6.19, the majority of the samples taken from the Whin Sill fall within the continental basalt field as would be expected.
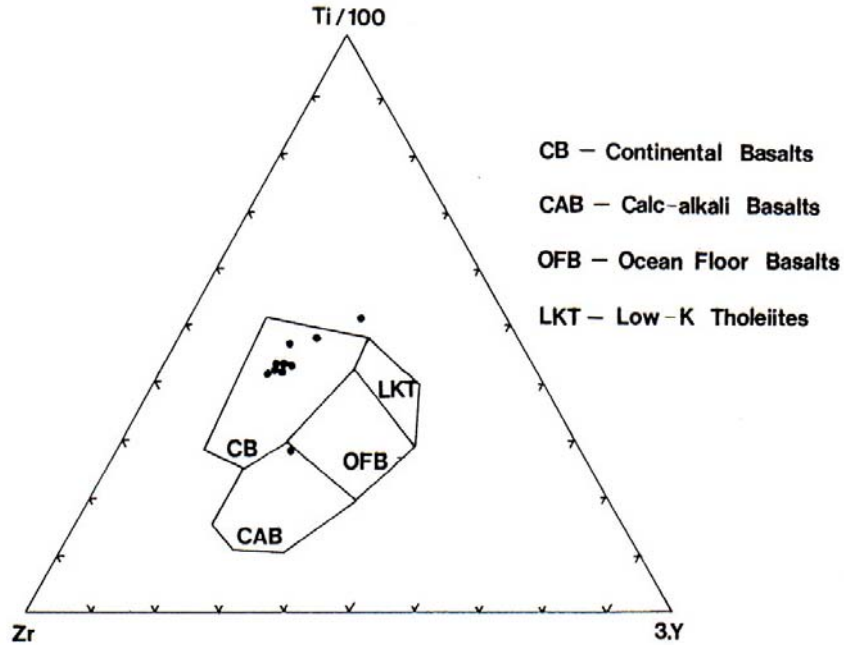
Figure 6.19: Triangular diagram Ti/100 – Zr – 3.Y showing samples
from the Whin Sill. After Pearce and Cann (1973).

If we compare this with the diagram by Pearce *et al* (1974) for determining between oceanic and continental basalts, figure 6.20, we find that the points for the Whin Sill plot on, or below the boundary, again emphasizing that the Whin Sill is of a continental basaltic nature.
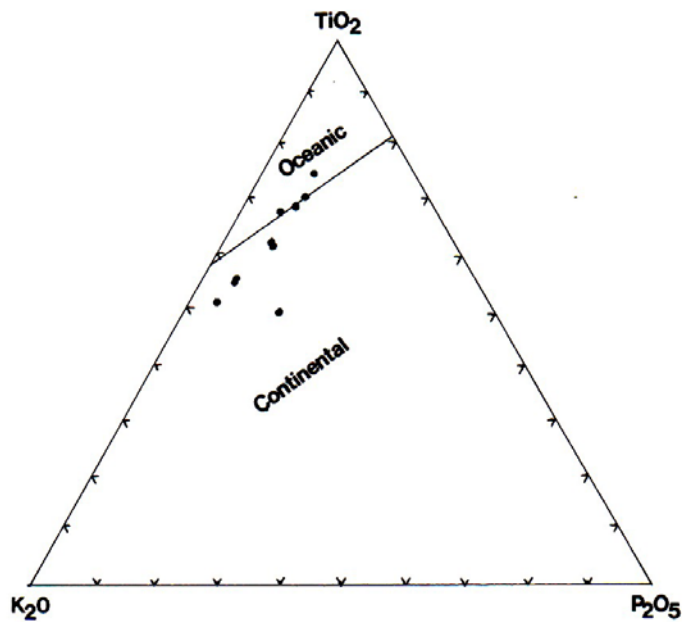
Figure 6.20: Triangular variation diagram TiO_2 – K_2O – P_2O_5, showing
samples from the Whin Sill. After Pearce *et al* (1974).

7.0 <u>CONTACT ROCKS</u>

It has been estimated by Dunham and Kaye (1965) that the Whin Sill magma was intruded at a temperature of approximately 1100 to 1150°C and that at its most thickest point in Teesdale it took around sixty years to cool. The sedimentary rocks adjacent to the sill show some signs of metamorphism but not to any considerable degree. Visible effects lying either above or below he contacts have been recorded up to distances of 30 m from the intrusion itself (Robson, 1980) and changes have been observed in coals as far as 425 m above the sill (Jones and Cooper, 1970 <u>In</u> Burgess and Holliday, 1979).

7.1 <u>Limestones</u>

The effects of metamorphism are very slight, the white or pale grey limestones with low organic content, such as the Melmerby Scar Limestone, Robinson Limestone and Single Post Limestone are marmorized into a coarse, granular white marble where bedding is obliterated and vertical joints become the major foliation. As we move away from the contacts the saccharoidal nature of these limestones decreases and bioclastic debris becomes increasingly apparent. Dark grey limestones, with greater organic content such as sample DC 9 taken from Scoberry Bridge (Plate 7.0), show little alteration other than minor recrystallization. Rayner and Hemingway (1974) have identified the development of garnet, vesuvianite and wollastonite in impure limestones converted to calcsilicate rocks.

Plate 7.0: Photomicrograph of thin section DC 9 in P.P.L. showing bioclastic
debris in impure limestones from Scoberry Bridge.

7.2 Sandstones

Sandstones have been hardened and converted to metaquartzite close to the sill and compaction has produced polygonal quartz grains with sutured grain boundaries, as shown in plate 7.1. Deformation of the crystal lattice has produced strained and stressed quartz which is easily identifiable by sweeping extinction in X.P.L. and can be seen in plate 7.1. Destruction of the original clastic structure has taken place and secondary growth of quartz between the grains has lead to 'ghost' grain boundaries being produced. As the Whin Sill thins towards the River Lune and Lunedale fault metamorphic effects become less in the surrounding sedimentary rocks. Sample DC 16 (Plate 7.2) was taken from the River Lune cutting and consists of almost unaltered sandstones with a silt matrix and calcite cement.
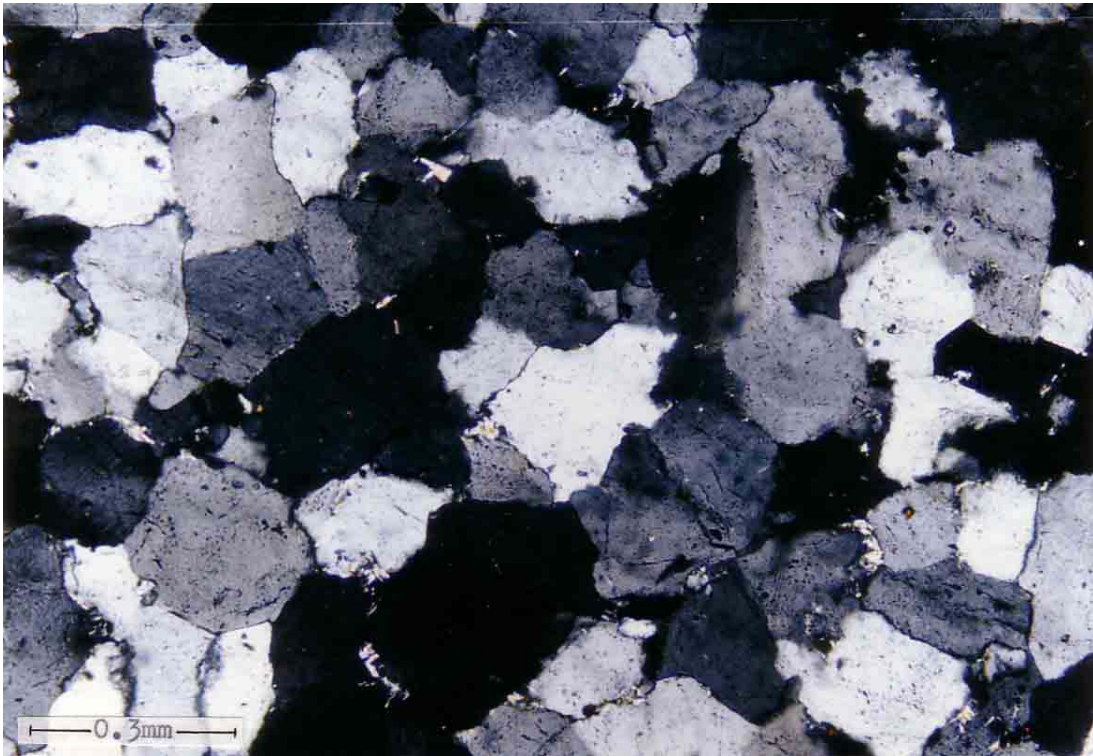
Plate 7.1: Photomicrograph of thin section DC 13a in X.P.L. showing polygonal quartz Grains with sutured grain boundaries and also strained and stressed quartz.

7.3 Siltstones

Many carbonaceous mudstones and micaceous siltstones have taken on an olive-green colour where metamorphosed by the emplacement of the Whin Sill. Occasional spotting is visible throughout sample DC 7 taken from the raft at Wynch Bridge (Plate 7.3) and Harbord (1962) In Rayner and Hemingway (1974) has shown that spotting results from the development of patches of iron-rich chlorite. The spots shown in plate 7.4 with exceptionally high relief and reddish brown colour are most likely rutile crystals (TiO_2), formed by the breakdown of ilmenite, surrounded by epidote rosettes ($Ca(Fe^{3+})Al_2(OH)Si_3O_{12}$) showing high relief and yellowish green colouring.
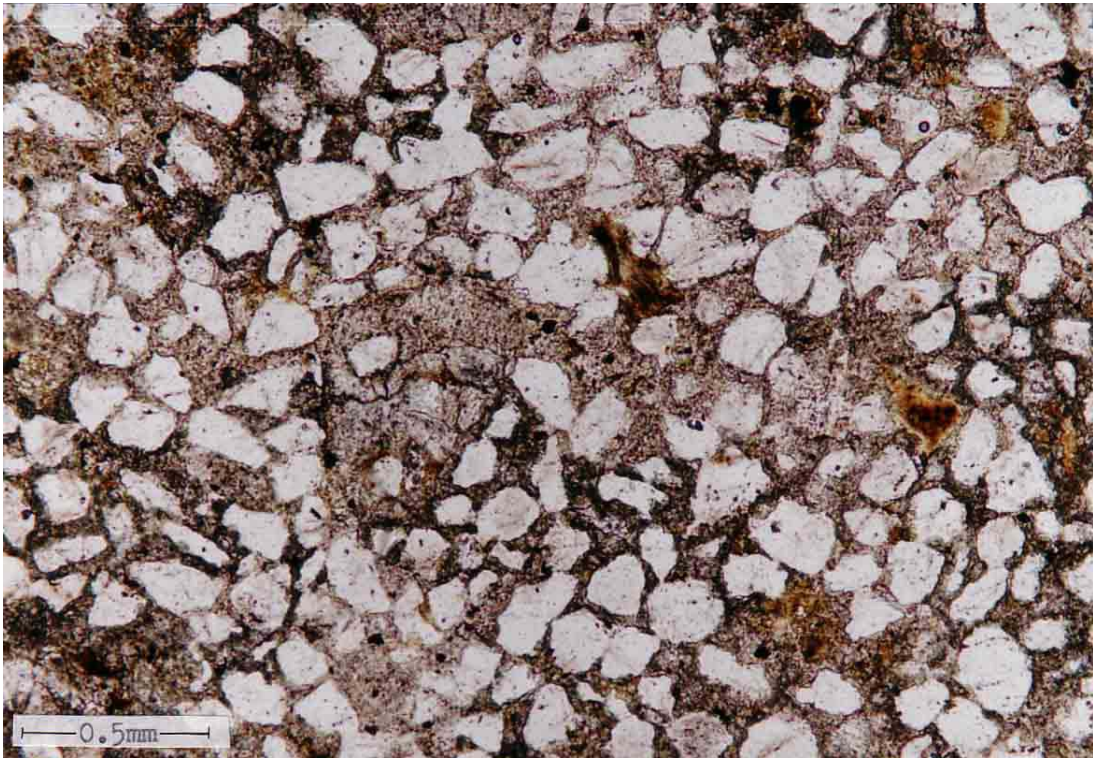
Plate 7.2: Photomicrograph of thin section DC 16 in P.P.L. (unaltered sandstone).

Despite the complex relationships between the country rocks above and below the Whin Sill, there is very little or no field evidence at the sill contacts that suggests any chemical contamination of country rocks into the magma, but there is evidence of assimilation of the country rock into the Whin Sill magma in the form of rafts of baked sediments such as the one found at Wynch Bridge (Section 3.7). This theory is opposed by some of the geochemical and mineralogical evidence in section 6.1 which suggests some possible contamination by the country rocks at both the upper and lower contacts, although as already discussed we may dismiss the chilled outer shell of magma as representing the initial composition of the Whin Sill.

Geochemistry is required from the surrounding contact rocks to evaluate any form of chemical contamination with the margins of the Whin Sill magma any further.
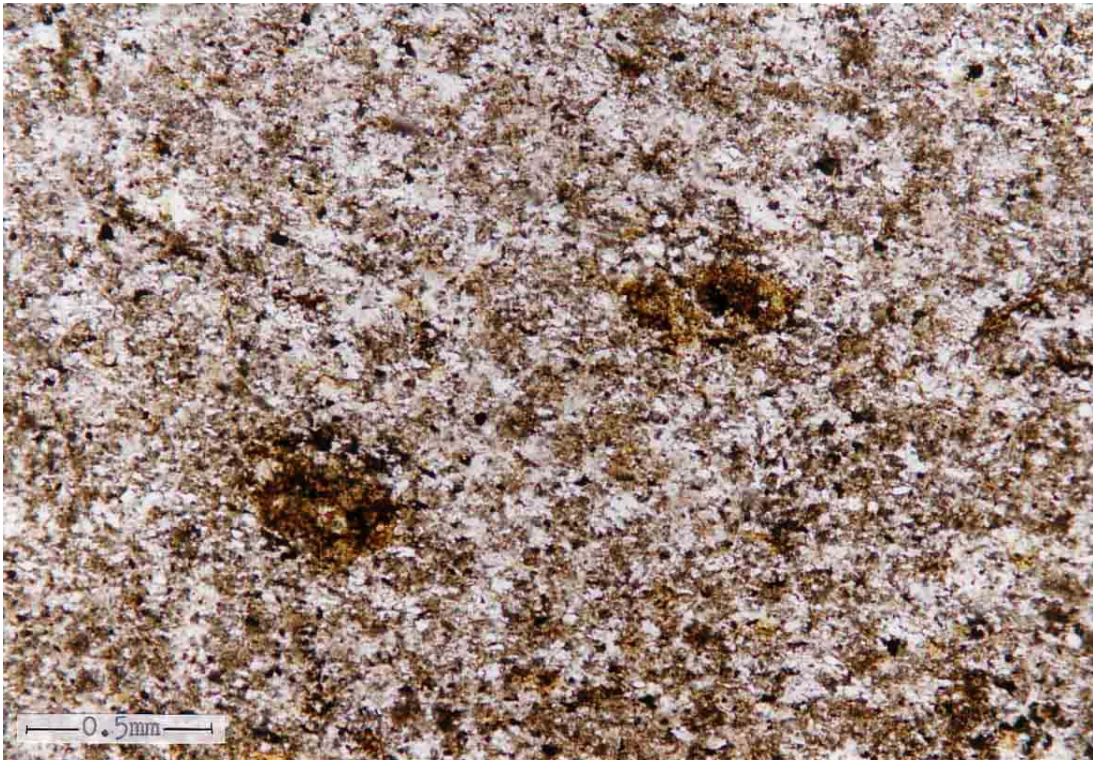
Plate 7.3: Photomicrograph of thin section DC 7 in P.P.L. showing
occasional spotting in metamorphosed siltstone.
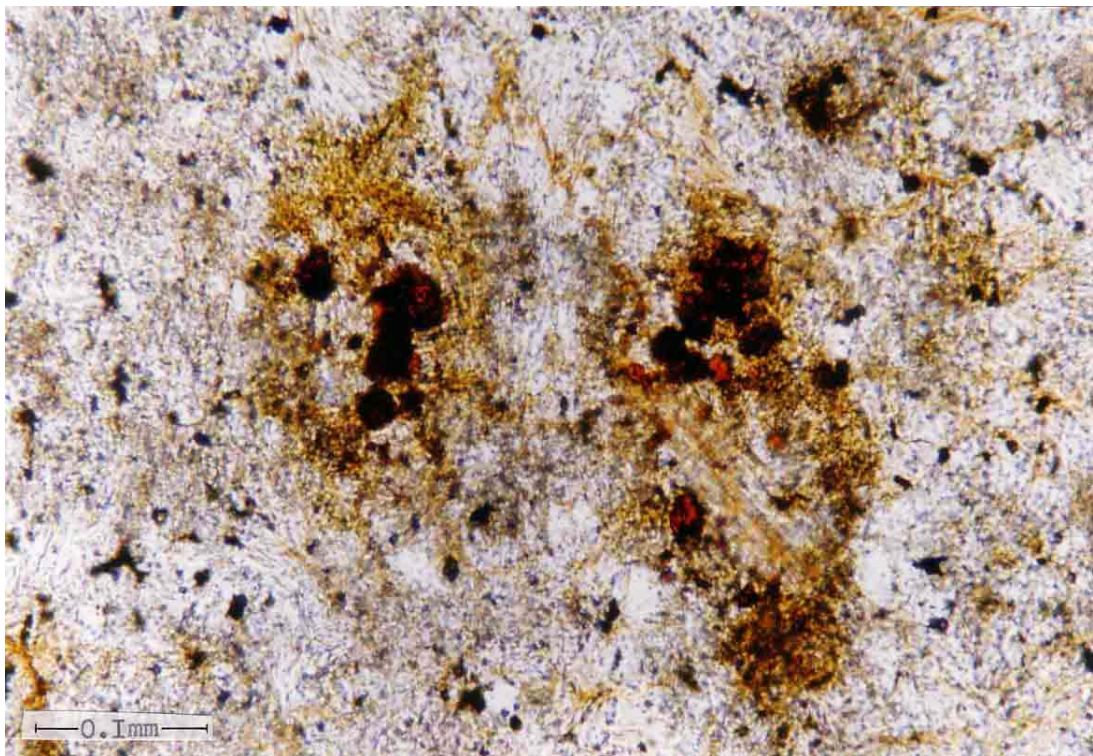
Plate 7.4: Photomicrograph of thin section DC 7 in P.P.L. showing epidote
rosettes and rutile crystals in metamorphosed siltstone.

8.0   DISCUSSION

The magma which produced the Whin Sill complex was most likely generated in the mantle from many batches of tholeiitic magma, and triangular tectonic discriminant diagrams indicate a tectonic setting of continental basaltic nature. The iron-rich nature of the sill, shown in figures 6.5 and 6.6, indicates that the initial magma may possibly have already undergone some form of differentiation before intrusion through tensional dyke channels into its present location. A possible site of differentiation would be a high-level magma chamber which was undergoing crystallization whilst at the same time being continuously fed with fresh basaltic magma from below. Even if the magma supply were of constant composition the liquid in the magma chamber would have become partly differentiated before being mixed with new magma, giving a mixed product different from both the original magma and from any normal product of closed system differentiation. Crystallization within a high-level magma chamber would explain the presence of micro-phenocrysts throughout the sill, notably plates 5.6 and 5.7. Grain sizes increase symmetrically away from both the upper and lower contacts, figure 6.0, due to chilling, and this fine-grained chilled outer shell of magma most likely represents the bulk composition of the Whin Sill magma. Due to relatively quick solidification of the sill (*c.* 75 years) very little, if any, contamination by the surrounding country rock has taken place. Basic plutonic and minor intrusions usually show a chilled margin, as is the case with the Whin Sill; a chilled margin such as this would tend to isolate the remaining magma from the country rocks. Hall (1987) states that contamination usually 'plays a minor role in the evolution of basalts.', although in the case of the Whin Sill a marked increase in free quartz and SiO_2 towards the contacts suggests some contamination from the surrounding sandstone strata. Field relationships between the country rocks above and below the Whin Sill show no sign of any chemical reaction between the country rocks and the whin magma and a perfectly concordant boundary can be seen (plates 3.2, 3.3 and 3.4), however, there is evidence of inclusion of rafts of baked sediment at a number of localities, a rotated raft in this work being found at the location of Wynch Bridge (Section 3.7) and a wedge of sandstone at the River Lune location (Section 3.1) but again, other than baking of the sediment there is no evidence of chemical contamination between the rafts and the Whin Sill magma. At the time of intrusion the heat of the magma (*c.* 1100 - 1150°C) and the emission of volatiles caused minor metamorphism to the sedimentary rocks adjacent to the sill. The contact rocks of the Whin Sill consists or partially recrystallized limestones, sandstones and silt/mudstones. The metamorphosed rocks, even from rafts within the sill itself, frequently contain identifiable fossils and show occasional spotting in the form of neocrystallization of minerals such as rutile and epidote, and hardening by the recrystallization of sutured quartz grains in sandstone. Differentiation effects within the sill are controlled by temperature gradients falling off towards the floor and roof rather than by internal motion such as convection currents and crystal settling as found in larger sills of this type, this would also account for the symmetrical array of grain sizes through the sill. Differentiation trends can be seen in sections through the sill and show a vertical variation in SiO_2, FeO and total loss on ignition all increasing towards the contacts and fe_2O_3, MgO, Na_2O and K_2O all decreasing towards the contacts. The increased volatile concentration and differentiation towards the centre of the sill most likely lead to the formation of the coarse-grained dolerite pegmatite occurring in flat lying concordant sheets up to 150 mm thick. This coarse-grained dolerite pegmatite shows markedly different chemical compositions to that of the

surrounding normal quartz-dolerite, but has a similar composition to the chilled margins although it is petrographically very different, with very coarse-grained poikolitic and granophric textures. The boundary between the coarse pegmatite is sharp and well defined as shown in plates 6.0 and 6.1 and indicates the sudden change from a magma under-saturated in volatiles to a volatile saturated magma. There is no distinct evidence of layering or crystal settling within the sill, although there is some evidence of liquid immiscibility to some extent as large sulphide droplets can be seen close to the lower contact in sample DC 2 from Crossthwaite quarry. These are formed by early segregation of immiscible sulphide liquids within the magma, which then coalesce and accumulate towards the base of the intrusion. This vertical variation within the Whin Sill may be due to contamination from the surrounding country rocks or by magma differentiation, or by a combination of these factors, but we must not rule out the possibility of there being more than one intrusive phase. Randall (1989) assumes that the magma was emplaced in one episode to forma single cooling unit, whilst chemical variation within this work suggests that there may be two liquid trends fractionating from the same initial magma composition. This difference is very small and may again represent pulses of slightly varying magma from a high-level magma chamber beneath the continental crust, further investigation into this would require a larger number of samples, as we cannot distinguish between a definite trend or scatter with only ten samples. In general it can be seen that the Whin Sill has chemical characteristics intermediate between alkaline and tholeiitic magma types. Its petrographical and mineralogical affinities are dominantly tholeiitic.

8.1 Conclusion

The majority of the samples, data and descriptions within this work on the petrology, mineralogy and geochemistry of the Whin Sill have led to results which are comparable with the present state of knowledge, though there are a number of new ideas and facts that have come to light with this work.

If time, capital and equipment were more freely available a more detailed study of a section of through the Win Sill would most likely produce excellent results. Samples taken at very close intervals (<10 m) from the lower contact to the upper contact at one location would eliminate any lateral variation. Lateral variation can be seen in this study by comparing the samples at both the River Lune location and Crossthwaite quarry. Unfortunately there is no natural section that cuts from the top to the bottom of the sill, this type of data must be obtained from bore holes.

APPENDIX

Dolerites from the Whin Sill.

Darren Clark, January – February, 1992.

	DC2	DC3	DC4	DC5	DC6	DC8	DC12	DC14	DC18	DC19
SiO_2	52.27	51.12	51.37	50.75	50.87	52.47	54.07	50.48	51.30	49.91
Al_2O_3	14.48	13.45	14.10	14.06	14.36	14.43	14.20	14.27	14.69	14.45
Fe_2O_3	3.27	4.04	4.15	4.60	4.19	3.33	3.84	3.50	3.10	4.23
FeO	9.15	8.66	8.40	8.20	8.46	8.98	9.75	8.92	9.13	8.60
MgO	4.91	5.57	4.91	5.43	5.47	4.75	2.40	5.55	5.80	6.04
CaO	8.07	8.83	6.69	7.74	8.74	7.93	6.16	8.36	8.37	8.32
Na_2O	2.16	2.27	2.41	2.60	2.38	2.43	3.29	2.33	2.48	2.52
K_2O	0.54	0.93	2.20	1.89	0.90	0.76	1.61	0.76	0.81	1.25
MnO	2.60	2.66	2.61	2.55	2.58	2.49	2.29	2.54	2.53	2.57
TiO_2	0.17	0.15	0.16	0.15	0.14	0.16	0.15	0.15	0.15	0.15
P_2O_5	0.29	0.28	0.28	0.29	0.29	0.29	0.80	0.28	0.30	0.29
tot.LOI	2.54	2.13	2.30	2.31	2.13	2.54	2.64	2.60	2.61	1.81
total	100.45	100.07	99.58	100.56	100.56	100.75	100.19	99.76	100.28	100.13
LOI	1.52	1.17	1.37	1.40	1.19	1.54	1.56	1.61	1.60	0.85
tot.Fe_2O_3	13.44	13.65	13.49	13.71	13.59	13.31	14.67	13.42	13.25	13.78
Cr	52	47	53	56	56	53	3	59	54	67
Ni	58	55	55	58	58	57	17	59	60	58
Zn	118	118	120	121	128	118	168	129	124	122
Cu	59	59	57	60	61	61	54	59	61	56
Pb	7	6	6	7	7	7	7	7	7	7
Sr	382	412	589	428	389	378	400	378	381	420
Rb	33	44	66	48	37	37	57	39	50	68
Ba	249	389	402	306	304	290	487	297	332	276
Y	25	25	23	23	23	27	50	24	22	20
Zr	146	138	138	143	99	63	222	145	150	116
Nb	26	26	23	25	25	22	25	26	17	12
V	402	395	394	410	411	392	200	414	411	388
Sc	24	24	24	24	24	24	19	25	25	25
S	1179	1115	1127	1377	1164	1213	2366	1551	2866	1155
A	13.7	15.2	21.3	20.2	15.6	16.5	23.9	14.9	15.6	16.9
F	61.4	58.4	56.0	55.4	58.3	62.2	64.4	58.3	56.8	55.9
M	24.9	26.4	22.7	24.4	26.1	21.2	11.7	26.8	27.6	27.2
K	15.7	24.0	43.2	40.0	23.9	21.0	34.3	21.2	22.2	30.4
T	75.8	68.6	51.3	54.0	68.4	71.0	48.7	70.9	69.6	62.5
P	8.5	7.3	5.5	6.0	7.7	8.0	16.9	7.9	8.2	7.1
Mg#	42.0	44.7	41.9	44.0	44.4	37.9	24.5	45.1	46.5	46.5
Ni/Ti	0.00372	0.00345	0.00352	0.00379	0.00375	0.00371	0.00124	0.00387	0.00396	0.00377
Al/Ti	4.92	4.47	4.77	4.86	4.92	4.97	5.09	4.95	4.78	4.97
Ti ppm	15587	15933	15647	15308	15455	15359	13712	15251	15165	15378
Cr/Ti	0.0033	0.0029	0.0034	0.0037	0.0036	0.0035	0.0002	0.0039	0.0036	0.0044
FeO*/MgO	2.46	2.21	2.47	2.27	2.24	2.93	5.51	2.18	2.06	2.05
Sr/Ca	0.0066	0.0065	0.0123	0.0077	0.0062	0.0061	0.0091	0.0063	0.0064	0.0071
Ba/Ca	0.0043	0.0062	0.0084	0.0055	0.0048	0.0046	0.0111	0.0050	0.0055	0.0046
K/(K+N)	0.20	0.29	0.48	0.42	0.27	0.24	0.33	0.25	0.25	0.33
T/P	8.97	9.36	9.32	8.94	8.84	8.82	2.88	8.97	8.49	8.84
Zr/P_2O_5	503.1	485.5	491.1	501.9	339.5	217.0	279.3	512.8	503.0	399.0
2.Nb	46.0	46.2	45.0	45.6	51.3	51.2	32.4	46.0	36.3	33.1
Zr/4	32.1	31.1	33.1	32.9	25.4	18.0	35.8	32.7	40.0	39.9
Y	21.9	22.7	21.9	21.5	23.4	30.8	31.8	21.3	23.8	27.0
Ti/100	41.4	42.8	43.2	41.7	48.0	51.7	27.0	41.3	41.2	46.8
Zr	38.8	37.0	37.9	39.1	30.7	21.2	43.8	39.4	40.7	35.3
3.Y	19.8	20.2	18.9	19.1	21.2	27.1	29.2	19.3	18.2	17.9

REFERENCES

Adams, A. E. *et al*. 1984. <u>Atlas of Sedimentary Rocks Under the Microscope</u> Longman, Harlow.

Burgess, I. C. and Holliday, D. W. 1979. Geology of the country around Brough-under Stainmore. <u>Mem</u>. <u>Geol</u>. <u>Surv</u>. <u>G.B</u>., Sheet 31, 131pp.

Carmichael, I. S. E. *et al*. 1974. <u>Igneous Petrology</u> McGraw-Hill, London.

Clough, C. T. 1876. The section at the High Force, Teesdale. <u>Quart</u>. <u>Jl geol</u>. <u>Soc</u>. <u>Lond</u>: 32, 466-471.

Dunham, A. C. 1970 Whin Sills and Dykes. 92-100 <u>In</u>: Johnson, J. A. L. and Hickling, G. (eds), <u>Trans</u>. <u>Nat</u>. <u>Hist</u>. <u>Soc</u>. <u>Northumb</u>: 41, No. 1, 152.

Dunham, A. C. and Kaye, M. J. 1965. The Petrology of the Little Whin Sill, County Durham. <u>Proc</u>. <u>Yorks</u>. <u>Geol</u>. <u>Soc</u>: 35, 229-277.

Dunham, A. C. and Strasser-King, V. E. H. 1981. Petrology of the Great Whin Sill in the Throckley Borehole, Northumberland. <u>Rep</u>. <u>Inst</u>. <u>Geol</u>. <u>Sci</u>., No. 81/4.

Dunham, A. C. and Strasser-King, V. E. H. 1982. Late Carboniferous intrusions of northern Britain. <u>In</u>: Sutherland, D. S. (ed), Igneous Rocks of the British Isles. 277-283, Wiley, Chichester.

Emeleus, C. H. 1974. Igneous Rocks. <u>In</u>: Rayner, D. H. and Hemingway, J. E. (eds), <u>The Geology and Mineral Resources of Yorkshire</u>: 265-269. Yorkshire Geological Society. Maney, Leeds.

Fitch, F. J. and Miller, J. A. 1967. The Age of the Whin Sill. <u>Geological</u> <u>Journal</u>: 5, 233-250.

Francis, E. H. 1982. Magma and sediment. I. Emplacement mechanisms of late Carboniferous tholeiite sills in northern Britain. <u>Jl geol</u>. <u>Soc</u>. <u>Lond</u>: 139, 1-20.

Gribble, C. D. and Halk, A. J. 1985. <u>A Practical Introduction To Optical Mineralogy</u> Allen & Unwin, London.

Hall, A. 1987. <u>Igneous Petrology</u> Longman, Harlow.

Harrison, R. K. 1968 Petrology of the Little and Great Whin Sills in the Woodland Borehole, Co. Durnham. <u>Bull</u>. <u>Geol</u>. <u>Surv</u>. <u>G</u>. <u>B</u>: 28, 38-54.

Holmes, A. and Harwood, H. F. 1928. The Age and Composition of the Whin Sill and Related Dykes of the North of England. <u>Mineralog</u>. <u>Mag</u>: 21, 493-542.

Johnson, G. A. L. and Dunham, K. C. 1973. Ordovician, Carboniferous and Intrusive Rocks of Upper Teesdale. <u>In</u>: Capewell, J. G. (ed), <u>Geologists' Association Guides : The Durham Area</u>: 15, 6-11.

Kendall, P. F. and Wroot, H. E. 1924. <u>Geology of Yorkshire: An Illustration of the Evolution of Northern England</u>: Vol. 11, 824-829.

MacKenzie, W. S. *et al*. 1982. <u>Atlas of Igneous Rocks and their Textures</u> Longman, London.

Onuma, N., Hirano, M. and Isshiki, N. 1983. Genesis of Basalt Magmas and their Derivatives under the Izu Islands, Japan, Inferred from Sr/Ca – Ba/Ca Systematics. <u>Journal of Volcanology and Geothermal research</u>: 18, 511-529.

Pearce, J. A. and Cann, J. R. 1973 Tectonic Setting of Basic Volcanic Rocks Determined Using Trace Element Analyses. <u>Earth and Planetary Science Letters</u>: 19, 190-300.

Pearce, T. H., Gorman, B. E. and Birkett, T. C. 1974. The $TiO_2 - K_2O - P_2O_5$ Diagram : A Method of Discriminating Between Oceanic and Non-oceanic Basalts. <u>Earth and Planetary Science Letters</u>: 24, 419-426.

Randall, B. O. A. 1989. Dolerite-pegmatites from the Whin Sill near Barrasford, Northumberland. <u>Proc</u>. <u>Yorks</u>. <u>Geol</u>. <u>Soc</u>: Vol. 47(3), 249-265.

Robson, D. A. 1980. The Geology of North-Eastern England. <u>Trans</u>. <u>Nat</u>. <u>Hist</u>. <u>Soc</u>. <u>Northumb</u>: 67-75.

Spears, D. A. 1961. Joints in the Whin Sill and Associated Sediments in Upper Teesdale, Northern Pennines. <u>Proc</u>. <u>Yorks</u>. <u>Geol</u>. <u>Soc</u>: 33, 21-30.

Taylor, B. J. *et al*. 1971. <u>British Regional Geology : Northern England</u> 4th Ed. 68-69. Natural Environmental research Council Institute of Geological Sciences. Her Majesties Stationary Office, London.

Teall, J. J. H. 1984. On the Chemical and Microscopial Characters of the Whin Sill. <u>Quart</u>. <u>Jl geol</u>. <u>Soc</u>. <u>Lond</u>: 40, 640-657.

Thorpe, R. S. and Macdonald, R. 1985. Geochemical evidence for the emplacement of the Whin Sill complex of northern England. <u>Geol</u>. <u>Mag</u>: 122(4), 389-396.

Tomkeiff, S. I. 1929. A Contribution to the Petrology of the Whin Sill. <u>Mineralog</u>. <u>Mag</u>: 22, 100-122.

Yardley, B. W. K. *et al*. 1990. <u>Atlas of Metamorphic Rocks and their Textures</u> Longman, Harlow.

ACKNOWLEDGEMENTS